RHO-BWI-LD-20
Informal Report

Preliminary Description of Hydrologic Characteristics and Contaminant Transport Potential of Rocks in the Pasco Basin, South-Central Washington

R. A. Deju
K. R. Fecht

March 1979

Prepared for the United States
Department of Energy
Under Contract EY-77-C-06-1030

Rockwell International

Rockwell Hanford Operations
Energy Systems Group
Richland, WA 99352

DISCLAIMER

Rockwell International
Rockwell Hanford Operations
Energy Systems Group
Richland, WA 99352

PREPARED FOR THE UNITED STATES DEPARTMENT OF ENERGY
UNDER CONTRACT EY-77-C-06-1030

PRELIMINARY REPORT

This Report contains information of a preliminary nature. It is subject to revision or correction and therefore does not represent a final Report. It was prepared primarily for internal use within The Rockwell Hanford Operations. Any expressed views and opinions are those of the Author and not necessarily of the Company.

NOTICE

RHO-BWI-LD-20

Informal Report

PRELIMINARY DESCRIPTION OF HYDROLOGIC CHARACTERISTICS AND CONTAMINANT TRANSPORT POTENTIAL OF ROCKS IN THE PASCO BASIN SOUTH-CENTRAL WASHINGTON

R. A. Deju
Director
Basalt Waste Isolation Program

and

K. R. Fecht
Geosciences Unit
Research Department

March 1979

Rockwell International
Rockwell Hanford Operations
Energy Systems Group
Richland, Washington 99352

ABSTRACT

This report aims at consolidating existing data useful in defining the hydrologic characteristics of the Pasco Basin within south-central Washington. In addition, the report aims at compiling the properties required to evaluate contaminant transport potential within individual subsurface strata in this basin. The intent of consolidating such data in one document is to produce a preliminary conceptual model that describes the hydrologic regime and the contaminant transport potential that exists in individual strata within the Pasco Basin. This report will be used in subsequent studies as a data base for modeling the hydrologic regime and ascertaining whether or not the preliminary conceptual model is accurate.

The Pasco Basin itself is a tract of semi-arid land covering about 2,000 square miles in south-central Washington. The regional geology of this basin is dominated by tholeiitic flood basalts of the Columbia Plateau. The surface hydrology of the basin is dominated by the Yakima, Snake, and Columbia rivers. The first two are tributaries of the latter. Short-lived ephemeral streams through portions of the basin may flow for a short period of time after a heavy rainfall or snowmelt.

The subsurface hydrology of the Pasco Basin is characterized by an unconfined aquifer carrying the bulk of the water discharged within the basin. This aquifer overlies a series of confined aquifers carrying progressively smaller amounts of ground water as a function of depth. The ground water also increases in age as a function of depth.

The hydraulic properties of the various aquifers and non-water-bearing strata have been characterized and reported here. A summary of the basic properties is tabulated in Table 6.11. The hydrochemical data obtained have also been summarized in this report. Water characteristics vary as a function of the strata where the water is entrained.

The contaminant transport properties of the rocks in the Pasco Basin have been analyzed in Chapter 8.0 of this report with emphasis on the dispersion and sorption coefficients and the characteristics of the potential reactions between emplaced waste and the surrounding medium.

The final chapter of this report presents some basic modeling considerations of the hydrogeologic systems in the basin with a brief discussion of model input requirements and their relationship to available data.

TABLE OF CONTENTS

Table of Contents (continued)

Table of Contents (continued)

Table of Contents (continued)

LIST OF TABLES

List of Tables (continued)

List of Tables (continued)

LIST OF FIGURES

List of Figures (continued)

1.0 INTRODUCTION

1.1 PROGRAM OVERVIEW

In February 1976, the U. S. Energy Research and Development Administration (currently the U. S. Department of Energy) expanded the commercial radioactive waste management program and established the National Waste Terminal Storage Program. Its mission was to provide multiple facilities in various deep geologic formations within the United States. The Office of Waste Isolation was established within the Union Carbide Corporation-Nuclear Division to provide program management of the National Waste Terminal Storage Program. The overall program consisted of investigating a number of geologic rock types to determine their suitability for terminal storage of radioactive waste. Basalts, such as the Columbia Plateau basalts, which underlie a large portion of the Pacific Northwest and the Hanford Site, were selected for initial geologic reconnaissance. Atlantic Richfield Hanford Company was asked in May 1976, by the Office of Waste Isolation, to plan and execute a basalt feasibility study. Geologic exploration of Columbia Plateau basalts was needed to determine the feasibility of utilizing those formations as a site for terminal storage of commercial nuclear waste.

In September 1977, the National Waste Terminal Storage Program was restructured. While emphasis was still on a salt repository, additional funds were given to support investigations of two U. S. Department of Energy sites--Hanford and Nevada. The Hanford program is presently the responsibility of the U. S. Department of Energy-Richland Operations Office. Rockwell Hanford Operations (successor to Atlantic Richfield Hanford Company) is the prime contractor responsible for this work. The Basalt Waste Isolation Program within Rockwell Hanford Operations has been chartered with the responsibility of conducting these investigations. This program is divided into seven areas:

- Systems Integration encompasses the definition of technical criteria, planning, and systems analysis, as well as repository siting and mine model development;
- Geology encompasses all geologic studies needed for basalt qualification, repository siting, and conceptual design;
- Hydrologic Studies includes all tests required to define any existing ground water flow systems and to obtain the hydrologic information needed for basalt qualification, repository siting, and conceptual design;
- Engineered Barriers includes the thermal assessment of the repository environment and the effect of waste form and other engineered barriers on repository feasibility and effectiveness;
- Engineering Testing involves the conduct of tests to obtain laboratory and in situ engineering properties necessary for conceptual design and basalt qualification;

- Near-Surface Test Facility Construction involves the construction of a Near-Surface Test Facility for in situ testing of the thermo-mechanical behavior of basalt;

- Repository Engineering includes the engineering work leading to design and completion of a basalt repository.

1.2 PURPOSE AND SCOPE

This report aims at consolidating existing data useful in defining the hydrologic characteristics of the Pasco Basin within south-central Washington. In addition, the report aims at compiling the properties required to evaluate contaminant transport potential within individual subsurface strata in this basin. The intent of consolidating such data in one document is to produce a preliminary conceptual model that describes the hydrologic regime and the contaminant transport potential that exists in individual strata within the Pasco Basin. This report will be used in subsequent studies as a data base for modeling the hydrologic regime and ascertaining whether or not the preliminary conceptual model is accurate.

This report draws upon existing data available from numerous studies by county, state, and Federal agencies, private institutions, universities, and research centers. Data from these studies have been carefully analyzed to assess their validity and ensure the accuracy of our interpretation.

1.3 ACKNOWLEDGMENTS

The authors gratefully acknowledge the cooperation from the staff of the Hydrology Unit of the Research Department who gathered much of the data. Special thanks go to Dr. C. W. Myers, Mr. R. L. Biggerstaff, and Dr. M. R. Fox, who acted as reviewers of this document.

2.0 GENERAL CHARACTERISTICS

2.1 LOCATION

The Pasco Basin is a tract of semi-arid land covering about 2,000 square miles in south-central Washington (Figure 2.1). The basin boundaries lie between 46°00' and 46°50' north latitude and 118°50' and 120°30' west longitude, mostly within Benton, Franklin, and Grant counties. This section of Washington has a sparse covering of natural vegetation, primarily suited for grazing, although large areas in the basin have gradually been put under irrigation during the past few years.

2.2 DEMOGRAPHY

The major cities in the area are Richland, Kennewick, and Pasco, all of which are centered in the southern portion of the basin at the confluence of the Yakima, Snake, and Columbia rivers. The population of these 3 cities, based on 1970 census information, is approximately 66,000. Current estimates place the population of the three cities at about 90,000.

2.3 CLIMATE

The Pasco Basin climate is dominated by the high Cascade Range to the west and the prevailing direction of storm fronts from the Pacific Ocean eastward over these high mountains. The orographic effect is dramatic, in that the region has a very mild temperature and is dry. There are occasional periods of high winds. Summers are generally hot and dry; most of the moisture comes during winters, which are relatively mild.

The average maximum temperatures in January and July are 2.6° and 33.2° C, respectively. The average minimum temperatures for the same months are -5.5° and 16.1° C, respectively. The average relative humidity varies from a low of 31.8 percent in July to a high of 80.4 percent in December. The minimum diurnal temperature in winter seasons ranges from -32.8° to -5.6° C; the diurnal maximum temperatures in summer seasons vary from 37.8° to 36.1° C.[1]

Average annual precipitation is 6.25 inches. Thirty-seven percent of the annual precipitation occurs during November, December, and January; whereas only 10 percent occurs in July, August, and September.[1] A slight secondary maximum in precipitation occurs in late spring. About 45 percent of all precipitation that occurs during the months of December through February is in the form of snow.

Mean monthly wind speeds range from about 5 miles per hour in the winter to 9 miles per hour in the summer. July hourly average wind speed varies from a low of about 5 miles per hour in mid-morning to a high of 13 miles per hour in the late evening. The corresponding speeds in January have the same trend, but have less than a 0.6-mile-per-hour

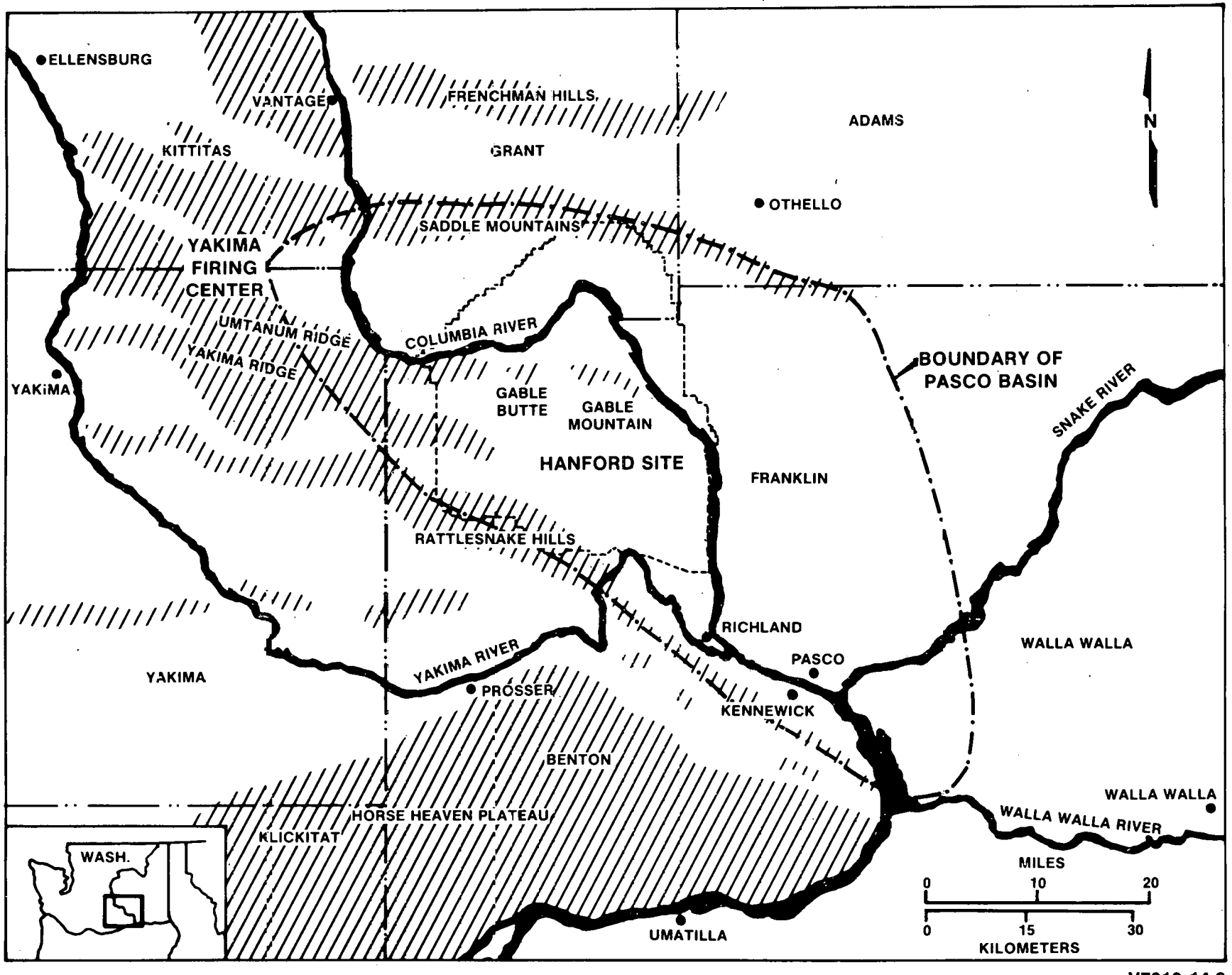

FIGURE 2.1

LOCATION OF THE PASCO BASIN

difference. The prevailing wind directions are from the north-northwest through northwest. The strongest winds tend to be from the southwest. The highest observed peak wind gusts of 41 miles per hour or greater have been observed on the average of at least once in every month of the year, although the winter months tend to have a higher frequency of high-wind periods.

2.4 LAND AND WATER USE

Land within the Pasco Basin is used for agriculture and for Federal Government installations. Agricultural land is generally north and east of the Columbia River and south of the Yakima River (Figure 2.1). Most of the agricultural land is used for growing irrigated crops. Within the Pasco Basin vicinity, the annual quantity of irrigation water pumped from the Columbia and Yakima rivers and from wells is estimated at 10^{10} cubic feet.[2] Government installations include the 476-square-mile U. S. Department of Energy site in the north-central portion of the Pasco Basin and the U. S. Army-Yakima Firing Center in the northwest portion of the basin.

2.5 PHYSIOGRAPHY

The Pasco Basin is a structural and topographic low within the Columbia Plateau. The Pasco Basin is bounded by the Saddle Mountains to the north, Umtanum and Yakima ridges to the west, the Rattlesnake and Horse Heaven hills to the south, and a broad regional monocline (known locally as the Jackass Mountain monocline) to the east.

The central portion of the basin is partially filled with continental clastic sediments transported into the area by river systems from the surrounding highlands. The general surface topography of these sediments forms a broad plain which varies in elevation between 400 and 900 feet.

Locally, a diversity of landforms is found within the basin. In the north-central portion of the basin, two basaltic ridges, Gable Mountain and Gable Butte, crop out above the fluvial plain. These two ridges are the eastern extension of the Umtanum Ridge beneath the basin. Catastrophic flooding during the Late Pleistocene has scoured scabland tracts and coulees in the eastern portion of the basin and aggraded extensive bar deposits in the western two-thirds of the basin. Erosion by the Columbia River and Late Pleistocene floods has formed steep bluffs in the northeast portion of the basin.

In addition, other landforms also characterize the basin. Landslides are prominent along the basaltic ridges bounding the basin and along the river bluffs. Both active and stabilized sand dunes also are prominent features forming a veneer over most of the Pasco Basin.

2.6 REFERENCES

1. W. A. Stone, D. E. Jenne, and M. J. Thorp, Climatography of the Hanford Area, BNWL-1605, Battelle, Pacific Northwest Laboratories, Richland, Washington (1972) p. 230.

2. J. L. Liverman, Final Environmental Statement - Waste Management Operations - Hanford Reservation, Richland, Washington, ERDA-1538, United States Energy Research and Development Administration, Washington, D. C. (December 1975).

3.0 GEOLOGY

3.1 REGIONAL GEOLOGY

3.1.1 Miocene Volcanic Rocks

The regional geology surrounding the Pasco Basin is dominated by a tholeiitic flood basalt province in the Columbia Plateau and adjacent Blue Mountains of Washington, northern Oregon, and adjacent Idaho (Figure 3.1). The flood basalt province is a layered mass of more than 50,000 cubic miles of basalt covering an area of more than 60,000 square miles. The flood basalts and associated rocks form a plano-convex lens. The upper surface of the lens slopes gently inward, except where locally modified by fold systems.

The basalts erupted from linear fissure systems in the eastern and southern portion of the plateau.[1,2] Most of the basalt was emplaced during a 3-million-year volcanic pulse between 16 and 13 million years before present.[3] However, sporadic fissure eruptions continued until about 6 million years before present.[4]

The flood basalts are collectively designated the Columbia River Basalt Group, and have been subdivided into five formations.[5] The lower two formations are the Imnaha Basalt[6] and the Picture Gorge Basalt.[1] The upper three formations, the Grande Ronde Basalt, the Wanapum Basalt, and the Saddle Mountain Basalt, collectively constitute the Yakima Basalt Subgroup.

In general, progressively older basalt formations crop out toward the margins of the plateau (Figure 3.2). The oldest formation in the Columbia River Basalt Group is the Imnaha Basalt. The Imnaha Basalt unconformably overlies deformed pre-Tertiary rock and is found only in northeastern Oregon and adjacent portions of Idaho and Washington. At its type locality in Oregon, the Imnaha Basalt is about 1,700 feet thick.[7,8] The Imnaha lavas emanated, at least in part, from feeder dikes in northeastern Oregon.[7]

Picture Gorge Basalt crops out in north-central Oregon. These lavas are about 15 million years old[3] and unconformably overlie tuffaceous rocks of the John Day Formation.[2] To the south, the andesitic and rhyolitic rocks of the Strawberry Volcanics underlie, interfinger with, and overlie the Picture Gorge Basalt.[9] The thickness of the Picture Gorge Basalt is up to 2,600 feet.[5]

The Grande Ronde Basalt is the most widespread formation in the Columbia River Basalt Group (Figure 3.2).[10] It covers all of the Columbia Plateau in Washington, extends south into the Blue Mountains, and is present along the lower Columbia River valley. The thickest section of Grande Ronde Basalt is in the Pasco Basin, where the unit is at least 500 feet thick. The formation crops out against older rocks along its margins.

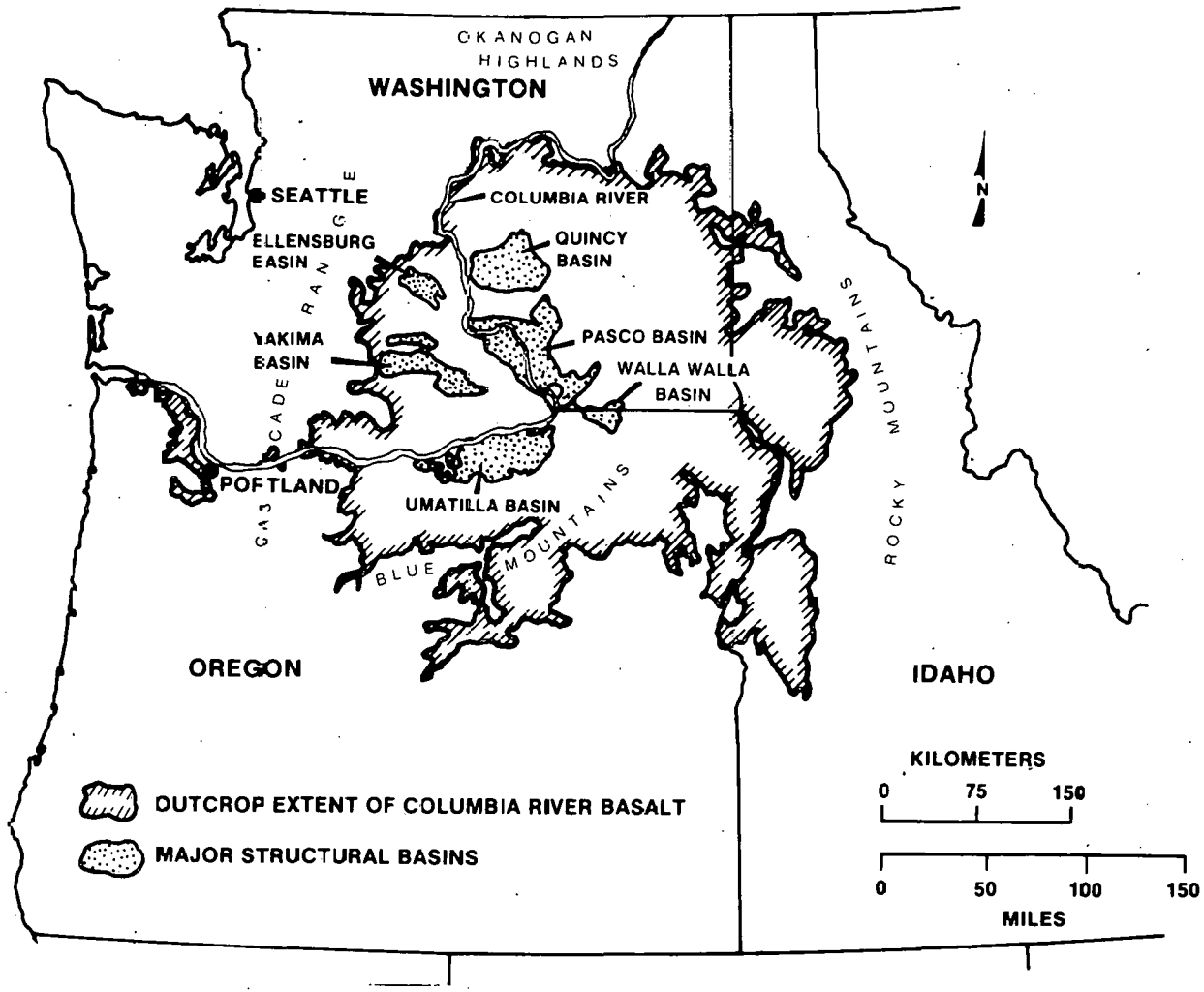

FIGURE 3.1

GEOGRAPHIC EXTENT OF COLUMBIA RIVER BASALT

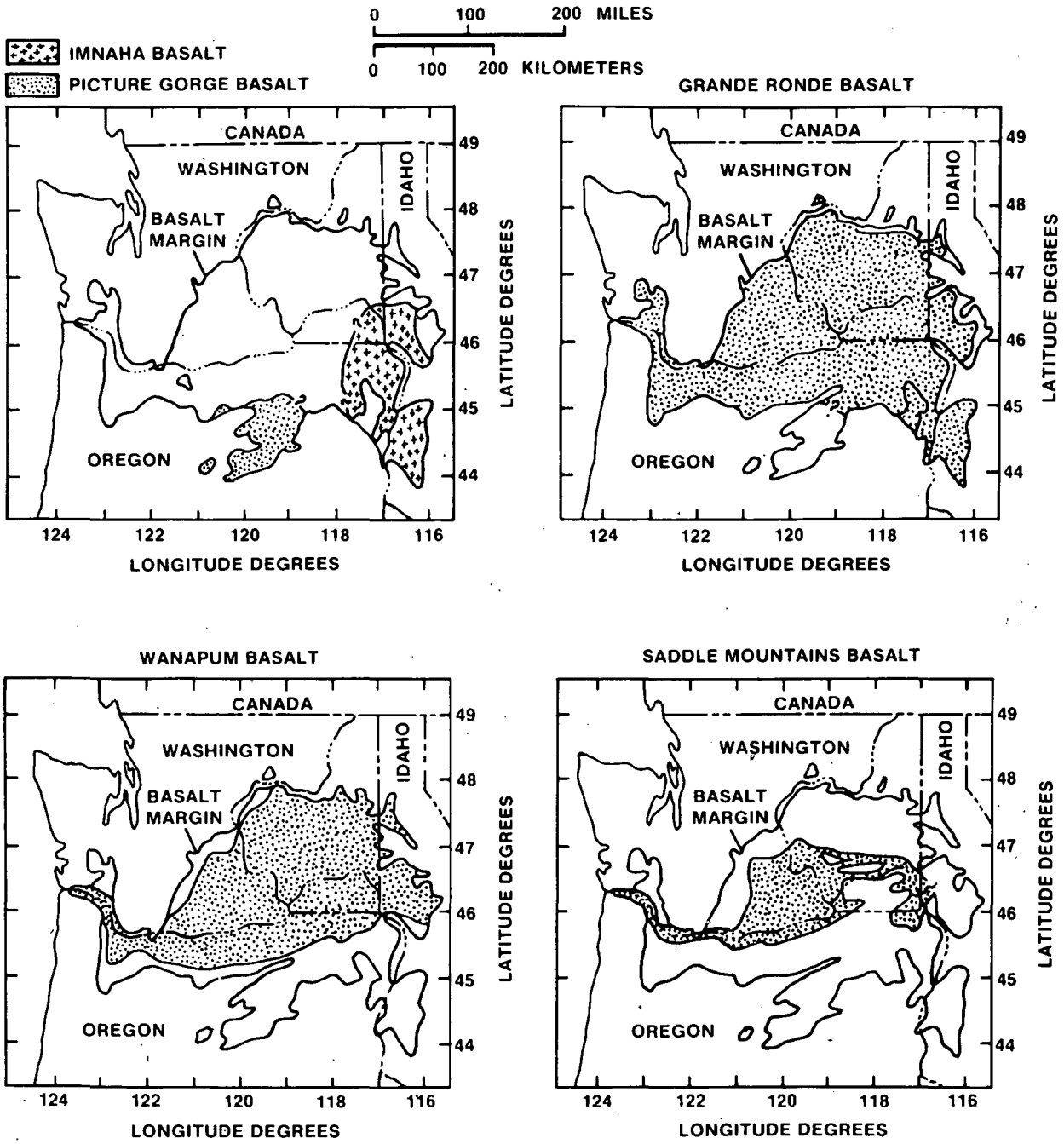

FIGURE 3.2

DISTRIBUTION OF FORMATIONS WITHIN THE COLUMBIA RIVER BASALT GROUP

(Modified from Swanson and Wright[10])

However, in north-central Oregon, the Grande Ronde interfingers with the Picture Gorge Basalt.[5] The Grande Ronde Basalt rests conformably on the Imnaha Basalt, with no evidence of a major time break.[11,12] This evidence indicates the Grande Ronde Basalt is at least in part coeval with the Picture Gorge, but older than Imnaha. The top of the Grande Ronde is generally overlain by the Vantage member of the Ellensburg Formation or a zone of weathering.

The Wanapum Basalt conformably overlies the Grande Ronde Basalt in the central portion of the plateau. Swanson, et al.,[5] conclude that on a "regional scale, however, the Wanapum Basalt disconformably overlies progressively older parts of the Grande Ronde Basalt eastward from the center of the plateau." This suggests that downwarping of the Plateau started in Grande Ronde time. At one locality in southeastern Washington, Wanapum Basalt is known to interfinger with Grande Ronde Basalt.[5]

The Saddle Mountains Basalt is generally conformable with the Wanapum Basalt. Locally, however, particularly on the Yakima fold, flows of the Saddle Mountains Basalt form angular unconformities with Wanapum Basalt. The Saddle Mountains Basalt is largely confined to the center of the plateau, where downwarping has continued since Grande Ronde time, but there are some small exposures in the Lewiston Basin and intercanyon flows which filled the ancestral Snake River valleys.[13] The age of the Saddle Mountains Basalt is about 13.5 to 6 million years before present;[4,14] it represents the waning period of Columbia River Basalt volcanism. Eruptions were sporadic during this time interval, allowing thicker sequences of interbedded sediments to accumulate in the central portions of the plateau.

3.1.2 Miocene Sedimentary Rocks

During quiescent periods in Columbia River Basalt volcanism, continental clastic sediments were transported onto the Columbia Plateau from the surrounding highlands. In the northeast portion of the plateau, lacustrine and fluvial sediments of the Latah Formation occur beneath, interfinger with, and overlie the Columbia River Basalt Group.[15,16] A sequence of tuffaceous lacustrine sediments underlies and interfingers with the Columbia River Basalt Group in the southwestern portion of the plateau. These sediments are designated as the Payette Formation. Along the western margin, the Columbia River Basalt Group is interfingered with and overlain by volcaniclastic sediments of the Ellensburg Formation.[17] These sediments were derived largely from the Cascade Range, they are found near the center of the plateau, and become increasingly abundant from Wanapum through Saddle Mountains time. In the southwest portion of the plateau, the Mascall Formation is interfingered with and overlies the Columbia River Basalt Group.[2,5]

3.1.3 Plio-Pleistocene Sediments

Deformation during the later stages of Columbia River Basalt volcanism resulted in the emergence of the Yakima fold system in the plateau interior. Growth of these folds created a system of structural ridges and basins, which include the Ellensburg Basin, Quincy Basin, Yakima Basin, Pasco Basin, and Umatilla Basin (Figure 3.1). Thick sequences of sediments transported from the surrounding highlands accumulated in these basins.

Clastic sediments of the Pliocene Ringold Formation accumulated in the Quincy, Pasco, and Walla Walla basins in the central portion of the plateau.[18,19,20] Catastrophic floods at the close of the Pleistocene Epoch resulted in the deposition of thick sequences of glaciofluvial sediments in these central plateau basins.[21] The flood deposits overlie the Ringold Formation and the Columbia River Basalt Group.

On the western margin of the plateau in the Yakima and Ellensburg basins, Ellensburg sediments continued to aggrade after cessation of Columbia River Basalt volcanism. The Pliocene Thorp gravels[22,23] overlie the Ellensburg Formation in the Ellensburg Basin. The Ringold Formation and glaciofluvial sediments are present in the lower Yakima Basin. In the Umatilla Basin, The Dalles Formation[24] was deposited on the Columbia River Basalt. Impoundment of floodwaters in Glacial Lake Lewis during the Late Pleistocene resulted in the deposition of glaciofluvial sediments in the Umatilla Basin.[21]

3.2 PASCO BASIN GEOLOGY

3.2.1 Stratigraphy

3.2.1.1 Basement Rock

The basement rocks underlying the basaltic lava flows in the Pasco Basin are of uncertain composition. Pre-basalt rock types can be projected from the margins of the Columbia Plateau, 100 to 150 miles away, and are inferred to exist locally in the central plateau area, perhaps beneath the Pasco Basin. For example, data from the Basalt Explorer Well, northeast of the Pasco Basin, indicate that sandstones and shales comparable to sedimentary rocks of the Cascade Range may lie beneath the Pasco Basin. Recent magnetotelluric surveys indicate a very deep conductive section, possibly representing these sediments.[25] Beneath these sediments are probably granitic rocks comparable to those in the Okanogan Highlands, the Snoqualmie Pass area of the Cascade Range, in the Moscow Basin area of Idaho, in the lower part of the Basalt Explorer Well, and parts of the core of the Blue Mountains, Oregon. The granitic rocks there were intruded into largely Paleozoic and early Mesozoic metavolcanic and metasedimentary rocks whose equivalents might also occur beneath the Pasco Basin.

3.2.1.2 Columbia River Basalt Group

In the Pasco Basin, near the center of the area covered by the Columbia River Basalt, the total basalt sequence is more than 10,000 feet thick[26] and perhaps as much as 19,000 feet thick.[25] In the Pasco Basin, a 5,000-foot thick sequence of Columbia River Basalt apparently overlies a series of older basalt of Oligocene to Eocene age.[5] Approximately 100 basalt flows, including both Columbia River Basalt and older lavas, have been identified from geophysical logs obtained from a 10,600-foot deep borehole located along the western margin of the Pasco Basin.

The stratigraphic nomenclature for the Pasco Basin is given in Figure 3.3. The three formations which constitute the Yakima Basalt Subgroup have been subdivided into additional mappable units (members and flows).[27] Based on extensive borehole and mapping studies, many of these units have been determined to be laterally continuous across the Pasco Basin (Figures 3.4 and 3.5).

Individual basalt units within the Pasco Basin vary in thickness from flows greater than 325 feet in thickness to flow units a few feet thick. The internal characteristics of these flow units show a high variability in jointing patterns between flows, but a typical flow usually consists of: (1) a lower zone or lower colonnade, generally 1/2 to 1/3 the thickness of the flow having nearly symmetrical columnar joints defining prismatic columns oriented approximately perpendicular to the flow top; and (2) an upper zone or entablature, generally 1/2 to 2/3 the thickness of the flow and consisting of a much more irregular jointing pattern where columnar joints, if present, are less distinct than in the colonnade (Figure 3.6).[28,29] The flow tops are typically vesicular and most flows have a thin vesicular zone at the base.

3.2.1.3 Ringold Formation

The Ringold Formation is Pliocene in age[20] and was deposited in response to a flattening of the gradient of the Columbia and Snake rivers. systems, perhaps related to the uplift of the Horse Heaven Hills and consequent deposition of the sediments carried.[30] The Ringold Formation in the Pasco Basin has accumulated to a thickness of up to 1,300 feet.

The Ringold Formation can generally be divided into three units on the basis of texture: clay and silts with lenses of gravel of the lower Ringold unit; occasionally cemented sand and gravel of the middle Ringold unit; and silts and fine sands of the upper Ringold unit (Figure 3.7).[31]

The lower portion of the Ringold Formation is, in general, conformable with the surface of the underlying basalt bedrock. The lower Ringold unit is thickest in the central portion of the Pasco Basin and thins to the margins of the basin. The matrix-supported conglomerate of the middle Ringold unit overlies the lower unit. The upper Ringold unit is generally confined to the margins of the basin; elsewhere, it either has not been deposited, or has been eroded by ancestral river systems and by Late Pleistocene catastrophic flooding of the basin.

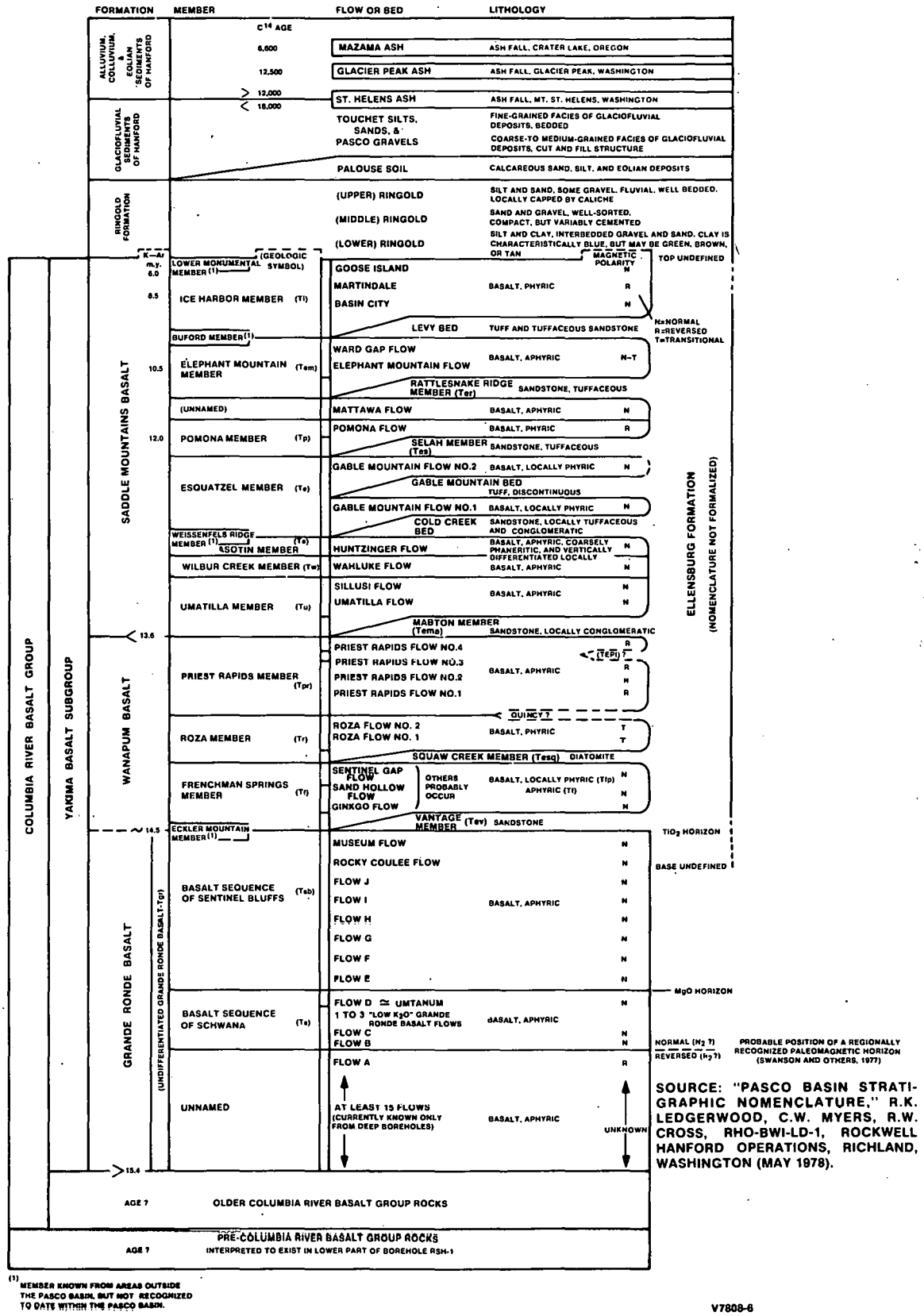

SOURCE: "PASCO BASIN STRATIGRAPHIC NOMENCLATURE," R.K. LEDGERWOOD, C.W. MYERS, R.W. CROSS, RHO-BWI-LD-1, ROCKWELL HANFORD OPERATIONS, RICHLAND, WASHINGTON (MAY 1978).

FIGURE 3.3

PASCO BASIN STRATIGRAPHIC NOMENCLATURE

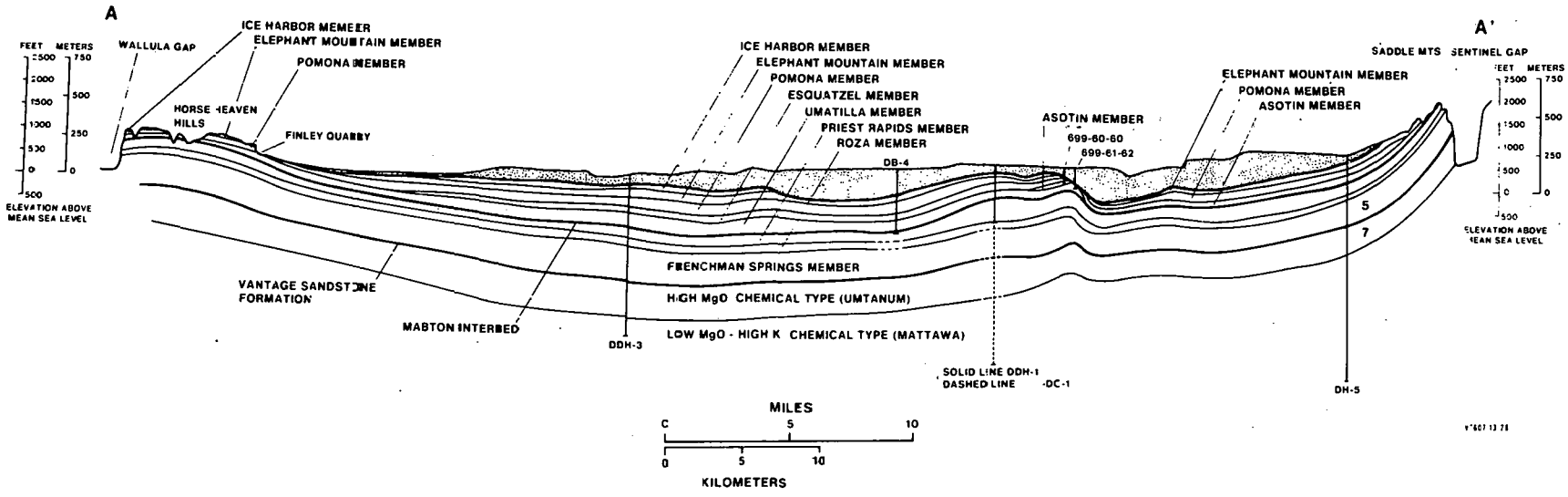

FIGURE 3.4

GENERALIZED CROSS SECTION
A-A' PARALLEL TO MAIN AXIS OF THE PASCO BASIN

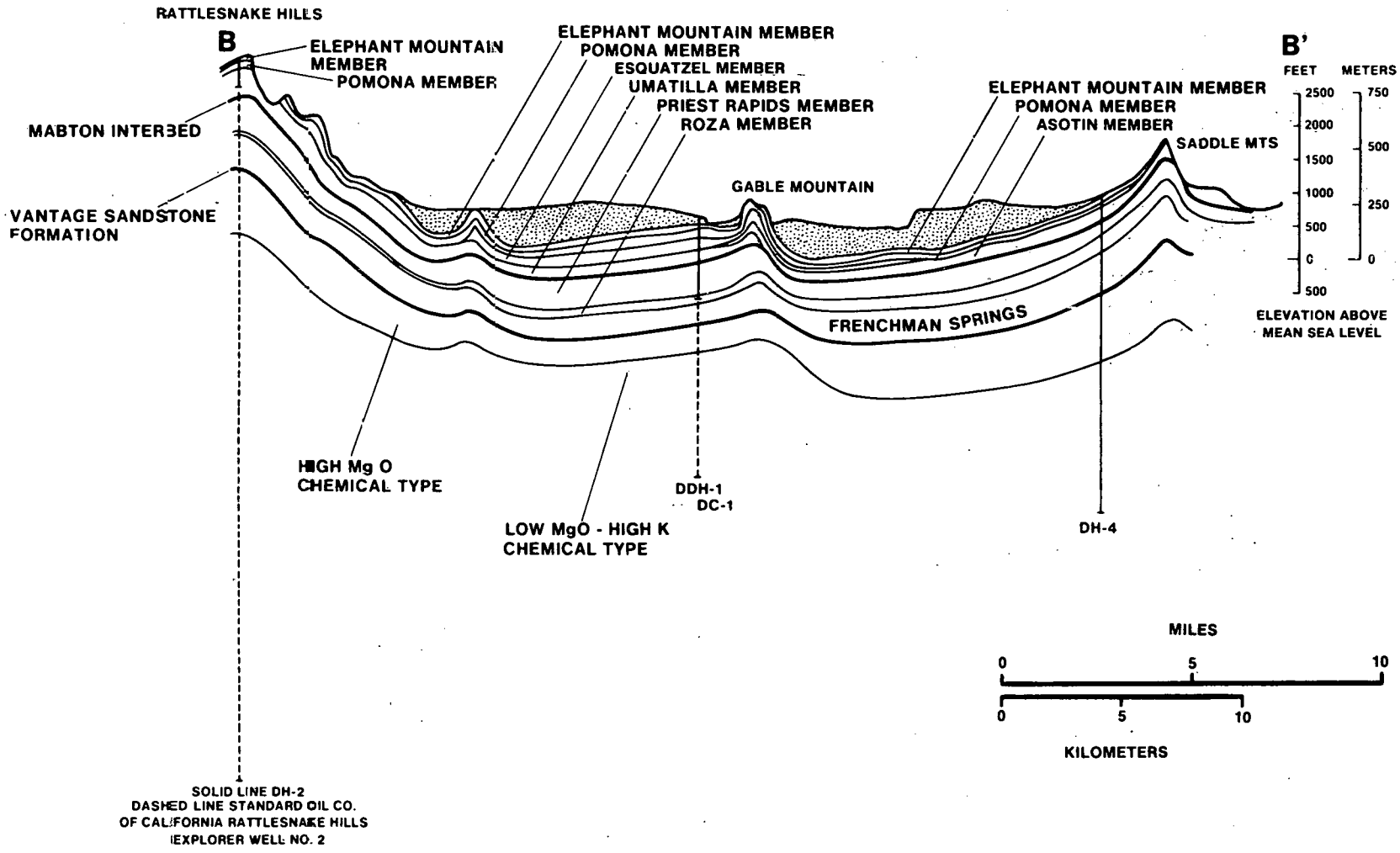

FIGURE 3.5

GENERALIZED CROSS SECTION
B-B' NORMAL TO MAIN AXIS OF THE PASCO BASIN

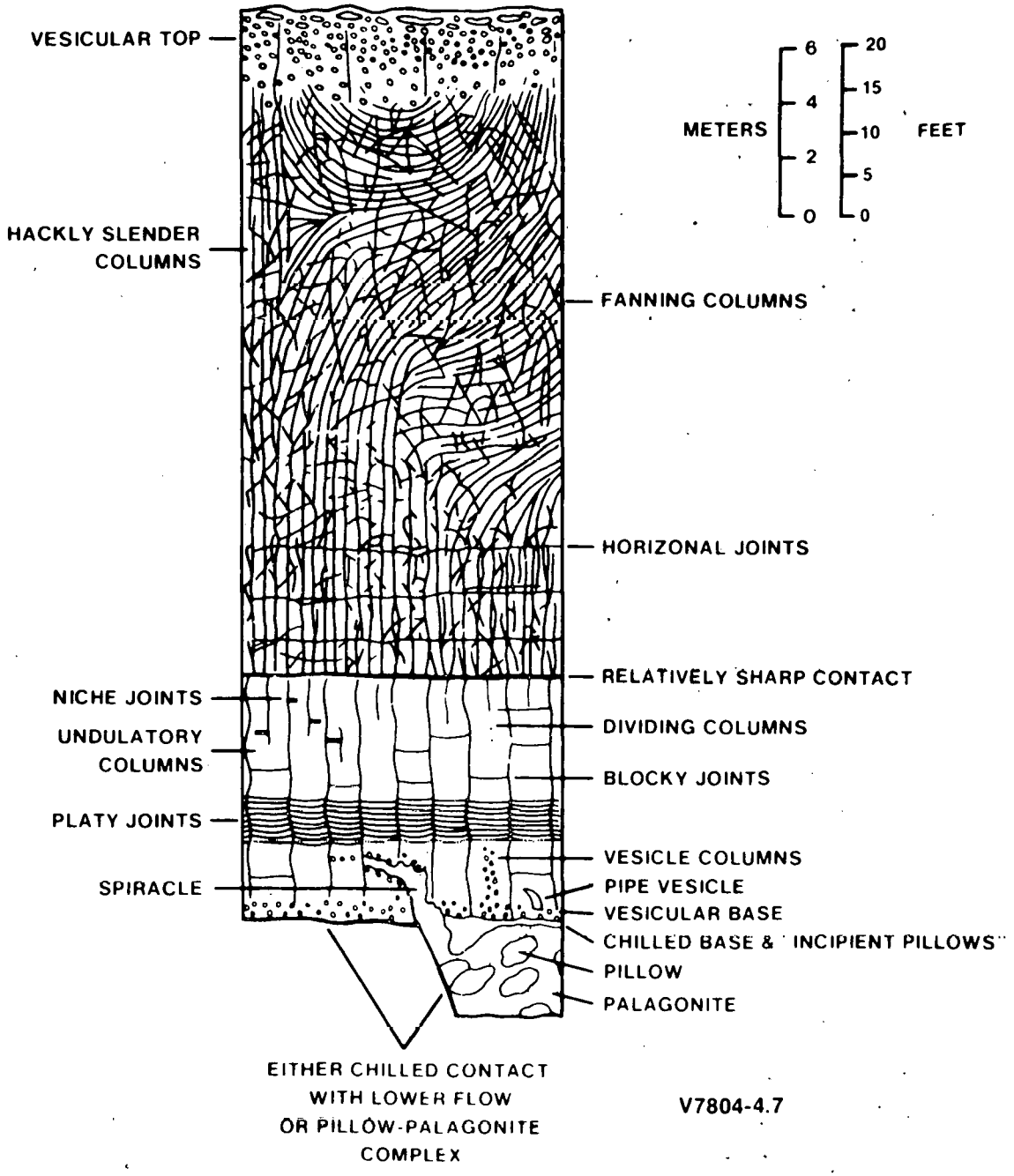

FIGURE 3.6

MAJOR INTRAFLOW STRUCTURES
OF TYPICAL COLUMBIA RIVER BASALT FLOW

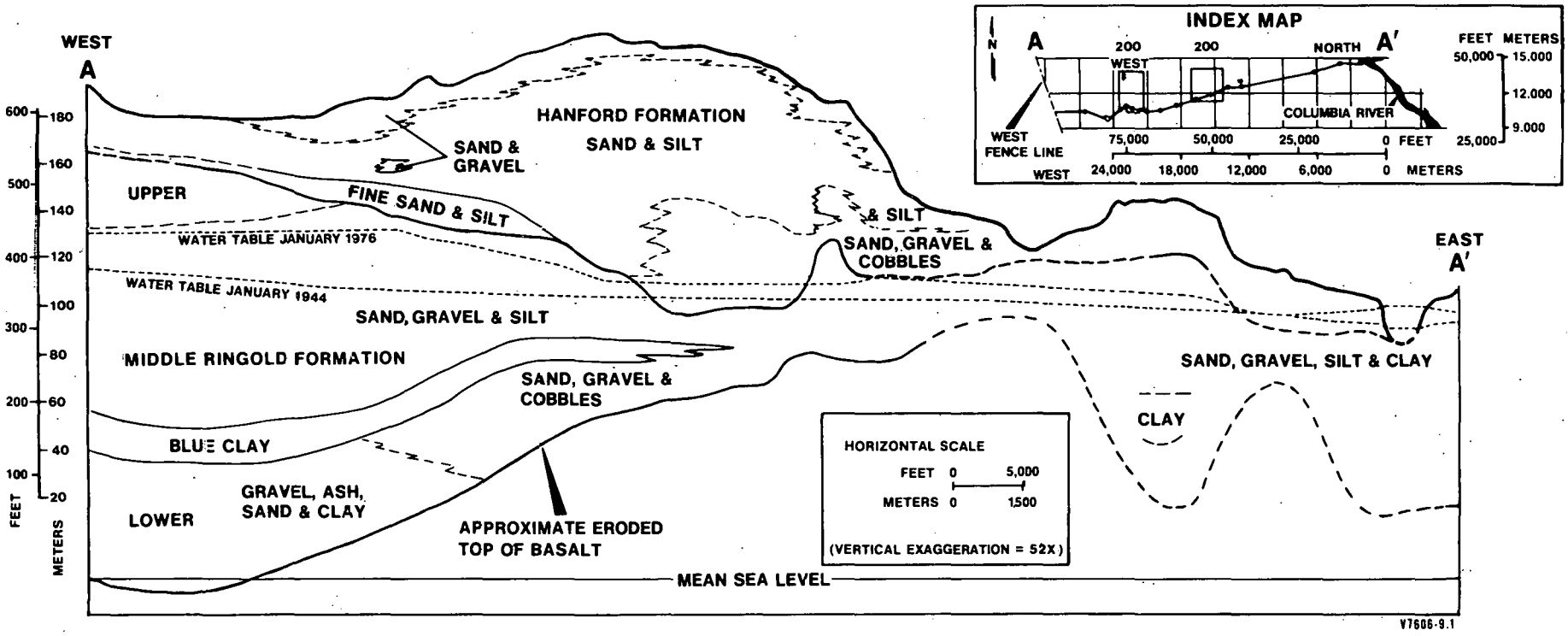

FIGURE 3.7

GEOLOGIC CROSS SECTION
HANFORD SITE

3.2.1.4 Palouse Soils

An eolian silt (loess) and fine sand overlie part of the eroded surface of the Ringold Formation and caliche bed beneath the western part of the Hanford Site (Figure 3.7).[32] It is considered to be the equivalent to the earlier Palouse soils (loesses) of eastern Washington and western Idaho. It indicates a climate comparable to that of today, with effective wind transport and deposition of sediment.

3.2.1.5 Hanford Formation (Informal Name)

The Ringold Formation and the basalts and sedimentary interbeds were locally eroded and truncated by multiple floods that occurred as ice-dammed lakes released catastrophic torrents of water and ice when the ice dams were breached near the close of the ice age.[21,33] The floods scoured the land surface leaving a network of buried channels crossing the Pasco Basin filled with the outwash sands and gravels, forming the Hanford formation.

The glaciofluvial sediments in the Pasco Basin were deposited on the Columbia River Basalt Group and Ringold Formation (Figure 3.7). These sediments can be divided into the coarser sands, gravels, and boulders and are referred to as the Pasco Gravels;[27] the fine-grained sand and silt units are called the Touchet Beds.[34]

The Touchet Beds represent low-energy (slack water) sediments deposited in Glacial Lake Lewis, which formed when floodwaters were backed up behind the Wallula Gap constriction. The Pasco Gravels represent high energy deposition in areas of more rapid water flow. In general, the Touchet Beds are found on the margins of the basin and the Pasco Gravels in and near the center of the basin. The characteristic variability of sediment size and degree of sorting within the "gravel" unit can be attributed to changes in water velocity and water level which occurred during the flooding process. The thickness of the Hanford formation varies significantly within the basin, with the thickest occurrence in the region of buried channels.

3.2.1.6 Eolian Deposit

Loess and sand dunes mantle the surface of the Pasco Basin. These deposits are primarily reworked sediments of the Hanford formation from surrounding areas. The thickness of the wind-blown sediments varies considerably, ranging from zero to more than 100 feet in some dunes.

3.2.2 Structure

3.2.2.1 Folds

The most prominent structural features in the Pasco Basin and vicinity are anticlinal ridges known as the Yakima folds which divide the Columbia Plateau into several structural and physiographic basins. Although the orientation of the folds is generally east-west, they are east-west-trending, west-northwest-trending, and northeast-trending segments (Figure 3.8).

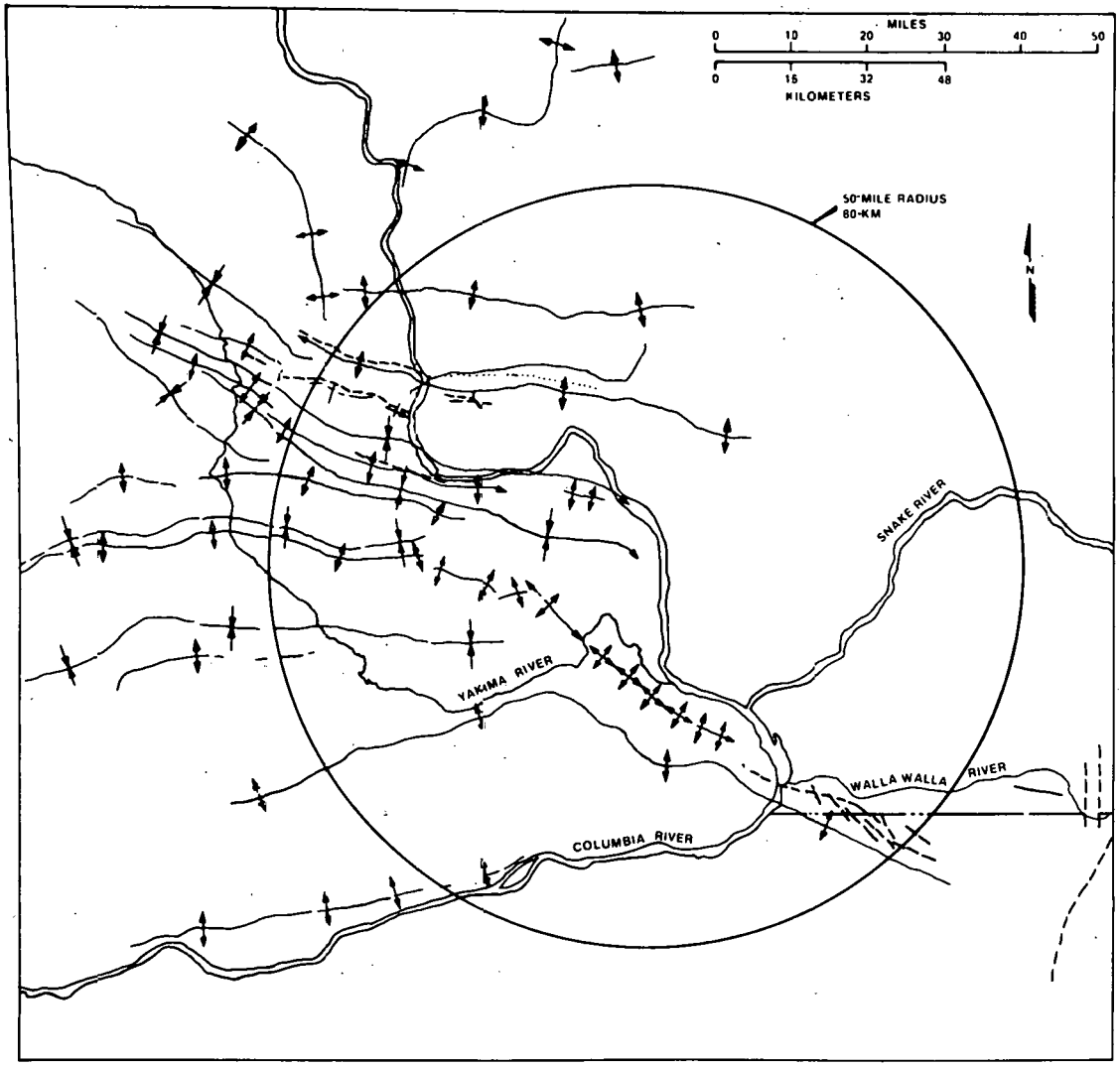

FIGURE 3.8

STRUCTURAL FEATURES OF THE PASCO BASIN AREA

3.2.2.2 Faults

The major faults mapped in the Pasco Basin vicinity are generally associated with folds in the basalt and typically sub-parallel fold axes. Many of the anticlinal structures shown on Figure 3.8 have associated faults along part of their extent.

3.3 REFERENCES

1. D. A. Swanson, T. L. Wright, and R. T. Helz, "Linear Vent Systems and Estimated Rates of Magma Production and Eruption for the Yakima Basalt on the Columbia Plateau," American Journal of Science, 275 (1975) p. 877-905.

2. A. C. Waters, "Stratigraphic and Lithologic Variations in Columbia River Basalt," American Journal of Science, 259 (1961) p. 583-611.

3. A. K. Baksi and N. D. Watkins, "Volcanic Production Rates - Comparison of Oceanic Ridges, Islands, and Columbia Plateau Basalts," Science, 180 (1973) p. 493-496.

4. E. H. McKee, D. A. Swanson, and T. L. Wright, "Duration and Volume of Columbia River Basalt Volcanism, Washington, Oregon, and Idaho," Geological Society of America, Abstract with Programs, 9 (1977) p. 463-464.

5. D. A. Swanson, T. L. Wright, P. R. Hooper and R. D. Bentley, Revisions in Stratigraphic Nomenclature of the Columbia River Basalt Group, U. S. Geological Survey Bulletin 1457 (1978).

6. P. R. Hooper, "Petrology and Chemistry of the Rock Creek Flow, Columbia River Basalt, Idaho," Geological Society of America Bulletin, 85 (1974) p. 15-26.

7. W. D. Kleck, "Chemistry, Petrography, Stratigraphy of the Columbia River Group in the Imnaha River Valley Region, Eastern Oregon, and Western Idaho," Ph.D. Dissertation, Washington State University Pullman, Washington (1976) 203 p.

8. T. L. Vallier and P. R. Hooper, "Geologic Guide to Hells Canyon, Snake River," Geological Society of America, Cordilleran Section Meeting, Field Guide No. 5, Pullman, Washington (1976) 38 p.

9. T. L. Robyn, Geology and Petrology of the Strawberry Volcanics, Northeast Oregon, Ph.D. Dissertation, Oregon State University, Eugene, Oregon (1977) 197 p.

10. D. A. Swanson and T. L. Wright, "Bedrock Geology of the Northern Columbia Plateau and Adjacent Areas," in V. R. Baker and D. Nummedal (editors), The Channeled Scabland, Office of Space Administration National Aeronautics and Space Administration, Washington, D. C. (1978) 185 p.

11. V. E. Camp, Petrochemical Stratigraphy and Structure of the Columbia River Basalt, Lewiston Basin Area, Idaho-Washington, Ph.D. Dissertation, Washington State University, Pullman, Washington (1976) 201 p.

References (continued)

12. G. S. Holden and P. R. Hooper, "Petrology and Chemistry of the Columbia River Basalt Section, Rocky Canyon, West-Central Idaho," Geological Society of America Bulletin, 87 (1976) p. 215-225.

13. D. A. Swanson, T. L. Wright, V. E. Camp, J. N. Gardner, R. T. Helz, S. A. Price, and M. E. Ross, Reconnaissance Geologic Map of the Columbia River Basalt Group, Pullman and Walla Walla Quadrangles, Southeast Washington and Adjacent Idaho, U. S. Geological Survey Open-File Report 77-100 (1977).

14. Staff, Research and Engineering, Preliminary Feasibility Study on Storage of Radioactive Wastes in Columbia River Basalts, ARH-ST-137, Atlantic Richfield Hanford Company, Richland, Washington (1976) p. 168.

15. V.R.D. Kirkham and M. M. Johnson, "The Latah Formation in Idaho," Journal of Geology, 38 (1929) p. 483-504.

16. J. W. Hosterman, Clay Deposits of Spokane County, Washington U. S. Geological Survey Bulletin 1270 (1969) p. 96.

17. G. O. Smith, Geology and Water Resources of a Portion of Yakima County, Washington, U. S. Geological Survey Water Supply Paper 55 (1901).

18. J. C. Merriam and J. P. Buwalda, "Age of Strata Referred to the Ellensburg Formation in the White Bluffs of the Columbia River," University of California Publication of Geological Sciences, 10 (1916).

19. R. C. Newcomb, "Ringold Formation of Pleistocene Age in Type Locality, the White Bluffs Washington," American Journal of Science, 256 (1958).

20. E. P. Gustafson, The Vertebrate Faunas of the Pliocene Ringold Formation, South-Central Washington, Museum of Natural History Bulletin No. 23, University of Oregon, Eugene, Oregon (1978).

21. J H. Bretz, Washington's Channeled Scabland, Washington Division of Mines and Geology, Bulletin 45 (1959).

22. S. C. Porter, "Pleistocene Glaciation in the Southern Part of the North Cascade Range, Washington," Geological Society of America Bulletin, 87 (1976) p. 61-75.

23. R. W. Taber, R. B. Waitt, V. A. Frizzell, D. A. Swanson, and G. R. Byerly, Preliminary Map of the Wenatchee 1:100,000 Quadrangle, Washington, U. S. Geological Survey Open File Map (1977) p. 40.

24. T. Condon, The Two Islands and What Came of Them, J. K. Gill Company, Portland, Oregon (1902) p. 221.

25. Staff, Basalt Waste Isolation Program, Annual Report - Fiscal Year 1978, RHO-BWI-78-100, Rockwell Hanford Operations, Richland, Washington (1978).

References (continued)

26. J. R. Raymond and D. D. Tillson, Evaluation of a Thick Basalt Sequence in South-Central Washington, BNWL-776, Battelle, Pacific Northwest Laboratories, Richland, Washington (1968).

27. R. K. Ledgerwood, C. W. Myers, and R. W. Cross, Pasco Basin Stratigraphic Nomenclature, RHO-BWI-LD-1, Rockwell Hanford Operations, Richland, Washington (1978).

28. S. I. Tomkeiff, "The Basalt Lavas of the Giant's Causeway District of Northern Ireland," Bulletin of Volcanism, 6 (1940).

29. D. A. Swanson, "Yakima Basalt of the Tieton River Area, South-Central Washington," Geological Society of America Bulletin, 78 (1967).

30. R. C. Newcomb, J. R. Strand and F. J. Frank, Geology and Ground-Water Characteristics of the Hanford Reservation of the U. S. Atomic Energy Commission, Washington, U. S. Geological Survey Professional Paper 717 (1972) 78 p.

31. D. J. Brown, Subsurface Geology of the Hanford Separations Areas, HW-61780, General Electric Company, Richland, Washington (1959) 21 p.

32. D. J. Brown, An Eolian Deposit Beneath 200 West Area, HW-67549, General Electric Company, Richland, Washington (1970).

33. V. R. Baker, Paleohydrology and Sedimentology of the Lake Missoula Flooding in Eastern Washington, Geological Society of America Special Paper 144 (1973).

34. R. F. Flint, "Origin of the Cheney-Palouse Scabland Tract," Geological Society of America Bulletin, 49 (1938).

4.0 SURFACE HYDROLOGY

4.1 GENERAL

The Pasco Basin lies within the Columbia River Basin. This major surface drainage system (Figure 4.1) covers parts of five physiographic provinces in the United States, namely: (1) Pacific Border; (2) Cascade Range; (3) Columbia Plateau; (4) Northern Rocky Mountains; and (5) Middle Rocky Mountains. It also includes a portion of the British Columbia Physiographic Province in Canada. The Columbia River Basin is drained by the 1,243-mile-long Columbia River and its major tributaries: Kootenai; Pend Oreille; Spokane; Okanogan; Wenatchee; Yakima; Snake; Lewis; Cowlitz; John Day; Deschutes; and Willamette rivers.

The headwaters of the Columbia River are at Columbia Lake (Figure 4.1) in British Columbia, between the Canadian Rockies and the Selkirk Mountains, 2,650 feet above sea level. The river empties into the Pacific Ocean near Astoria, Oregon at 45°15' latitude and 124°05' longitude.

The Columbia River flows northwest for the first 218 miles, then south for 280 miles, crosses the United States-Canadian border into northeast Washington, and flows south, then west, and again south across central Washington in a sweeping curve called the Big Bend. Just below the mouth of the Snake River south of Pasco, Washington, the Columbia turns west for 210 miles and cuts across the Cascade Range, forming the boundary between Oregon and Washington. Near Vancouver, Washington the river turns north for 50 miles, then west for the final 55 miles to the Pacific Ocean.

4.2 DRAINAGE OF THE PASCO BASIN

The Pasco Basin is drained by the Yakima, Snake, and Columbia rivers. Short-lived ephemeral streams through portions of the Pasco Basin may flow for a short period of time after a heavy rainfall or snowmelt.

The Yakima River is a major tributary of the Columbia River (Figure 4.1). It has an overall length of about 180 miles and a drainage basin of about 6,000 square miles. The river heads in the rugged eastern slopes of the Cascade Range and flows southeastward into the semi-arid region of Central Washington. The Snake River starts in the state of Wyoming and flows westward to the confluence with the Columbia just south of Pasco, Washington.

The surface hydrology of the Pasco Basin[1] has been extensively studied, especially as part of the Hanford waste management programs and as part of studies by the U. S Army-Corps of Engineers. The Hanford studies include not only an analysis of the Columbia and Yakima rivers, but also extensive

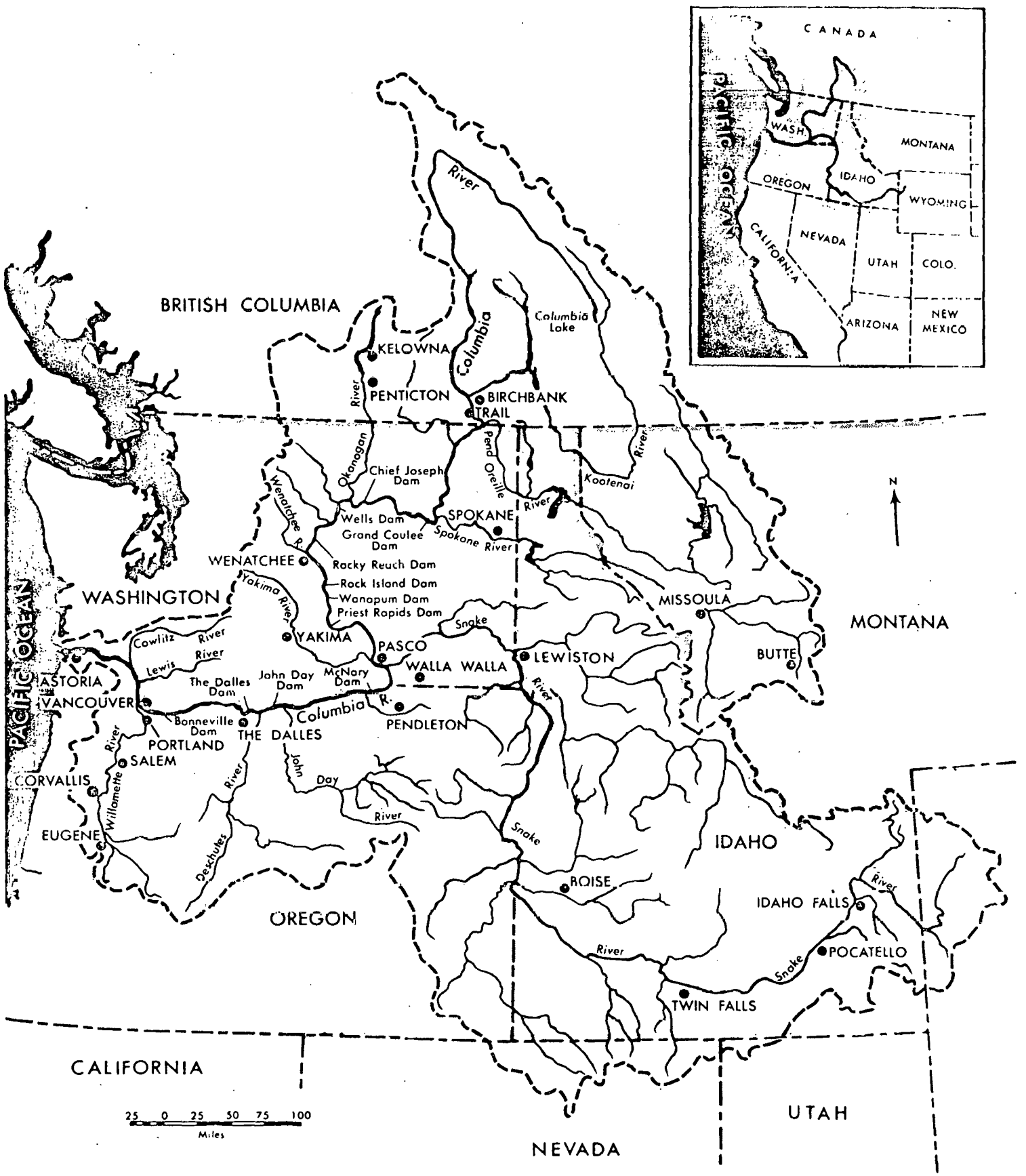

FIGURE 4.1

THE COLUMBIA RIVER BASIN

investigations as to the nature of a number of man-made ditches and ponds which are used for the disposal of low-level radioactive waste (Figure 4.2), certain industrial waste, and cooling water from various processes. A complete list of the ditches and ponds, together with their physical dimensions and radioactive inventories, has been compiled.(1)

Direct precipitation over the Pasco Basin mostly evaporates, leaving a minimal amount of water as land runoff and/or infiltration. Except for minor periods of time during the spring, land runoff in the Pasco Basin is negligible.

More precipitation falls during the winter at the Hanford Meteorological Station and at Richland, Washington than during the summer. Thirty-seven percent of the total typically falls during November, December, and January, whereas only 10 percent falls during July, August, and September.(2)

Thus, precipitation is least when the potential evapotranspiration (PE) is greatest and largest when the PE is least. This tends to make both the mean annual surplus and mean deficits (which are the sum of the mean monthly surpluses, and the sum of the mean monthly deficits) larger than if the precipitation were uniformly distributed in time.

Figure 4.3 shows the relation of mean-annual precipitation, PE, surplus, and deficit as a function of altitude obtained from 64 stations in and around the Yakima River Basin, which is adjacent to the Pasco Basin.(3)

The precipitation at Richland and the Hanford Meteorological Station(2) shown on Figure 4.3 suggests that these curves should fit the Pasco Basin conditions fairly well. However, limited precipitation data from the Arid Lands Ecology Reserve(2) on the west side of the Hanford Site suggest that the precipitation rate increases more slowly with altitude in the Pasco Basin than it does in the Yakima River Basin. Precipitation at the top of Rattlesnake Hills appears to be only 70 to 90 percent greater than at the Hanford Meteorological Station; whereas the curve of Figure 4.3 suggests that it should be 500-600 percent greater. If this is indeed the case, the surpluses will be smaller and deficits larger than those shown. This is significant to the ground water hydrology of the Pasco Basin because recharge must be less than the calculated surplus.(4)

The Columbia River reaches from Priest Rapids Dam (river mile 397) (Figure 4.2) to the head of the reservoir behind McNary Dam (approximately river mile 351) are the last free-flowing stretch of the Columbia River within the United States. The main channel is braided around the island reaches and submerged rock ledges and gravel bars causing repeated pooling and channeling. The riverbed material is mobile and dependent on river velocities; it is typically sand, gravel, and rocks up to 8 inches in diameter. Small fractions of silts and clays are associated with the sands in areas of low-velocity deposition, becoming more dominant approaching the upstream face of each river dam.

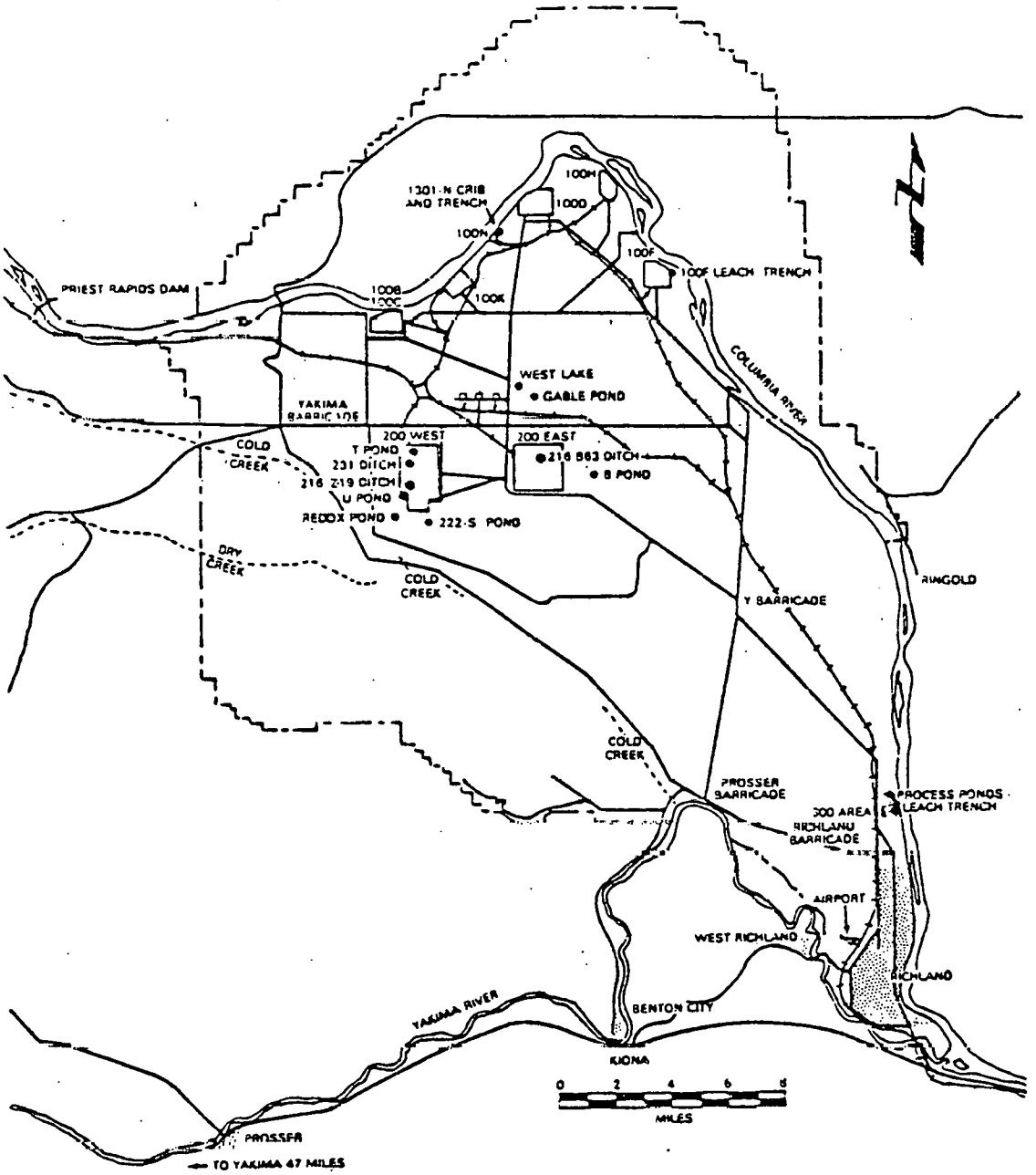

FIGURE 4.2

SURFACE WATER AREAS ON THE HANFORD SITE

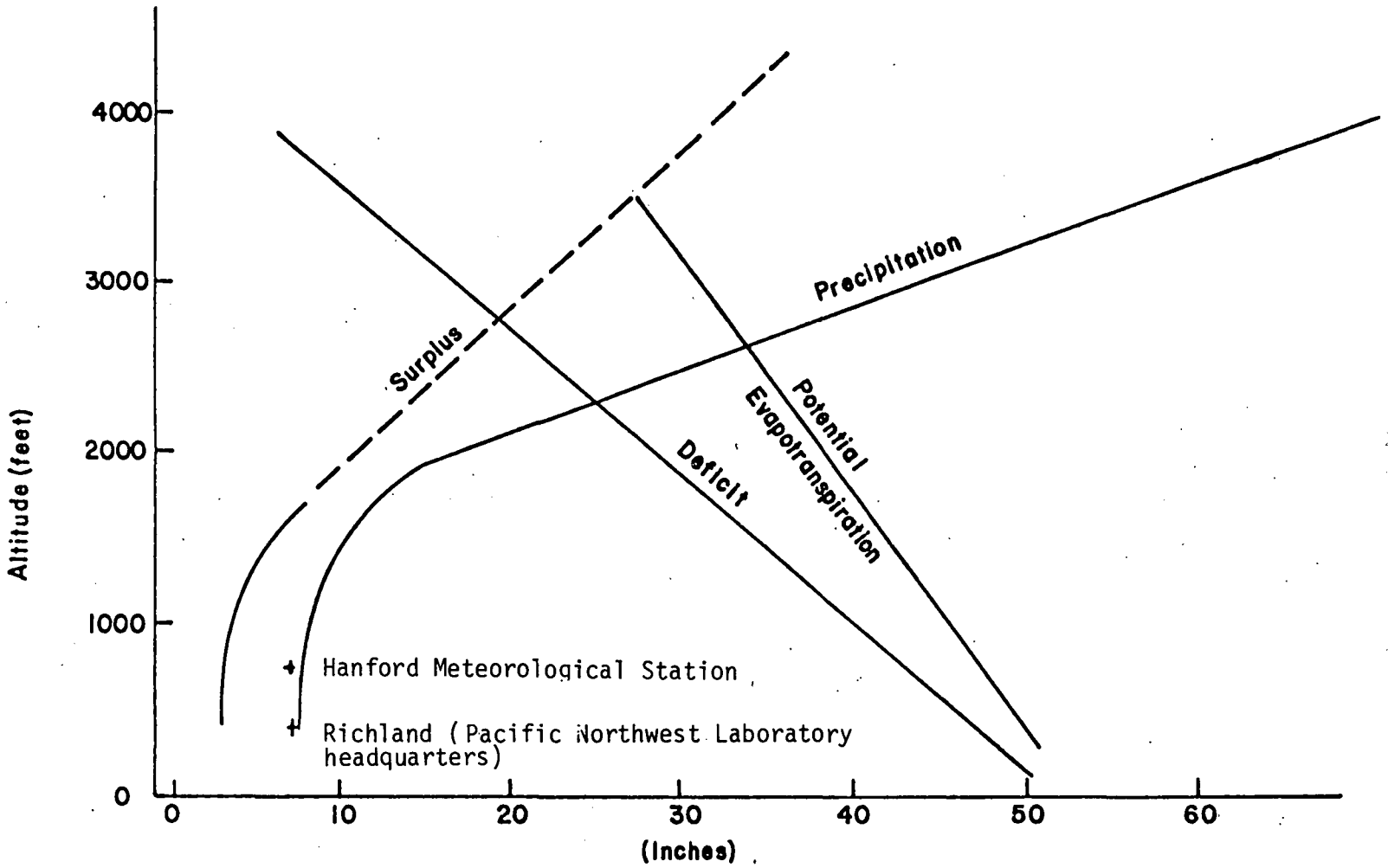

FIGURE 4.3

RELATION OF MEAN ANNUAL PRECIPITATION, POTENTIAL EVAPOTRANSPIRATION, SURPLUS, DEFICIT TO ALTITUDE IN THE YAKIMA RIVER BASIN

(From Summers and Deju, 1974[3])

Velocity measurements in the Columbia River have been made at selected locations, usually in conjunction with temperature and radioactivity surveys, and have included both surface velocity and velocity as a function of depth. Surface and vertical velocity profiles have been drawn from these measurements.[1] The maximum velocities measured vary from less than 3 feet per second (fps) to over 11 fps, depending upon the river cross section and flow rate.

From the reactors located on the Hanford Site to several miles below the Snake River mouth, bed sediments of the Columbia River are typically sand, intermixed with gravel and rock as large as eight inches in diameter. Streambeds of eddying areas in this relatively fast-water reach are usually composed of sand. Sand, silt, and clay are deposited in slack water areas behind McNary Dam. Between the upstream reach (which has a coarse-sediment bed) and the deposits of small-size sediments near McNary Dam, the streambed in deep channels is sand and, in shallow areas, is a mixture of sand, silt, and some clay. Some sediment is present in the Bonneville Dam reservoir. In general, the bed in most stretches of the river between the reservoirs either has been scoured to bedrock or has been covered with a thin deposit of coarse gravel.

Concentrations of suspended sediment carried by the Columbia River vary considerably throughout the year because of the seasonal contributions of tributaries. However, during all seasons, the Snake River usually is the major contributor of suspended sediments. During slack water, the dams along the Columbia and Snake rivers normally interrupt the transport of suspended sediment as well as the bedload; during high water, the sediment is resuspended. Thus, most of the suspended sediment is discharged to the Pacific Ocean during the late spring and early summer at the time of highest flow rate.

Bedload sediment transport, appreciable only in the lower Columbia, is probably small, perhaps on the order of 10 percent of the total sediment load, exclusive of dissolved materials.[1]

4.3 POTENTIAL FLOODS

A calculation of the effect of a Columbia River flood that might occur in the next 1,000 years on the Hanford Site has been performed and reported.[1] The flooding condition used in the analysis is the dam-regulated "Probable Maximum Flood" (PMF) previously predicted[1] by the U. S. Army-Corps of Engineers. This prediction was derived using extensive data and computer modeling techniques and incorporating assumptions of a combination of conditions which were the most severe considered "reasonably possible" for the Columbia River Basin. Contributing factors of winter snow accumulation, spring melting, and runoff-season rainstorms were maximized.

The basic cause of the PMF would be spring snowmelt runoff in the mountains of the Columbia River Watershed following exceptionally cold and wet weather during the October to April snow accumulation season. It was assumed that, over the Columbia River Basin as a whole, the October to April precipitation equaled 1.3 times the normal annual precipitation. Unusually rapid melting due to meteorological conditions was predicted as a result of the assumption of extreme seasonal values for air temperatures, dew point, solar radiation albedo, and wind speed.

In addition, two hydrologically significant (the most severe considered "reasonably possible") basin-wide rainstorms were assumed. It was also assumed that rain contributions to the PMF fell entirely during two 5-day periods during the snowmelt season. The first was arbitrarily chosen in mid-May, the second was timed to maximize the natural peak discharge of the lower Columbia River. This calculation shows that, even under these circumstances, the flood would be restricted to a narrow zone adjacent to the Columbia River.

The probable maximum 24-hour precipitation that can be expected in the Pasco Basin region near Hanford at least once in 1 million years is about 11 inches.[5] The maximum recorded 24-hour precipitation has been 1.94 inches. Even an 11-inch, 24-hour downpour flooding would be confined to the immediate areas along the Columbia River.

Estimates of the consequences of hypothetical (artificial) floods have been reported.[6] A worst-case event would result from a postulated 50 percent breach of Grand Coulee Dam. The ensuing flood of 7.9×10^6 feet per second would crest at about 460 feet above mean sea level in the channel between 200 East Area and Gable Mountain.

4.4 REFERENCES

1. J. L. Liverman, Final Environmental Statement - Waste Management Operations - Hanford Reservation, Richland, Washington, ERDA-1538 United States Energy Research and Development Administration, Washington, D. C. (December 1975).

2. W. A. Stone, D. E. Jenne, and M. J. Thorp, Climatography of the Hanford Area, BNWL-1605, Battelle, Pacific Northwest Laboratories, Richland, Washington (1972) 230 p.

3. W. K. Summers and R. A. Deju, Final Report, A Preliminary Review of the Regional Hydrology of the Hanford Reservation, ARH-C-5, Atlantic Richfield Hanford Company, Richland, Washington (November 1974).

4. W. K. Summers and Associates, A Survey of the Ground-Water Geology and Hydrology of the Pasco Basin, Washington, RHO-BWI-C-41, Rockwell Hanford Operations, Richland, Washington (December 1978).

5. Probable Maximum Precipitation, Northwest States, U. S. Department of Commerce, Environmental Science Service Administration, Weather Bureau, Hydro-Meteorological Report No. 43., Washington, D. C. (November 1966).

6. Evaluation of Impact of Potential Flooding Criteria on the Hanford Project, RL-76-4, The U. S. Department of Energy-Richland Operations Office, Richland, Washington (1976).

5.0 SUBSURFACE HYDROLOGY

5.1 GENERAL

The Pasco Basin is only a part of the area covered by Columbia River Basalt (Figure 2.1). Located in south-central Washington, the Pasco Basin extends southward to near the Washington-Oregon border. It entirely encompasses the Hanford Site. Its boundary crosses the Columbia River just south of Lake Wallula and the Snake River, and just north of Sentinel Gap near the Saddle Mountains.

The Pasco Basin lies completely within the Columbia River Basalt Plateau which extends westward almost to Portland, Oregon; eastward into Idaho; southward to central Oregon; and northward to northern Washington.

The Pasco Basin, being a subset of the Columbia River Basin (Figure 4.1) includes a sequence of subsurface systems ranging from localized to intermediate to regional, where the latter two may have their origin outside the Pasco Basin.

5.2 DESCRIPTORS OF THE SUBSURFACE FLOW FIELD

The subsurface flow field of a given area can be characterized by defining: (1) descriptors of the subsurface flow system; (2) measuring the basic hydraulic properties; and (3) establishing reference fluid characteristics (Table 5.1). The basic descriptors of the fluid system give the geometric (areal and stratigraphic) and potentiometric (head) variations as a function of time and space. These descriptors will be discussed in this section of the report. Chapter 6.0 of this report discusses the basic hydraulic properties. The fluid characteristics required to model the subsurface hydrology of the Pasco Basin are not affected by the chemistry of the water, inasmuch as the total content of salts in the water is minimal. Thus, the standard values listed in Table 5.1 are appropriate.

5.3 DATA BASE

Much of the data for studying subsurface hydrologic systems come from surveys of the literature and an analysis of existing well records. This study began with the compilation of a bibliography covering reports dealing with the geology and ground water of the basalt both within the Pasco Basin[1] and outside the Pasco Basin, but within the Columbia River Basin with emphasis on the State of Washington.[2] A bibliography of the hydrologic studies on the overlying sediment was previously reported.[3]

Data from existing wells were compiled as part of our hydrologic base line studies. About 800 wells that penetrate basalt in the Pasco Basin have been identified and their base line information has been compiled into standard forms.[4] Of these wells, 268 have been drilled in basalts deeper than the

TABLE 5.1

GENERAL DATA REQUIREMENTS TO
DESCRIBE THE SUBSURFACE FLOW FIELD

DESCRIPTORS OF THE SUBSURFACE FLOW SYSTEM	HYDRAULIC PROPERTIES
1. Recharge and discharge locations and rates	1. Hydraulic Conductivity
2. Time-varying potentials along the boundaries of the system	2. Porosity
3. Geometric description of aquifer boundaries	3. Storage coefficient
4. Initial potential distribution	**FLUID PROPERTIES**
5. Soil moisture characteristics*	1. Density ρ = 1 gm/cm^3
	2. Compressibility $c = 1.45 \times 10^{-5}$ cm·sec^2/g
	3. Viscosity μ = 1 centipoise

*Only in the vadose zone.

Mabton interbed or its equivalent. Their data have been compiled in a separate report.[5] Data from selected wells within the Hanford Site not penetrating the basalts but bottoming out in the overlying sediment were also compiled.[6] These data include the description and summary logs of cuttings sampled from 114 wells within the Hanford Site.[7]

5.4 OVERALL CONCEPTUAL SYSTEM

Using the aforementioned data base, one can develop a concept for the flow systems underlying the Pasco Basin. Overall, we envision a series of systems ranging from regional to local that extends from the water table of the upper sediments to depths of several thousands of feet. Figure 5.1 depicts these flow systems in a cross section through the Pasco Basin.

Our conceptualization makes evidence of the following points.

- A regional flow system carries water (recharged, perhaps as far away as the Okanogan Highlands to the north or the Rocky Mountains to the east) that underflows the Pasco Basin and discharges downstream--perhaps to the Columbia River or directly to the Pacific Ocean. By the time the water reaches the Pasco Basin area, it is very very old, because it is moving under a very small hydraulic gradient within basalt flows of low hydraulic conductivity.

- Ground water also moves through intermediate flow systems that are recharged in regions beyond the Pasco Basin; conceivably, a flow system that has its origin in the Cascade Range underflowing the local flow systems and overflowing the regional system. There definitely exists an intermediate system that brings water from the eastern part of the Columbia River Basalt Plateau. These intermediate flow systems carry some of the water discharged to the Columbia River within the Pasco Basin.

- Local flow systems discharge water to local springs and streams as well as to the Columbia River. This water is very young and has its origins in recharge areas in the basin, such as Rattlesnake Hills and Saddle Mountains. These systems carry the bulk of the water discharged to the Columbia River within the Pasco Basin.

Within the Hanford Site, water table data show that two small local systems (Figure 5.2) resulting from waste management operations overlie the local system. These superimposed systems do not interact with the basin's local system except through their common boundary.

In the Pasco Basin, the local system appears to correspond to the unconfined aquifer in the overlying sediments. The intermediate flow system is really a collection of confined aquifers corresponding to flow tops and interbeds of the uppermost basalts. Some of these are interconnected in places, although the vertical hydraulic conductivity of most basalt is probably very small. As we progress downward in the section, the flow paths become longer and the intermediate flow systems can then truly be termed regional. Figure 5.3 summarizes the hydrostratigraphic relations in the Pasco Basin.

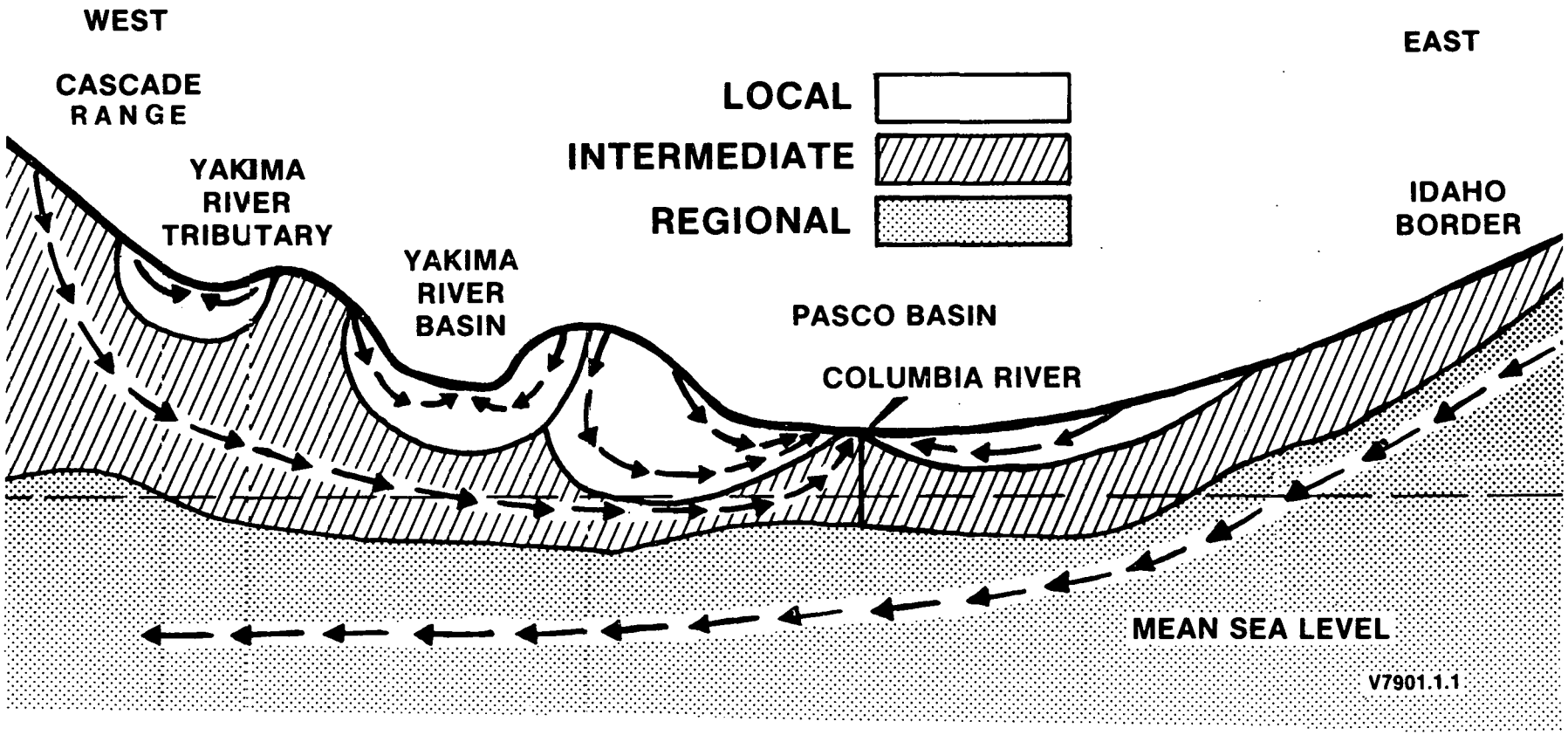

FIGURE 5.1

CONCEPTUAL SUBSURFACE FLOW SYSTEMS IN THE PASCO BASIN

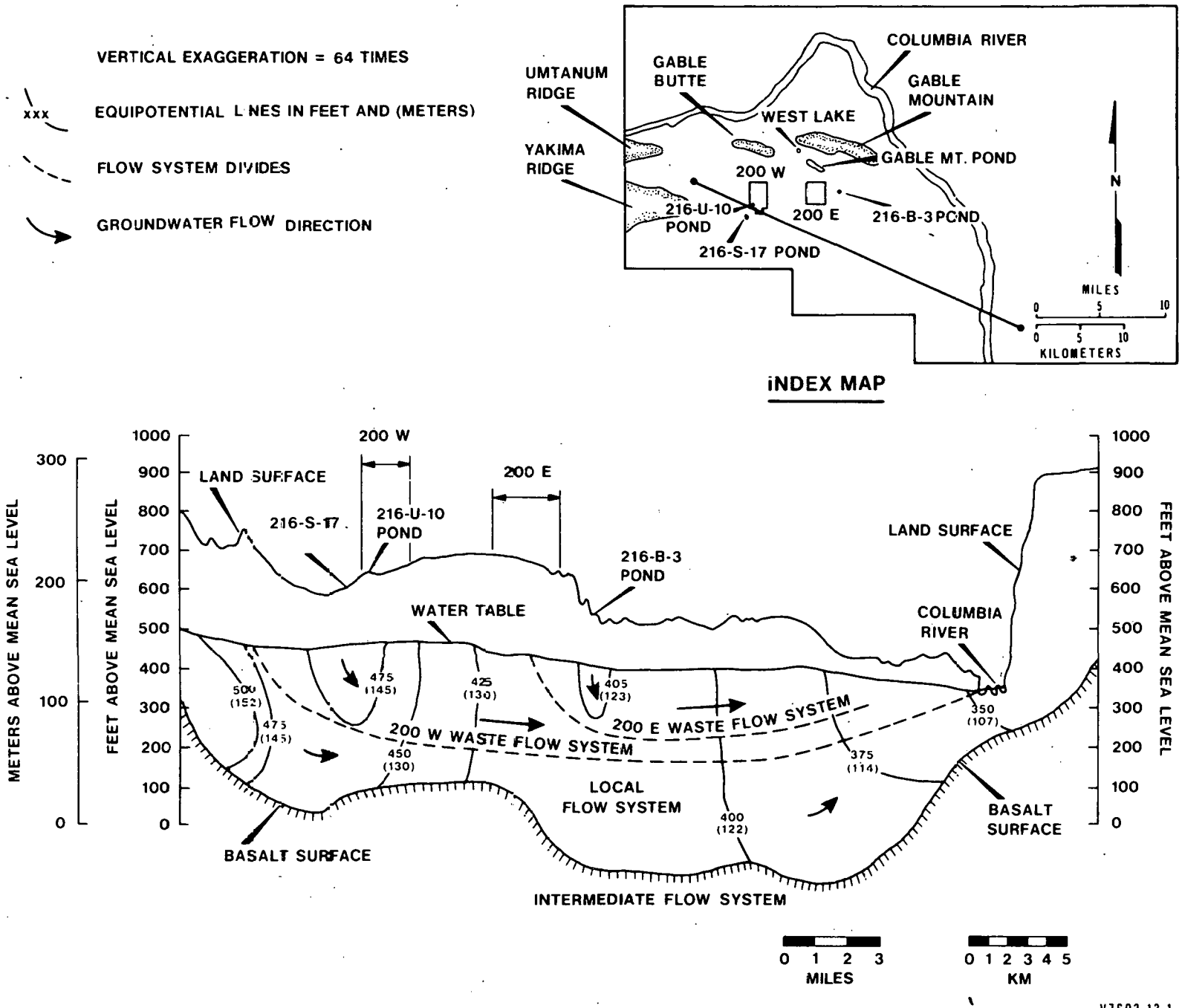

FIGURE 5.2

HANFORD SITE UPPER FLOW SYSTEMS

GEOLOGIC TIME SCALE			GEOLOGIC CHARACTERISTICS					HYDROGEOLOGY	
ERA	PERIOD	EPOCH	RADIOGENIC DATE YEARS B.P.	STRATIGRAPHIC	BED OR FLOW UNIT	LITHOLOGIC CHARACTER	THICKNESS IN METERS	HYDROLOGIC CHARACTER	AQUIFER
CENOZOIC	QUATERNARY	HOLOCENE	6,600	ALLUVIUM COLLUVIUM & EOLIAN SEDIMENTS		SANDS, SILTS, GRAVELS & CLAYS MODIFIED BY WIND EROSION	DUNES TO 20	OCCUR EVERYWHERE ABOVE THE WATER TABLE	DRY
					MAZAMA ASH	ASH FALL, CRATER LAKE, OREGON	.2-.3		
			← 10,000						
		PLEISTOCENE	12,500		GLACIER PEAK ASH	ASH FALL, GLACIER PEAK, WASHINGTON	.06		
			> 12,000 < 18,000		ST. HELENS ASH	ASH FALL, MT. ST. HELENS, WASHINGTON	.05		
				GLACIOFLUVIATILE SANDS & GRAVELS (HANFORD FORMATION)	TOUCHET SILTS	FINE-GRAINED FACIES OF THE GLACIOFLUVIATILE DEPOSITS. BEDDED IN QUIET WATER		OCCUR ABOVE THE WATER TABLE EXCEPT BETWEEN THE HIGH TERRACE PLATEAUS & THE COLUMBIA RIVER HAS VERY HIGH TRANSMISSIVITY & STORAGE	OCCASIONALLY AN UNCONFINED AQUIFER OR DRY
			40,000		PASCO GRAVELS	PREDOMINANTLY COARSE GRAINED GRAVELS. COBBLES & SANDS WITH CUT & FILL STRUCTURE	0-120		
					FALOUSE SOIL	CALCAREOUS SAND & SILT EOLIAN DEPOSIT, MAINLY DERIVED FROM RINGOLD FORMATION	0-25	OCCUR EVERYWHERE ABOVE THE WATER TABLE	DRY
				RINGOLD FORMATION	UPPER RINGOLD	LOCALLY CAPPED BY CALICHE. MOSTLY WELL-BEDDED FLUVIAL SILTS & SANDS WITH SOME GRAVELS	0-125	SANDS & GRAVEL BEDS HAVE VERY HIGH HYDRAULIC CONDUCTIVITY & STORAGE SOME BEDS OF SILTY CLAY OR CLAY ARE ESSENTIALLY IMPERMEABLE	UNCONFINED AQUIFER
					MIDDLE RINGOLD	SANDS & GRAVELS WELL SORTED COMPACT BUT VARIABLY CEMENTED	0-120		
			← 1,000,000						AQUICLUDE
	TERTIARY	PLIOCENE	15,000,000		LOWER RINGOLD	SILTS & CLAYS WITH INTERBEDDED GRAVELS & SANDS CLAY IS CHARACTERISTICALLY BLUE BUT MAY BE GREEN, BROWN OR TAN	0-125		CONFINED SYSTEMS: AQUIFER
			← 11,000,000	COLUMBIA RIVER BASALT GROUP	SADDLE MOUNTAINS AND WANAPUM BASALT	BASALT FLOWS AND INTERBEDS TUFF & TUFFACEOUS SANDSTONE	0-700	FLOWS ARE DENSE. VERTICAL HYDRAULIC CONDUCTIVITY IN THE FLOW IS LOW. HORIZONTAL HYDRAULIC CONDUCTIVITY & TRANSMISSIVITY OF INTERBEDDED SEDIMENTS IS LOW	CONFINED SYSTEMS: AQUITARD
		MIOCENE	15,000,000		VANTAGE SANDSTONE	WEAKLY CEMENTED SANDSTONE	0-10		CONFINED SYSTEMS: AQUIFER
					GRANDE RONDE BASALT	BASALT FLOWS & INTERBEDS	0-500		CONFINED SYSTEMS: AQUITARD
									CONFINED SYSTEMS: AQUIFER

V7611-10.6

FIGURE 5.3

HYDROGEOLOGIC CHARACTERISTICS OF THE PASCO BASIN

5.5 RECHARGE AND DISCHARGE

Recharge and discharge areas and rates for the local flow system (unconfined aquifer) in the Pasco Basin are better understood than for any of the deeper systems. Recharge and discharge to this system clearly occur within the Pasco Basin itself. Natural recharge to the unconfined system occurs in the Cold Creek and Dry Creek valleys along the margin of Rattlesnake Hills and Yakima Ridge (Figure 5.4). Some recharge also occurs along the Saddle Mountains and Umtanum Ridge. The Yakima River recharges the unconfined aquifer along its reach from Horn Rapids to Richland, Washington. The Columbia River represents a hydraulic discharge boundary for the local flow system. Ground water discharge and bank storage are affected by seasonal river stage fluctuations from one to three miles to either side of the Columbia River. Summers and Deju[8] analyzed the natural recharge and discharge areas in the Pasco Basin and prepared a map showing their location. They also analyzed the extent of synthetic recharge within the Pasco Basin resulting from waste management activities at the Hanford Site (Figure 5.2). The bulk of the synthetic recharge has resulted from disposal operations into five ponds (Figure 4.2), namely: (1) Gable Mountain Pond; (2) B Pond; (3) S Pond; (4) T Pond; and (5) U Pond. The volumes disposed to these ponds are well documented. Summers and Deju[8] calculated the volume contributed to synthetic recharge from these sources.

The major source of natural recharge to the unconfined aquifer is precipitation on Rattlesnake Hills, Yakima Ridge, and Umtanum Ridge which crop out to the south and west of the Pasco Basin. The water percolates under ground near the base of the highlands and moves east northeast.[9] Flow from springs emerging on the flanks of these hills and ridges generally sink into the ground within a mile of the sources.

The average flow of Cold Creek and other infiltration water in that section has been estimated at 72,000 cubic feet per day, of which perhaps half reaches the water table.[10] Estimated recharge from the Dry Creek and Rattlesnake Springs area averages about 36,000 cubic feet per day over the year. Additional recharge may be caused by leakage upward from the underlying confined aquifers along the western boundary of the Pasco Basin. Recent irrigation developments in the Cold Creek Valley could substantially augment the natural recharge from this area.

The natural recharge due to precipitation over the lowlands of the Hanford Site and east of the Columbia River is not measurable. A minor amount occurs where the water table is close to the land surface.[10] The Pasco Basin is in the rain shadow of the Cascade Range with average annual precipitation of 6.3 inches (the higher ridges receive about 12 inches per year). A maximum 24-hour precipitation of 1.94 inches and a maximum monthly precipitation of 3.08 inches have been recorded since 1912.[11] The primary return of rainfall to the atmosphere takes place almost immediately before deep penetration can occur. Drying of the land surface by wind and low-

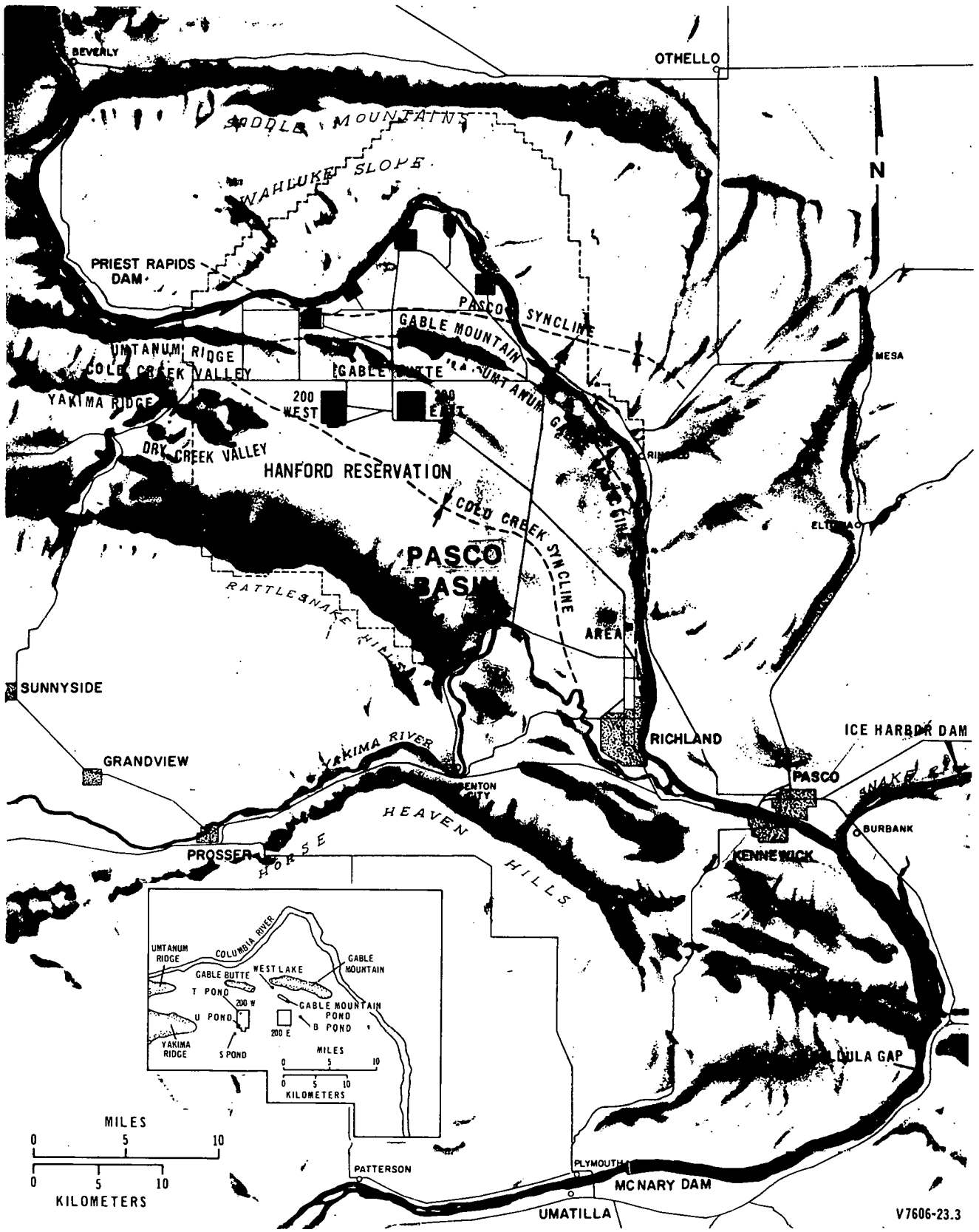

FIGURE 5.4

MAP OF THE PASCO BASIN INCLUDING THE HANFORD SITE

humidity air produces a gradient of water potential toward the surface. The evaporation potential during the summer months greatly exceeds total precipitation. Data on migration from natural precipitation in deep soils (below 30 feet) show movement rates of less than 1/2 inch per year at the one measurement site available.[12-14]

Tanaka, et al.,[15] have studied recharge to the eastern part of the Pasco Basin resulting from land irrigation as part of the Columbia Basin Irrigation Project. Based on numerical simulation, they calculate the natural recharge rate within the Pasco Basin resulting from the irrigation project as .33 inches per year. The bulk of the recharge is to the unconfined aquifer.

Recharge to the intermediate and regional flow systems comes from outside the Pasco Basin, possibly as far away as the Okanogan Highlands to the north, the Rocky Mountains to the east, or the Cascade Range to the west (see Section 5.4). Discharge takes place from infinitesimally slow flowage vertically to more pervious strata and ultimately to the Columbia River at points in the Columbia River between Lake Wallula and the Pacific Ocean.

5.6 GROUND WATER POTENTIALS AND AQUIFER GEOMETRY

5.6.1 The Unconfined Aquifer

The geometry of the local flow system (unconfined aquifer) beneath the Hanford Site is well documented. Flow models of the Hanford Site and the environmental impact statement for Hanford operations clearly define its geometric boundaries.[3]

The top of the unconfined aquifer is the water table (Figure 5.5). The aquifer bottom is either the top of the basalt sequence or silt and clay zones of the Ringold Formation (Figure 5.6). Both the water table map and the unconfined aquifer bottom map have been compiled using hundreds of wells.

The impermeable boundaries of the unconfined aquifers are the Rattlesnake Hills, Yakima Ridge, and Umtanum Ridge on the west and southwest sides of the Pasco Basin and the Saddle Mountains to the north. Gable Mountain and Gable Butte also impede the ground water flow. The Yakima River recharges the unconfined aquifer along its reach from Horn Rapids to Richland. The Columbia River forms a hydraulic potential boundary which is mainly a discharge boundary for the aquifer. However, the ground water flow from 1 to 3 miles inland from the Columbia River is affected by seasonable river stage fluctuations. This river bank storage phenomenon has been reduced by increased control of the river flow by dams upstream of the Hanford Site. The volume of river bank storage under the Hanford Site has been estimated to be from 2×10^9 cubic feet to 3.6×10^9 cubic feet for a typical year.

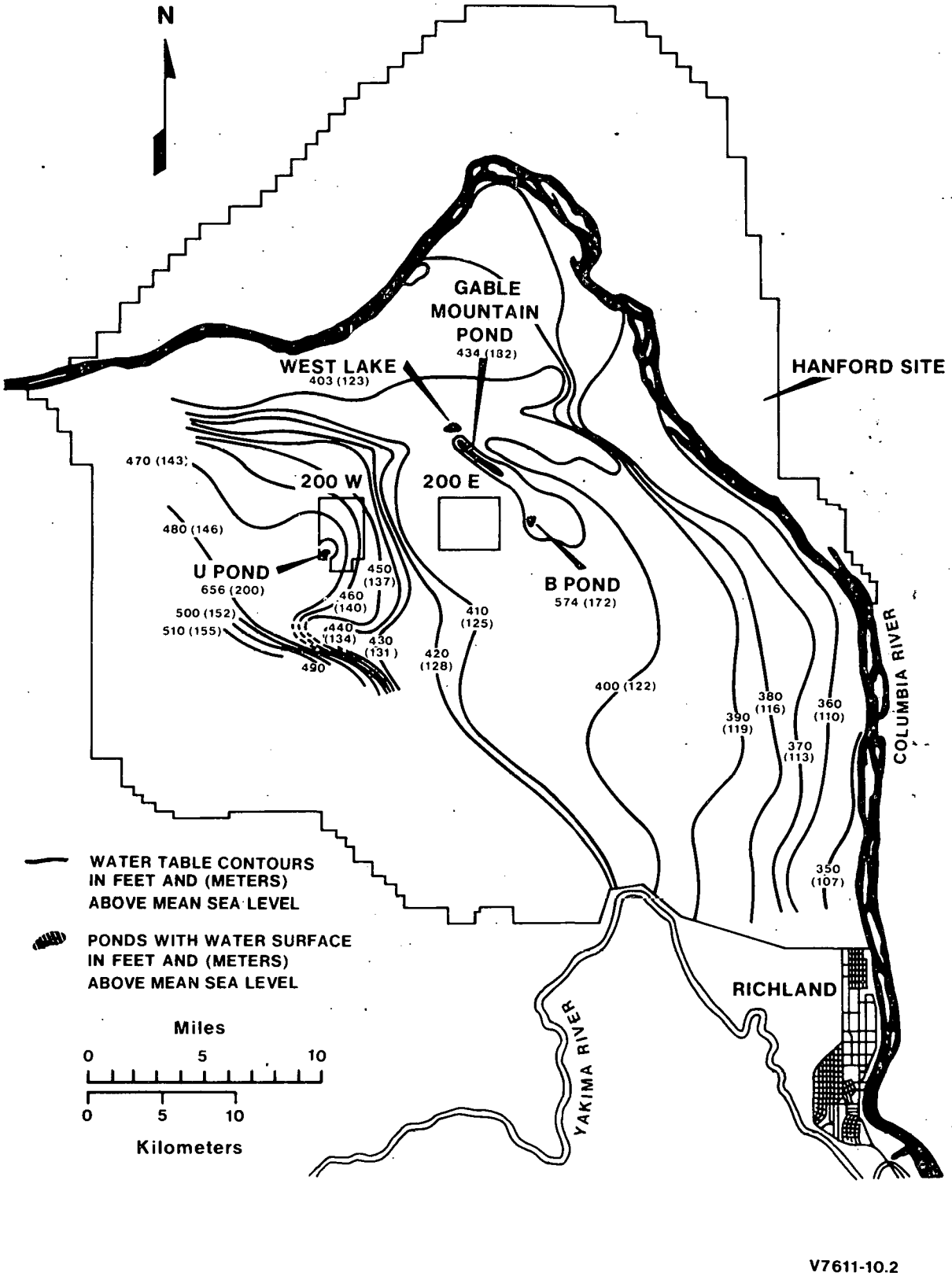

FIGURE 5.5

HANFORD SITE WATER TABLE MAP
DECEMBER 1976

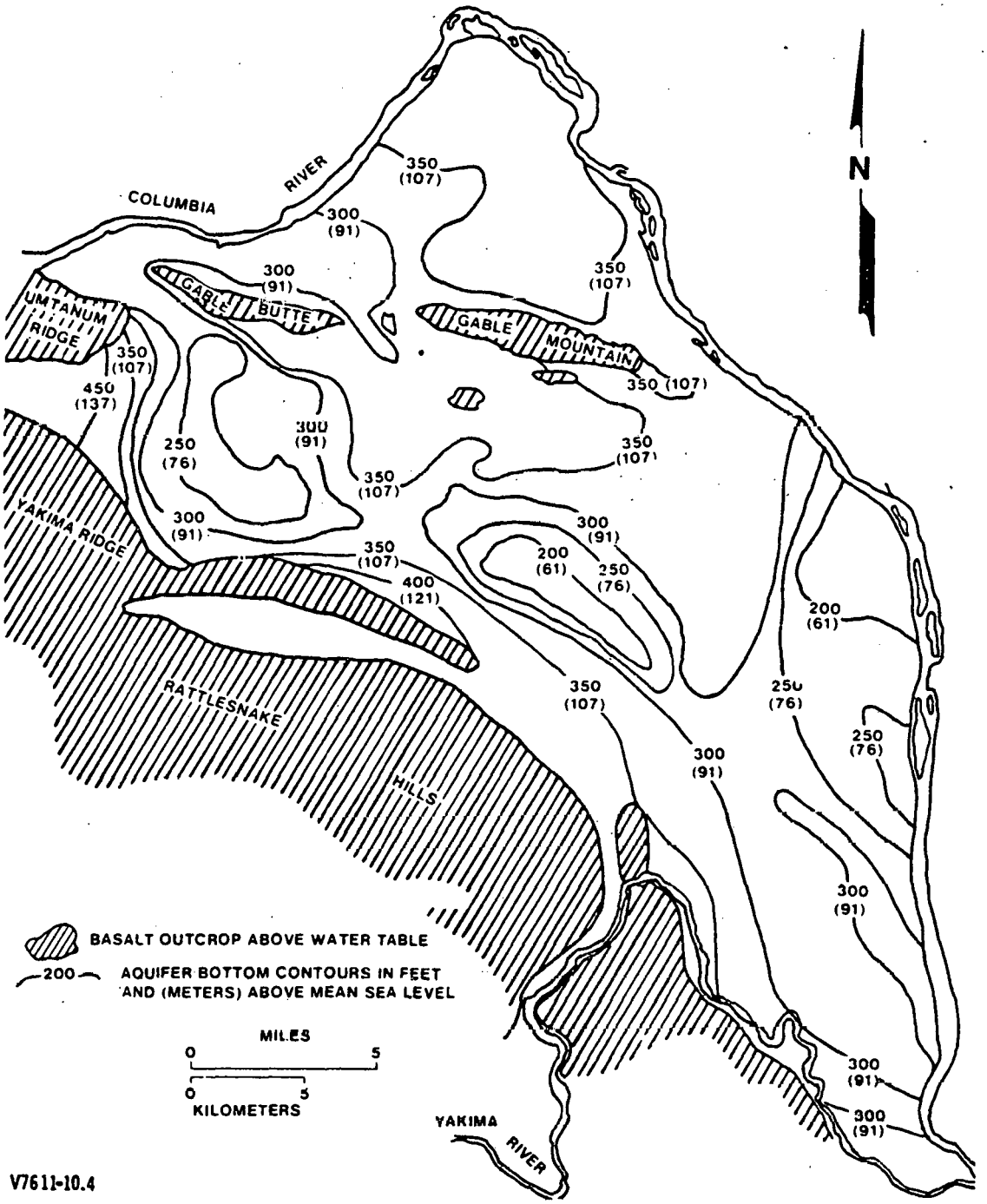

FIGURE 5.6

BOTTOM OF UNCONFINED AQUIFER SYSTEM

The unconfined aquifer under most of the Pasco Basin has a maximum thickness of 230 feet and extends approximately 30 miles north-south and 25 miles east-west at its maximum dimensions. Therefore, this system has a horizontal-to-vertical ratio of from 570:1 to 690:1. The maximum range in potential within this system is from 480 feet to 340 feet elevation. Primarily, horizontal flow within this system has been observed except in the immediate vicinity of recharge areas. Variation of hydraulic potential with depth within the unconfined aquifer has been determined to be negligible except in areas close to recharge sites.

The above reasoning leads to the deduction that the ground water velocity vector is perpendicular to the water table contours and points in the direction of lower hydraulic potential (water table elevation).

5.6.2 The Uppermost Confined Aquifers

The uppermost confined aquifers within the Pasco Basin include: (1) permeable units within the lower member of the Ringold Formation; and (2) sedimentary interbed and interflow contacts within the upper part of the Yakima Basalt Subgroup.

Recharge to the confined aquifers occurs from: (1) precipitation; (2) stream runoff; and/or (3) infiltration from an overlying unconfined aquifer.

Figure 5.7 shows the regional potentiometric surface within the uppermost confined aquifer systems (uppermost intermediate flow system) as defined from available core and piezometric well data. Ground water moves downgradient, perpendicular to equipotential lines, from areas of recharge and discharge ultimately to the Columbia River.

All of the uppermost confined aquifers down to the Mabton equivalent appear to recharge from ridges and plateaus fringing the Pasco Basin and discharge into the Columbia River or south of Pasco near Wallula Gap. It appears probable that the Horse Heaven Hills, an anticlinal ridge at the southern boundary of the Pasco Basin, causes ground water from the uppermost confined aquifers north of these hills to enter the Columbia River north of Wallula Gap.

Figure 5.7 shows the piezometric heads of the lower Ringold, Rattlesnake Ridge, and Mabton as measured in wells throughout the Pasco Basin. Although the data for the lower Ringold are limited to wells very near the Columbia River, it appears that along the banks of the river the lower Ringold aquifer is connected to the overlying unconfined aquifer. The Columbia River probably represents base level drainage for the lower Ringold aquifer.

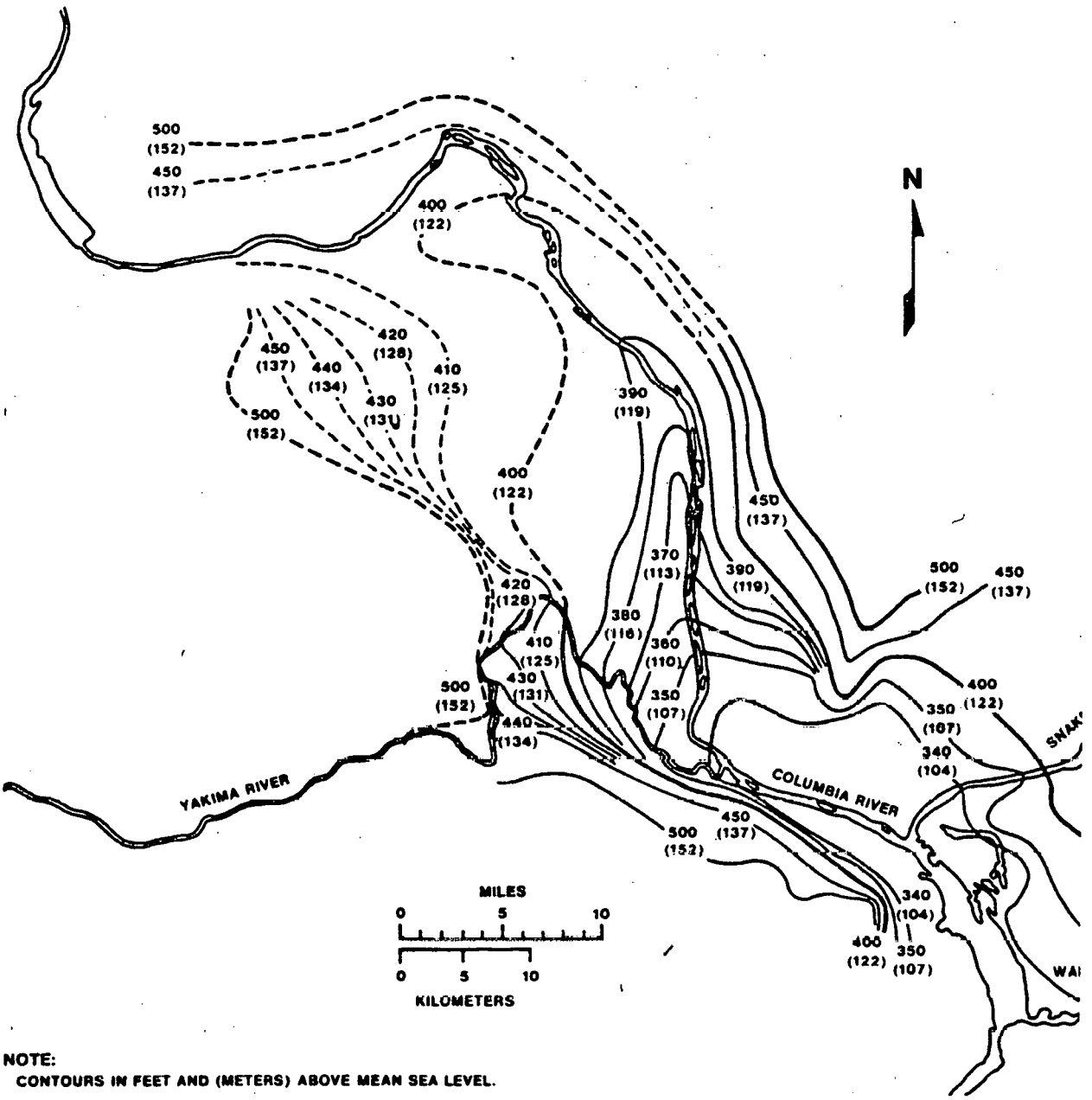

NOTE:
CONTOURS IN FEET AND (METERS) ABOVE MEAN SEA LEVEL.

FIGURE 5.7

PASCO BASIN UPPERMOST CONFINED AQUIFER POTENTIAL MAP

5.6.3 Deep Zones

A limited amount of data is available regarding the distribution of piezometric heads in deeper water-bearing zones within the Pasco Basin. These data come from measurements in Wells RSH-1, DC-1, DC-2, DC-6, and DC-8. Heads have been measured in these wells for various water-bearing intervals from the Saddle Mountains Basalt to basalts and andesites older than the Columbia River Basalt Group. Most measurements, however, were taken in the Grande Ronde sequence. Measurements on rocks older than the Columbia River Basalt Group are only available from Well RSH-1.

Reports of all deep head measurements are contained in Tables 5.2 through 5.6 and have been plotted on Figures 5.8 through 5.12. As the data and figures show, the piezometric head decreases with depth. The figures also show the existence of confining intervals, such as the Umtanum (Figure 5.9), which consistently act as barriers to vertical water flow. Vertical flowage in the deep zones of any of the holes is generally from the upper to the lower zones.

Using Wells DC-1, DC-2, and DC-6, one can note that the general flow system of individual horizons above and below the Umtanum unit show water flow from east to west. This is consistent with the concept postulated in Figure 5.2 for the regional flow system. Additional monitoring wells are needed to fully verify the direction of flow in these deep zones.

Based on measurements taken to date using Wells DC-1, DC-2, and DC-6, the regional westerly gradient is approximately 5 feet per mile. While it is difficult to infer the location of a discharge zone for the deep basalts, one can postulate with reasonable certainty that the direction from these zones to the Columbia River, if any, takes place below, or at the elevation of, Lake Wallula at least 60 miles from the center of the Pasco Basin.

A number of low-circulation zones was encountered during the testing, especially when heads were being measured in flow breccias. These low-circulation zones represent low-pressure horizons.

The decrease of heads with depth appears to continue to the pre-Columbia River Basalt Group rocks, at least as shown from the data at Well RSH-1.

TABLE 5.2

PIEZOMETRIC HEAD DATA
WELL RSH-1

TEST INTERVAL (feet)	INTERVAL DESCRIPTION	PIEZOMETRIC HEAD (feet above + or below - mean sea level)	FORMATION
1,929-2,005	Straddles one flow-top breccia zone, 1,956-1,990	+1,829	Grande Ronde, Sentinel Bluffs sequence
2,614-2,690	Flow-top breccia and 20-30 feet of entablature	+1,954	Grande Ronde, Schwana sequence top of Umtanum unit
3,213-3,289	Straddles flow-top breccia zone, 3,230-3,250	+1,360	Grande Ronde, Schwana sequence
4,119-4,195	Straddles one flow-top breccia zone, 4,152-4,195	+957	Grande Ronde, Schwana sequence
4,832-4,908	Straddles part of a flow-top breccia 4,815-4,850 and includes some intra-flow zones of variable density to 4,908	+999	Possible lowest flow of the Grande Ronde, Schwana sequence
5,921-5,997	Intra-flow zone of variable density	+855	Possible Pre-Columbia River Basalt andesites or basalts
8,275-8,351	Straddles one flow-top breccia zone, 8,300-8,355	-4,691	Possible Pre-Columbia River Basalt andesites or basalts

TABLE 5-3

PIEZOMETRIC HEAD DATA
WELL DC-1

TEST INTERVAL (feet)	INTERVAL DESCRIPTION	PIEZOMETRIC HEAD (feet above + or below - mean sea level)	FORMATION
362-416	Flow entablature or colonnade	+405	Saddle Mountains, Pomona Member
1,130-1,190	Straddles flow-top breccia zone	+400	Wanapum, Roza flow
1,970-2,160	Three thin flows and associated flow-top breccia zones and one thin interbed	+408	Wanapum, lowest Frenchman Springs Vantage Sandstone Grande Ronde, Sentinel Bluffs sequence, 2 thin flows
2,730-2,910	Three flow-top breccia zones, two moderately dense zones	+410	Grande Ronde, Sentinel Bluffs sequence, immediately above the Umtanum
3,360-3,597	Three flow-top breccia zones, three moderately dense zones	+390	Grande Ronde, Schwana sequence 2nd, 3rd, and 4th units below the Umtanum
3,774-3,934	One thin flow-top breccia zone; one thin intraflow low-density zone, rest of interval quite dense	+380	Grande Ronde, Schwana sequence 7 units below the Umtanum
4,080-4,283	Flow-top and intraflow low-density interior of a highly fractured or brecciated flow	+368	Grande Ronde, Schwana sequence 9 units below the Umtanum

TABLE 5.4

PIEZOMETRIC HEAD DATA
WELL DC-2

TEST INTERVAL (feet)	INTERVAL DESCRIPTION	PIEZOMETRIC HEAD (feet above + or below - mean sea level)	FORMATION
2,269-2,299	Dense, intraflow, probable colonnade	+470	Grande Ronde, Sentinel Bluffs sequence
2,340-2,370	Straddles flow-top breccia, 2,349-2,354	+443	Grande Ronde, Sentinel Bluffs sequence
2,626-2,655	Straddles flow-top breccia, 2,627-2,640	+438	Grande Ronde, Sentinel Bluffs sequence
2,795-2,825	Straddles 2 flow-top breccia zones, 2,797-2,810 and 2,818-2,825.	+421	Grande Ronde, Sentinel Bluffs sequence
2,960-2,990	Within flow-top breccia and vesicular zone, 2,958-2,992.	+395	Grande Ronde, Schwana sequence, top of Umtanum unit
3,160-3,190	Straddles flow-top breccia, 3,178-3,188	+377	Grande Ronde, Schwana sequence, top of low K_2O flow below the Umtanum unit
3,243-3,273	In a gradational flow-top contact zone, 3,244-3,300, vesicular and vuggy	+362	Grande Ronde, Schwana sequence, normal low MgO flow

TABLE 5.5

PIEZOMETRIC HEAD DATA
WELL DC-6

TEST INTERVAL (feet)	INTERVAL DESCRIPTION	PIEZOMETRIC HEAD (feet above + or below - mean sea level)	FORMATION
2,240-2,270	Straddles flow-top breccia, 2,263-2,270	+450	Grande Ronde, Sentinel Bluffs sequence
2,400-2,430	Straddles flow-top breccia and vesicular zone, 2,405-2,425	+447	Grande Ronde, Sentinel Bluffs sequence
2,454-2,484	Straddles a fissured flow-top breccia zone, 2,458-2,478, (making water during drilling)	+456	Grande Ronde, Sentinel Bluffs sequence
2,708-2,738	Straddles 2 breccia zones, 2,712-2,718 and 2,727-2,731, lost circulation zone, apparent interconnected vesicles	+423	Grande Ronde, Sentinel Bluffs sequence
2,896-2,936	Straddles 1 tight flow-top breccia zone, 2,903-2,910, with possible connected vugs 2,910-2,936	+454	Grande Ronde, Sentinel Bluffs sequence
3,025-3,055	Straddles a flow-top breccia zone, 3,036-3,054, lost circulation zone, interconnected fissures	+460	Grande Ronde, Schwana sequence, top of Umtanum unit
3,343-3,373	Straddles a flow-top breccia zone, 3,329-3,364 lost circulation zone, large fissures	+443	Grande Ronde, Schwana sequence, 2 flows below Umtanum unit
3,620-3,650	Straddles 3 thin breccia zones, 3,623-3,625, 3,634-3,638, and 3,643-3,648, lost circulation zone	+421	Grande Ronde, Schwana sequence
3,650-3,680	Straddles 1 breccia and vesicular zone, 3,662-3,668	+432	Grande Ronde, Schwana sequence
3,683-3,713	Straddles part of 1 flow-top breccia zone, 3,687-3,800, lost circulation zone, vesicular and highly fissured	+429	Grande Ronde, Schwana sequence
3,692-3,722	Straddles part of 1 flow-top breccia zone, 3,687-3,800, lost circulation zone, vesicular and highly fissured	+432	Grande Ronde, Schwana sequence

TABLE 5.6

PIEZOMETRIC HEAD DATA
WELL DC-8

TEST INTERVAL (feet)	INTERVAL DESCRIPTION	PIEZOMETRIC HEAD (feet above + or below - mean sea level)	FORMATION
1,710-1,740	Straddles an intraflow zone, 1,723-1,737 lost circulation zore, vesicular, vuggy and fracturec	+433	Wanapum, lower Priest Rapids
1,810-1,840	Within a flow-top breccia zone, 1,789-1,836, lost circulation zore, open fissures and interconnected vesicles	+431	Wanapum, top of Roza Member
1,990-2,020	Straddles an interbed, 2,001-2,010	+435	Wanapum, Roza Member, Squaw Creek interbed equivalent upper Frenchman Springs flow
2,033-2,063	Straddles flow-top breccia, 2,034-2,062	+422	Wanapum, Frenchman Springs undifferentiated flow

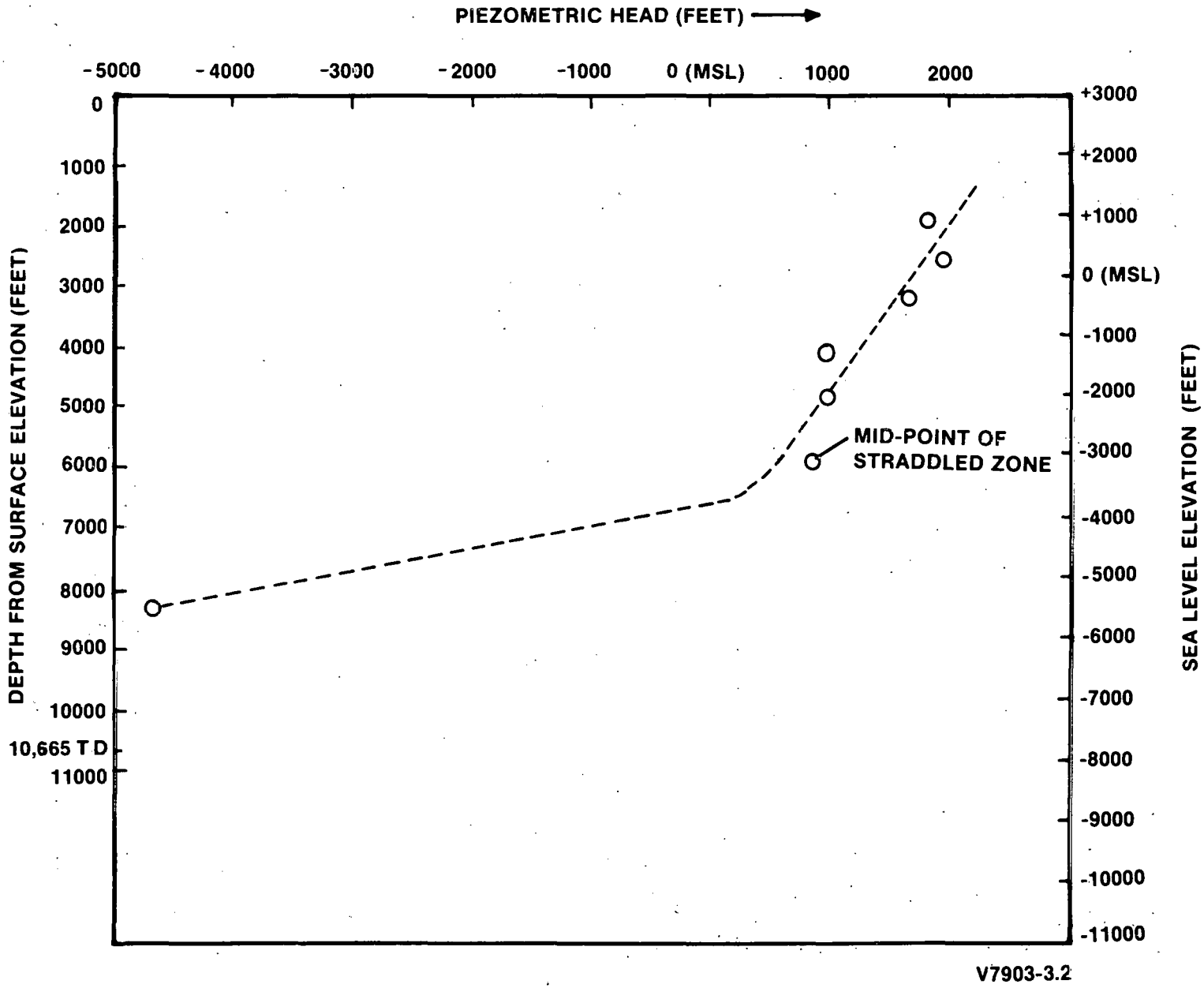

FIGURE 5.8

PIEZOMETRIC HEAD DATA, WELL RSH-1

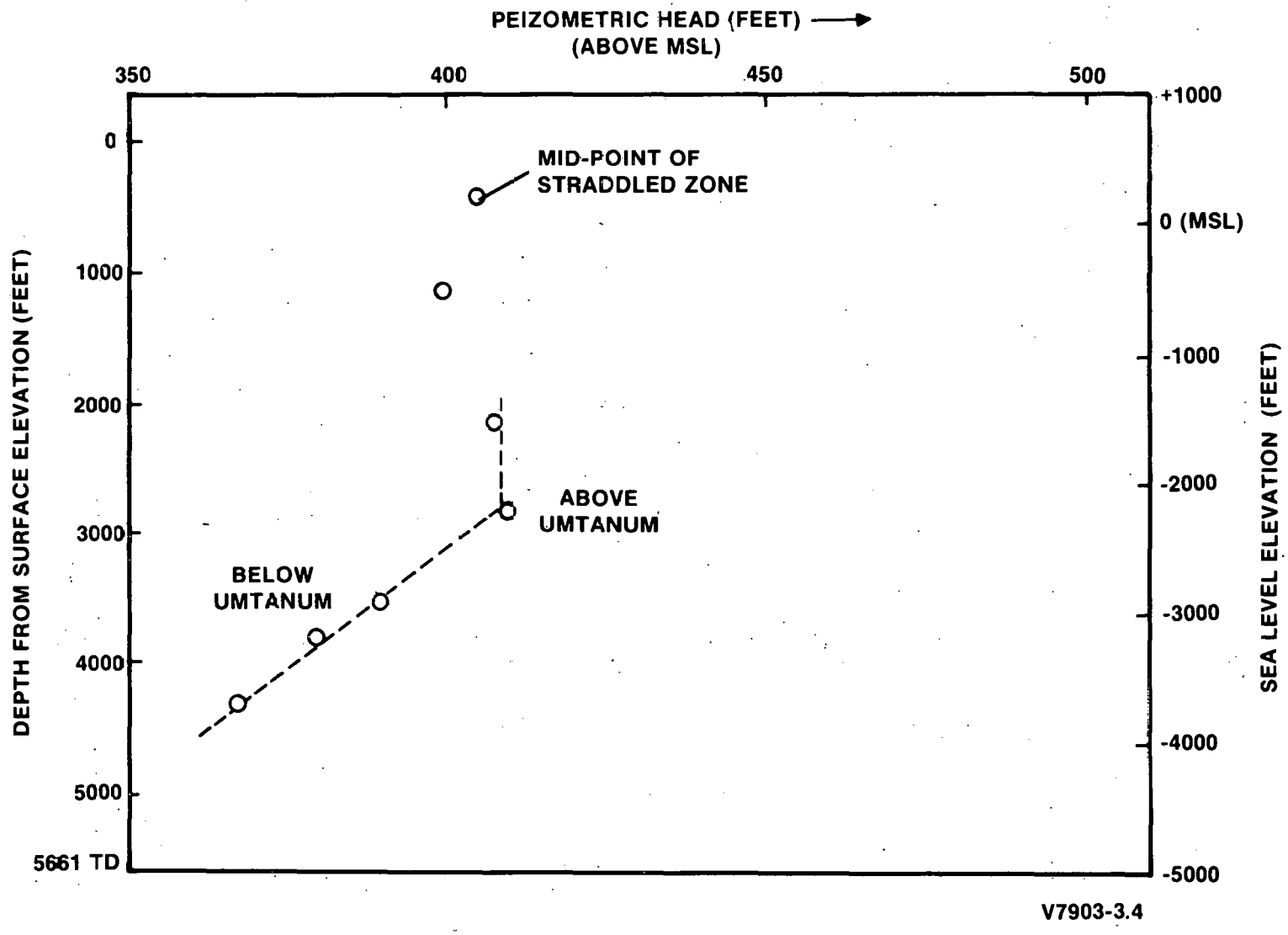

FIGURE 5.9

PIEZOMETRIC HEAD DATA, WELL DC-1

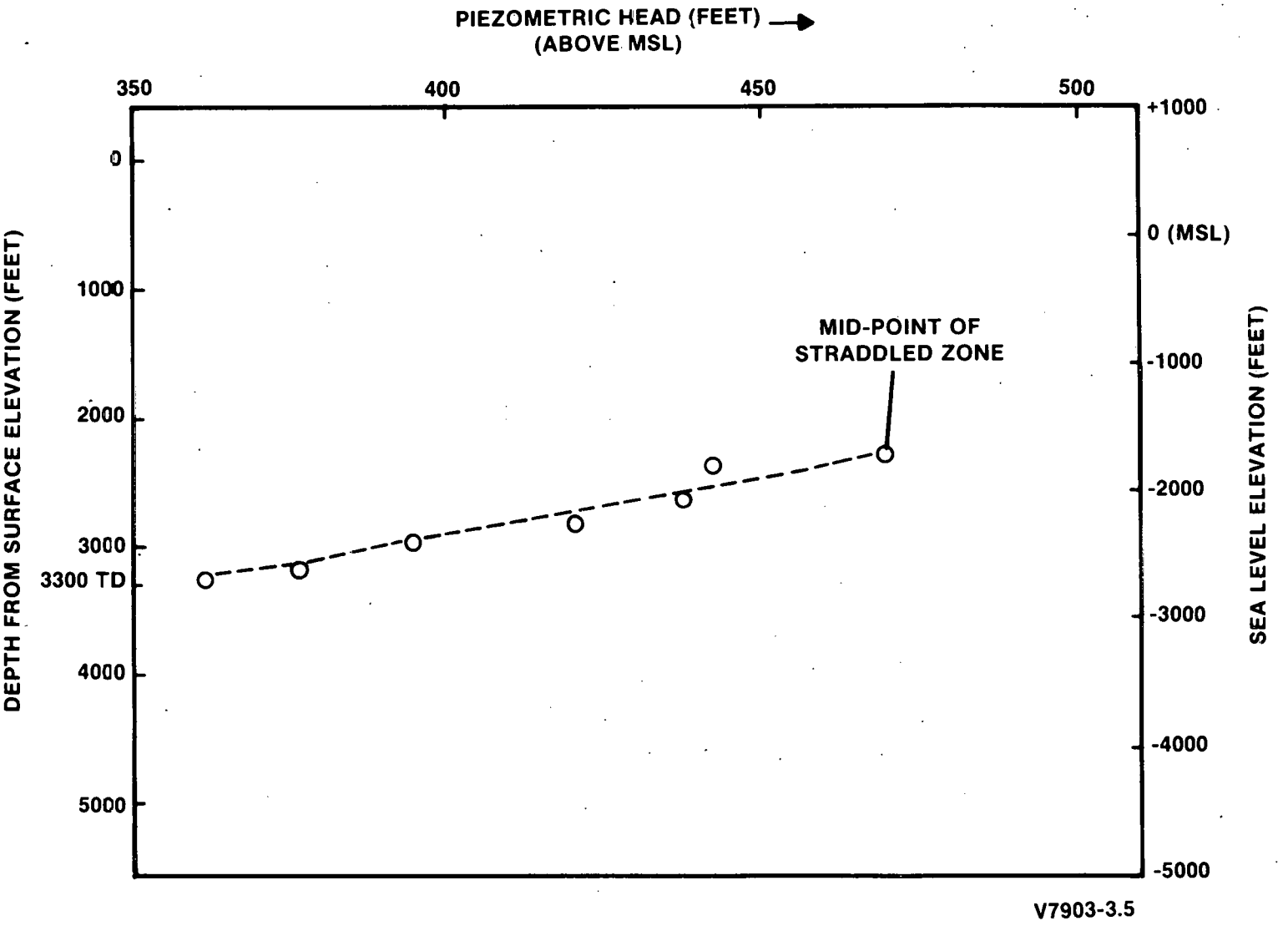

FIGURE 5.10

PIEZOMETRIC HEAD DATA, WELL DC-2

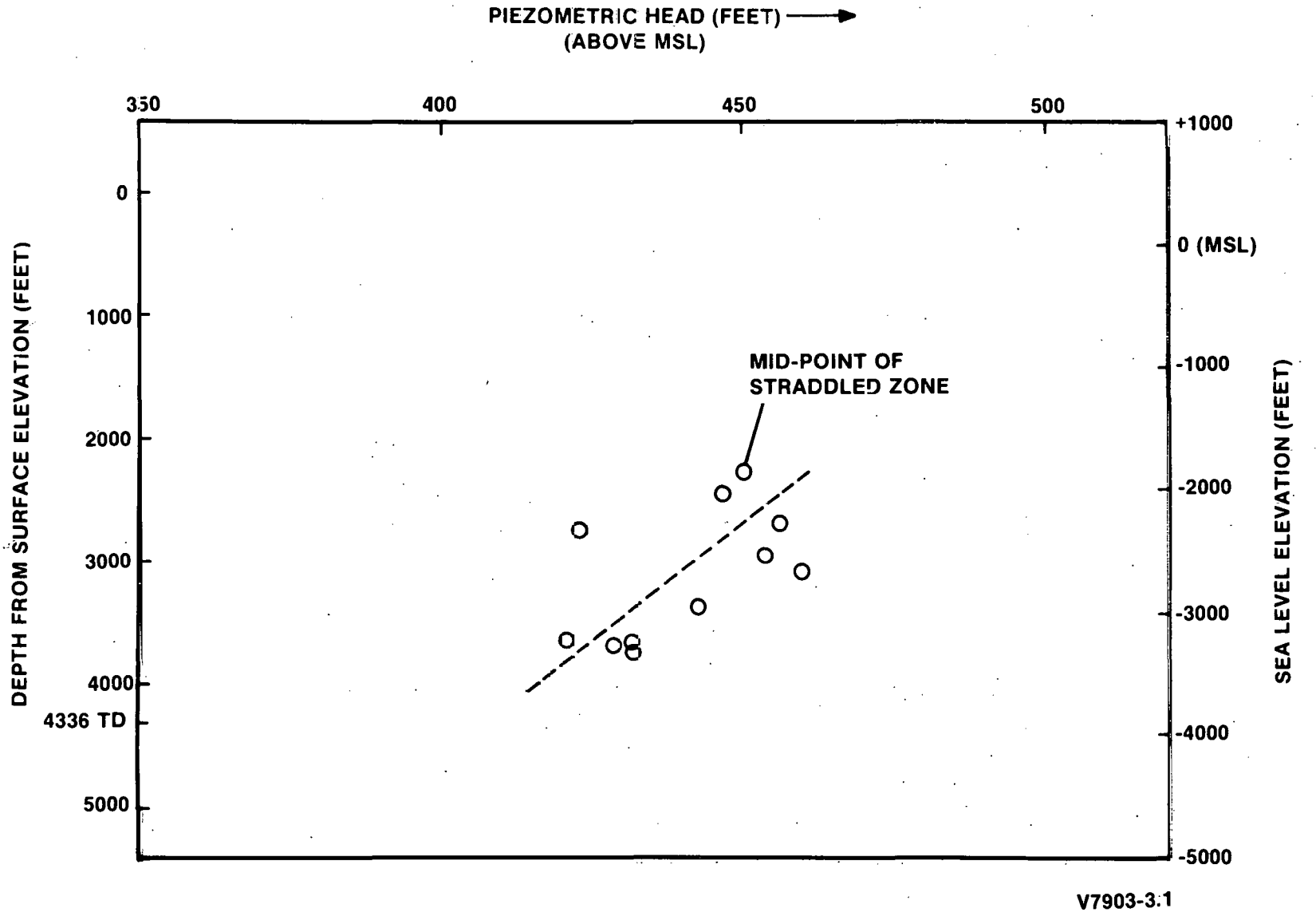

FIGURE 5.11

PIEZOMETRIC HEAD DATA, WELL DC-6

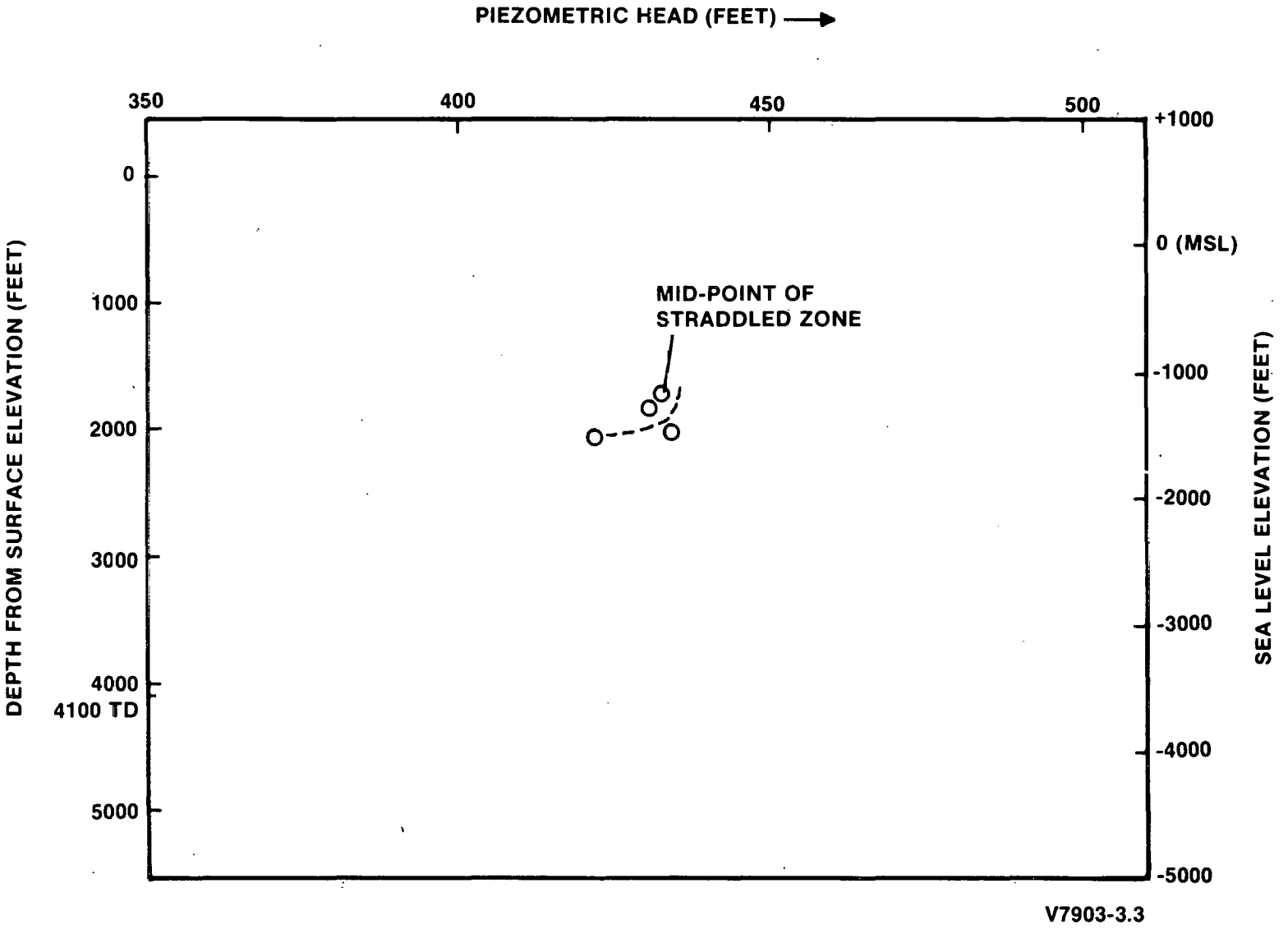

FIGURE 5.12

PIEZOMETRIC HEAD DATA, WELL DC-8

5.7 SOIL MOISTURE IN THE UNSATURATED ZONE

The unsaturated (vadose) zone has been defined by the U. S. Geological Survey's Committee on Redefinition of Ground-Water Terms[16] as:

> "...the zone between the land surface and the water table. Characteristically, this zone contains liquid water under less than atmospheric pressure, and water vapor and air or other gases usually at atmospheric pressure. In parts of this zone, interstices may be temporarily or permanently filled with water. Perched water bodies may exist within the unsaturated zone."

In the Pasco Basin, the thickness of the unsaturated zone varies from one foot to several hundred feet.

The movement of water in the unsaturated zone is influenced by the physical properties of the sediments in two ways: (1) the size and structural arrangement of the sediment particles determines the space configuration through which the water moves; and (2) the interaction between the sediments and the water gives rise to water-moving forces. In sediments where pores are completely filled with water, the fluid is single phase. Where water does not completely fill the pores, the hydraulic potential depends on the gravitational field and on the absorptive forces associated with interfacial boundaries in the sediments. Where air partially fills the soil pores, with water occupying the remaining void space, a two-phase flow can take place. As the percentage of liquid water decreases, it occupies the smallest capillaries that exist between soil particles.

Practically, measurement of the specific retention capacity of sediments is difficult because, under most conditions, water movement in sediments is exceedingly slow and equilibrium can be achieved only after extremely long periods of time. Thus, the specific-retention capacities measured for the sediments in the unsaturated zone represent the equilibrium conditions reached over the past several thousand years. The presence of a desiccated zone at the 30-foot depth in the region of the 200 Areas within the Hanford Site (Figure 4.2) indicates that no moisture is moving downward from the ground surface (at the 200 Areas test site) to the water table.

Several attempts have been made to measure drainage and water retention properties of the Hanford sediments using tension meters or suction plates. Whereas, these techniques are suitable for establishing irrigation and drainage practices for agricultural purposes, the techniques did not provide sufficient sensitivity for measuring moisture transport in sediments which contained about 1.5 percent to 3.0 percent water by weight.

The first major attempt to establish whether or not meteoric water percolates to the water table underlying the 200 Areas involved the use of thermocouple psychrometers. It was proposed that, because water migrates from a high-water potential to a lower potential, the potential gradient; i.e., the slope of the water potential curve versus depth, could be used to establish the direction of water transport as well as the magnitude of the driving force (isothermal condition).

In tests based on natural rainfall conditions, two lysimeters were constructued about one mile south of the 200 East Area. The two lysimeters have a diameter of 10 feet and a depth of 60 feet. The three sets of instrumentation provided for each lysimeter include: (1) a 1.5-inch aluminum alloy tube for use with a Nuclear of Chicago neutron log sensor; (2) a set of thermocouple psychrometers with temperature sensors attached; and (3) a stainless tube for recording pore pressure as a function of time and depth. One lysimeter has an open bottom; the other is closed. The purpose of closing the bottom of one lysimeter is to provide a more complete definition of the column of sediments within it by isolating it from complicating factors such as the effects of changing atmospheric pressures and vapor migration. The closed-bottom lysimeter would serve as a container to collect water if precipitation does indeed percolate to the water table on the 200 Areas plateau. If, on the other hand, evaporation exceeds percolation, the bottom zone of the closed-bottom lysimeter would slowly lose moisture. Thus, as the lysimeter begins to equilibrate, changes in the psychrometer readings and the direction of changes will predict whether or not percolation occurs. The observation has been made with the closed-bottom lysimeter during the 1973-1974 water year that a higher than average rainfall (170 percent of normal) reached a depth of 13 feet and then was removed by summer heat.

Tritium analyses of soil moisture were used to determine the depth of penetration of meteoric precipitation by evaluating tritium distribution from atmospheric fallout versus soil depth. Special sample-handling techniques were used to avoid contamination of soil samples with tritium from the atmosphere. Water was recovered from the soil samples by distillation and the very low tritium concentration in some samples was electrolytically increased by a factor of about 100 to permit more accurate gas counting. The results demonstrate that archaic water exists in virgin soil at depths from 23 feet to the water table. The tritium profiles are considered to be representative of uncontaminated areas of Hanford soils. The tritium concentration decreased exponentially from the surface to a depth of 17 feet and from a depth of 23 feet to the water table, the tritium units are in the range of values associated with archaic water, and water isolated from atmospheric contamination for the past 25 or more years.

In summary, observations to date indicate that the annual precipitation of meteoric water within the Pasco Basin does not percolate to the water table, but apparently moves downward only a few feet during the fall and winter months and is removed by evaporation and evapotranspiration during the summer.

5.8 REFERENCES

1. W. K. Summers and G. E. Schwab, Bibliography of the Geology and Ground Water of the Basalts of the Pasco Basin, Washington, RHO-BWI-C-15, Rockwell Hanford Operations, Richland, Washington (June 1978).

2. H. H. Tanaka and L. Wildrick, Hydrologic Bibliography of the Columbia River Basalts in Washington, RHO-BWI-C-14, Rockwell Hanford Operations, Richland, Washington (July 1978).

3. J. L. Liverman, Final Environmental Statement - Waste Management Operations - Hanford Reservation, Richland, Washington, ERDA-1538 United States Energy Research and Development Administration, Washington, D. C. (December 1975).

References (continued)

4. W. K. Summers and P. A. Weber, Data for Wells Penetrating Basalt in the Pasco Basin Area, Washington, RHO-BWI-C-19, Rockwell Hanford Operations, Richland, Washington (June 1978).

5. W. K. Summers and P. A. Weber, Descriptions of Wells Penetrating the Wanapum Basalt Formation in the Pasco Basin Area, Washington, RHO-BWI-C-22, Rockwell Hanford Operations, Richland, Washington (April 1978).

6. W. K. Summers and G. Schwab, Drillers' Logs of Wells in the Hanford Reservation, ARH-C-16, Atlantic Richfield Hanford Company, Richland, Washington (January 1977).

7. W. K. Summers and R. T. Hanson, Sample Descriptions and Summary Logs of Selected Wells within the Hanford Reservation, ARH-C-00014, Atlantic Richfield Hanford Company, Richland, Washington (January 1977).

8. W. K. Summers and R. A. Deju, Final Report, A Preliminary Review of the Regional Hydrology of the Hanford Reservation, ARH-C-5, Atlantic Richfield Hanford Company, Richland, Washington (November 1974).

9. W. H. Bierschenk, Aquifer Characteristics and Groundwater Movement at Hanford, HW-60601, General Electric Company, Richland, Washington (June 1959).

10. R. E. Newcomb, J. R. Strand, and F. J. Frank, "Geology and Groundwater Characteristics of the Hanford Reservation of the U. S. Atomic Energy Commission Washington," U. S. Geological Survey Professional Paper 717 (1972).

11. W. A. Stone, D. E. Jenne, and J. M. Thorp, Climatography of the Hanford Area, BNWL-1605, Battelle, Pacific Northwest Laboratories, Richland, Washington (June 1972) 230 p.

12. R. E. Isaacson, L. E. Brownell, R. W. Nelson, and E. L. Roetman, Soil Moisture Transport in Arid Site Vadose Zones, ARH-SA-169, Atlantic Richfield Hanford Company, Richland, Washington (January 1974).

13. J.J.C. Hsieh, L. E. Brownell, and A. E. Reisenauer, Lysimeter Experiment, Description, and Progress Report on Neutron Measurements, BNWL-1711, Battelle, Pacific Northwest Laboratories, Richland, Washington (1973).

14. J.J.C. Hsieh, A. E. Reisenauer, and L. E. Brownell, A Study of Soil Water Potential and Temperature in Hanford Soils, BNWL-1712, Battelle, Pacific Northwest Laboratories, Richland, Washington (1973).

15. H. H. Tanaka, A. J. Hansen, and J. A. Skrivan, "Digital-Model of Ground-Water Hydrology, Columbia Basin Irrigation Project Area, Washington," Water-Supply Bulletin 40, Washington State Department of Ecology, Olympia, Washington (1974).

16. "Definitions of Selected Ground-Water Terms, A Report of the Committee on Redefinition of Ground-Water Terms," U. S. Geological Survey Open File Report (August 1970).

6.0 HYDRAULIC PROPERTIES

6.1 GENERAL

The main hydraulic measurements made in ground water evaluations include:

- The hydraulic conductivity;
- The storage coefficient;
- The formation's porosity;
- The radius of influence of the test; and
- The skin factor of the well tested.

The last two parameters give an index of the representativeness of the test.

Other properties can then be calculated from the above parameters. Table 6.1 shows the measurement techniques used to determine the above parameters. Each technique is further discussed in Section 6.2.

TABLE 6.1

MEASUREMENT TECHNIQUES IN HYDRAULIC STUDIES

PARAMETER	MEASUREMENT TECHNIQUES
Hydraulic conductivity*	Pumping tests, drill stem tests, laboratory tests
Storage coefficient	Pumping tests, drill stem tests
Porosity	Calculated from the storage coefficient value or determined in the laboratory
Radius of influence	Pumping tests, drill stem tests
Skin factor	Pumping tests, drill stem tests

*Although hydraulic conductivity is really a tensor property, values measured in this study refer to horizontal hydraulic conductivity unless otherwise noted.

6.1.1 Hydraulic Conductivity

The hydraulic conductivity is a parameter quantifying the ability of a given stratum to conduct water through it under hydraulic gradients. It is a property dependent on both the moving fluid and the rock formation. The transmissivity of a formation, in turn, defines the overall ability of a water-bearing formation to transmit water. Transmissivity values are obtained by multiplying the hydraulic conductivity of a given stratum by its thickness.

6.1.2 Storage Coefficient

The storage coefficient is defined as the volume of water that an aquifer releases from or takes into storage per unit surface area of aquifer per unit change in the component of head normal to that surface.[1]

6.1.3 Porosity

In simple terms, the porosity of a formation is a measure of the interstices contained within the formation. Whenever the term effective porosity is used, it refers to a measure of connected interstices capable of transmitting water.

6.1.4 Radius of Influence

The radius of influence is a reasonable indication of the distance from the borehole that the formation was stressed during a well test. Generally, the greater the formation's hydraulic conductivity and the lower its effective porosity, the larger will be the radius of influence.

Several equations are available for estimating a test's radius of influence (r_i).[2-5] The equation used in this report is:[3]

$$r_i = \sqrt{\frac{4kt}{\Theta \mu c}} \qquad (6\text{-}1)$$

where

k = permeability (square centimeters)

t = test duration (seconds)

Θ = porosity (dimensionless)

μ = fluid viscosity (1 centipoise)

c = fluid compressibility (1.45×10^{-5} centimeter-square second per gram).

6.1.5 Skin Factor

This factor is an index for examining the pressure effect of a zone of different permeability immediately adjacent to the borehole. This alteration of near-field permeability (the skin) commonly results from pluggage of rock pore space by drilling fluids. Pressure tests conducted across such a zone would show artificially lower or higher permeability values depending upon the permeability of the host rock.

The skin factor has been quantitatively defined as:[6]

$$s = \frac{\Delta P \text{ (skin)}}{Q\mu/2\pi\ kh} \qquad (6\text{-}2)$$

where

ΔP = pressure drop across skin (feet per log cycle)

s = skin factor (dimensionless)

Q = production (barrels per day)

μ = viscosity (1 centipoise)

kh = transmissivity (millidarcy feet).

To calculate "s," it is necessary to measure the well pressure both before and after a test. The radius (r_s) of the skin zone around the well and the permability (k_s) in this zone are related to the skin factor as shown by the equation:[7]

$$s = \left(\frac{k}{k_s} - 1\right) \ln \frac{r_s}{r_w} \qquad (6\text{-}3)$$

where

r_s = radius of skin (feet).

r_w = well radius (feet).

If the permeability in the skin zone (k_s) is less than the rest of the rock formation, "s" will be positive. If the permeabilities are equal ($k = k_s$), the skin factor is zero. Finally, if the skin permeability is greater than that in the formation, "s" will be negative.

6.2 TESTING AND ANALYSIS TECHNIQUES

Hydraulic properties are either determined in situ using a variety of well tests or in the laboratory via well-established procedures. Laboratory tests on samples generally yield results which are quite different from well tests on the same strata. This difference is caused by the repacking of the sample and the sizable scale difference between the laboratory sample and the overall aquifer. In this section, we will describe the techniques that have been utilized in tests within the area of study.

6.2.1 Pumping Tests

The simplest of well tests consists of pumping a well and measuring changes in ground water drawdown as a function of time. These tests permit a determination of both the hydraulic conductivity and the storage coefficient. A number of procedures can be followed for testing and analyzing pumping tests.[8] All of these techniques require a knowledge of the physical characteristics of the well bore and a determination of the water level changes in the pumping well and in observation wells nearby as a known discharge is pumped from a preselected horizon. If water level measurements are only taken at the pumping well face, an accurate determination of the storage coefficient is not possible. In addition to measuring the water level lowering as a function of pumping a volume from a well bore, one usually measures the water level increase in the well bore subsequent to the end of pumpage. Measurements of water level data during this recovery period are usually more reliable since one is not disturbed by pump effects.

Pumping tests have been used almost exclusively to test the uppermost water-bearing zones, generally to depths not exceeding 1,000 feet, within the area of study. These tests, however, are not suitable for low-hydraulic conductivity horizons, such as the deep basalt interiors.

Analyses of pumping tests can be conducted using numerous well-documented techniques. Results of tests within the upper aquifers underneath the Hanford Site have been interpreted using the Deju-modified Jacob method for pump testing a well partially penetrating an unconfined aquifer.[8] The Boulton method[8] has also been used to interpret these tests. Other researchers conducting pumping tests in the Columbia Plateau have used the Theis, Hvorslev, and other methods.[9] Results from the various methods are comparable.

6.2.2 Drill Stem Tests

A drill stem test is a technique for evaluating the pressure response of a rock stratum to fluid injection or withdrawal. The results yield information about the hydraulic conductivity, storage coefficient, and other properties of the formation. These tests have been used in the deep basalts and interbeds. The test begins by lowering a package of "tools" into the borehole at the end of a tubing string. The tools consist

of packers, pressure recorders, spacing pipe, and mechanical locking devices (Figure 6.1). The packers used in the basalts are generally made of expandable rubber which are inflated to seal off and isolate the specific formation zones tested. By opening and closing various tool ports, the formation's fluid pressure is relieved by allowing fluid to flow into the drill pipe. For an injection test, the port openings allow fluid pressure to be applied against the formation. The recorders show the initial pressure buildup and then its decay into the formation. Withdrawal tests result in pressure release from the formation.

During the drill stem test, pressure records are normally obtained from three pressure recorders in the borehole. Each recorder monitors a separate borehole interval.

Figure 6.2 shows a typical pressure response recorded for a drill stem test during a single flow period. This response typifies the sequence of operations from tool installation to retrieval. Pressure increases from bottom to top and time increases from left to right. Beginning at point A, the pressure increases as the equipment is lowered into the borehole. The vibrations from A to B (and also F to G) represent movements of the recorder's stylus as the tools are lowered or raised and indicate the stylus is free and responding to pressure changes. The horizontal line at B gives the initial fluid pressure when the packer assembly is positioned opposite the desired rock formation. At C, the packers have been set and the test valve opened. Pressure drops as the fluid pressure within the tool equalizes with the formation pressure. Line C-D gives the initial flow period. At D, the test valve is closed and the formation pressure is allowed to freely build up to its hydrostatic pressure. Line D-E is the test's shut-in period. This pressure buildup provides data about the hydrologic properties of the rocks tested. The drill pipe is raised and rotated at E, unloading the hydrostatic pressure that had developed across the packed-off formation. The final hydrostatic pressure is read at F and, from F to G, the tools are being raised from the borehole.

The calculation of formation characteristics from drill stem test data is based upon the simplified equations for liquid systems.[10] The following assumptions are made concerning the formations tested and their entrained fluids:

- The flow obeys Darcy's law and its pattern is radial in influence;
- The reservoir is homogeneous, isotropic, horizontal, uniformly thick, and has infinite areal extent;
- The production or injection rate is constant; and
- The compressibility and absolute viscosity of the entrained fluid is reasonably constant over the working range of pressures and temperatures.

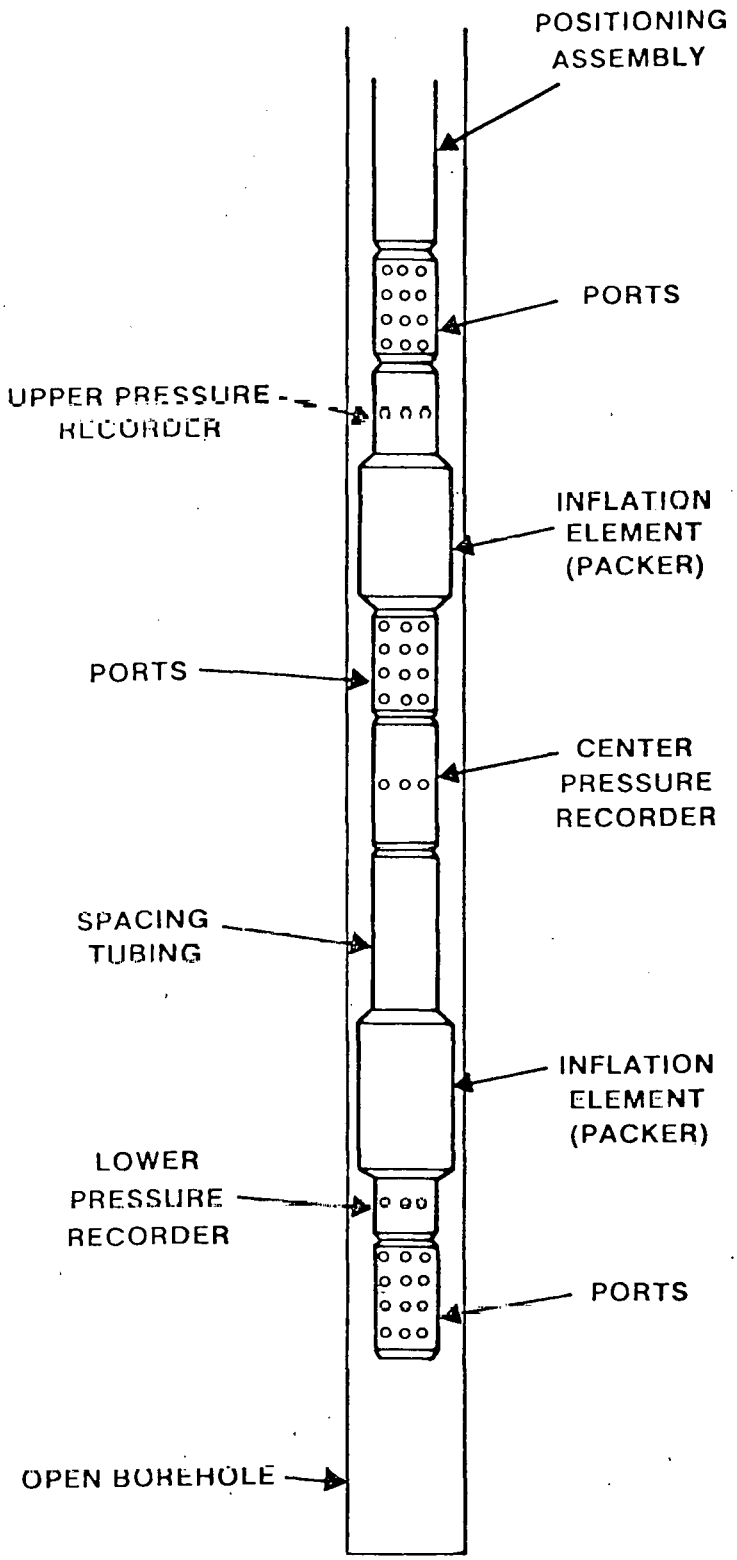

FIGURE 6.1

V7812-1.10

GENERALIZED DIAGRAM OF DRILL STEM EQUIPMENT

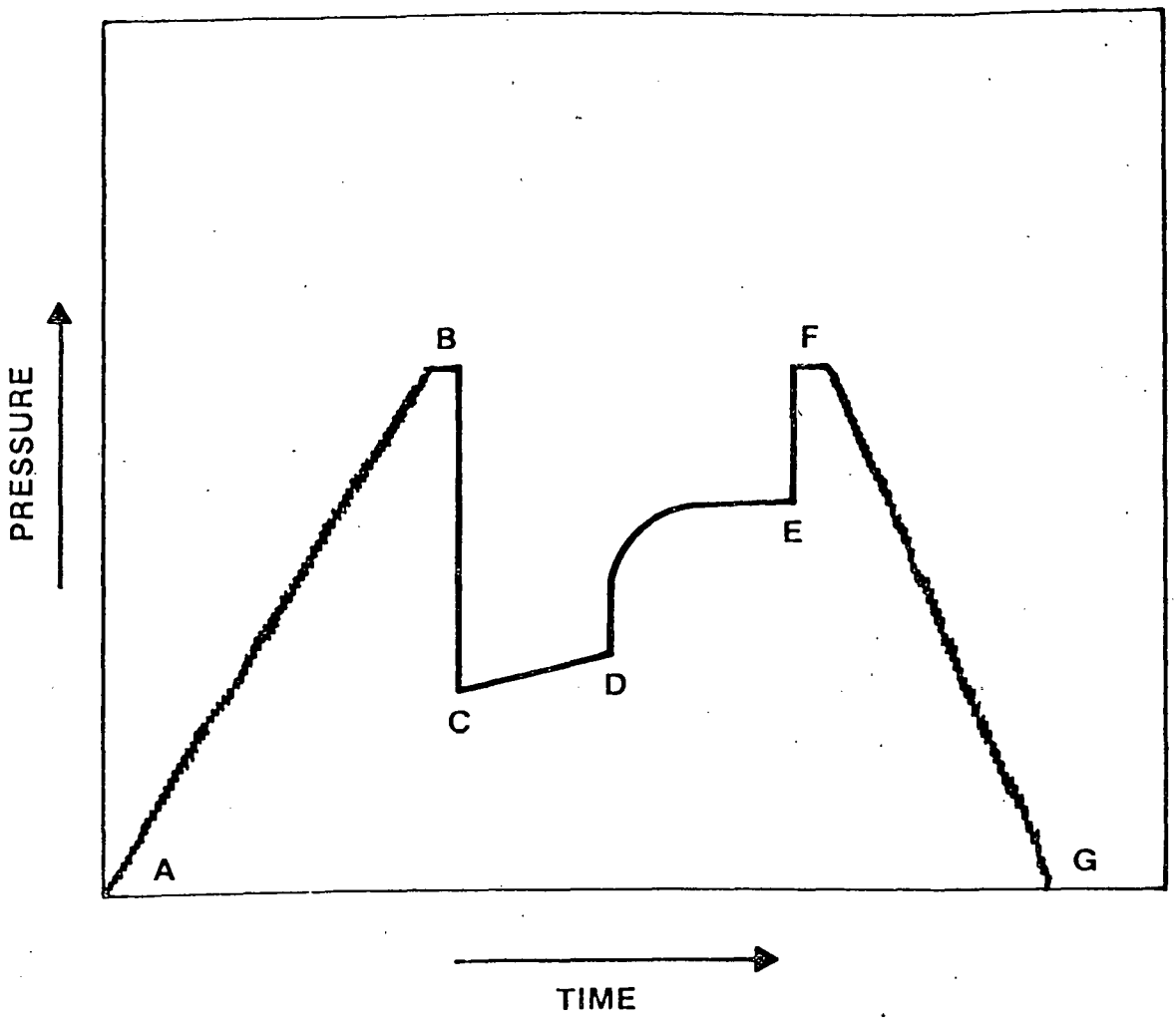

FIGURE 6.2

DRILL STEM PRESSURE RESPONSE FOR SINGLE FLOW PERIOD

Any variation from these assumptions will cause a deviation from an otherwise straight-line plot of the borehole pressure versus the time ratio $(t + \Delta t)/\Delta t$ as plotted on semi-logarithmic paper (t equals time of production or injection rate and Δt is the shut-in period).

A number of papers have been written discussing the interpretation of pressure buildup and decay curves. These pressure curves are read in time segments (t) and at their corresponding borehole pressures. These data are then plotted on semi-logarithmic paper in pounds per square inch versus the log of $(t + \Delta t)/\Delta t$. The slope (m) of the buildup curve is found as the difference of pressure over one log cycle. Basically, the data interpretation consists of calculating the fluid production rate by computing the number of barrels per day production of fluid using the pressure changes that take place during drill pipe fill up.

In addition to the measurement of hydraulic conductivity, one can also calculate the test radius of influence, the skin factor, and the storage coefficient. Values of the storage coefficient were calculated for this report using the curve-matching technique of Papadopulous, et al.[11]

6.2.3 Laboratory Studies

Laboratory studies on determination of porosity and hydraulic conductivity are included in this report. The hydraulic conductivity determination is made by measuring the permeability of a rock sample in a standard permeameter[1] and calculating the hydraulic conductivity using the equation:

$$K = \frac{k\rho g}{\mu} \qquad (6\text{-}4)$$

where

K = hydraulic conductivity

k = permeability

ρ = fluid density

g = acceleration of gravity

μ = viscosity.

The porosity determinations have been made by drying test specimens for periods of about 24 hours at temperatures of the order of 150° C, weighing them, and placing them in a vacuum chamber where the sample is subjected to a high vacuum for 4 hours. With the vacuum still on, distilled water is introduced so as to completely cover the sample. Evaluation continues until decreased bubbling indicates the air has been removed from the water. Pressure in the chamber is returned to atmospheric

and the sample kept submerged for 24 hours. The sample is then removed from the water, blotted, and quickly weighed. This procedure allows a determination of the pore volume. The total volume of the rock is measured using a standard precision mercury displacement volume determination device and an analytical balance.[12]

6.3 RESULTS

6.3.1 Unconfined Aquifer

The sedimentary material overlying the topmost basalt forms the unconfined aquifer of the Pasco Basin. This aquifer has been tested the most, especially within the Hanford Site. Newcomb, et al.,[13] report the results of pumping tests made prior to 1956 in the Hanford area. These tests were conducted in the glaciofluvial and Ringold material. The hydraulic conductivity values obtained average 6,000 feet per day in the glaciofluvial material and 60 feet per day in the Ringold conglomerate. Storage coefficient values reported by Newcomb, et al., [13] are 0.03 for the glaciofluvial material and 2×10^{-4} for the Ringold.

Comparable results were reported[14] for the glaciofluvial and Ringold material. In this report, the glaciofluvial material is found to have a hydraulic conductivity in the range from 1,200 to 12,000 feet per day, while the Ringold conglomerate was found to have a hydraulic conductivity in the range from 1 to 200 feet per day. The range of storage coefficients of the Ringold conglomerate is given as 8×10^{-4} to 2×10^{-1}, while that of the glaciofluvial material is given as 5×10^{-2} to 4×10^{-1}.

R. A. Deju[8] interpreted a number of pumping tests conducted by Pacific Northwest Laboratory. Results of these tests are summarized in Table 6.2. Well designation numbers refer to the Hanford coordinate system. Location of these wells is shown in Reference 14.

Results of these pumping tests have been used within the Hanford area to generate a map of the vertically averaged hydraulic conductivity distribution in the unconfined aquifer (Figure 6.3). Close scrutiny of this figure reveals a low hydraulic conductivity zone to the west of Hanford with an apparent buried stream channel running north-northwest to south-southeast passing between Gable Butte and Gable Mountain. The above results have been substantiated by a later study by Deju and Summers.[15]

Laboratory samples of cores from the unconfined aquifer material in wells at Hanford were used to obtain hydraulic conductivities. The laboratory-measured hydraulic conductivities are generally very low, probably due to sample repacking. These values are shown in Table 6.3.

TABLE 6.2

PUMPING TEST DATA RESULTS
FOR THE UNCONFINED AQUIFER[8]

WELL NUMBER	HYDRAULIC CONDUCTIVITY (feet per day)
699-77-54	97
199-K-10	260
199-K-12	250
699-87-55	130
699-61-66	>400
699-63-90	2,300
699-55-50	9,100
699-26-15	200
699-36-61	43
699-33-56	250
699-31-53	165
699-17-47	50
699-8-17	640
699-47-60	80
699-35-9	45
699-26-89	2
699-S12-3	9

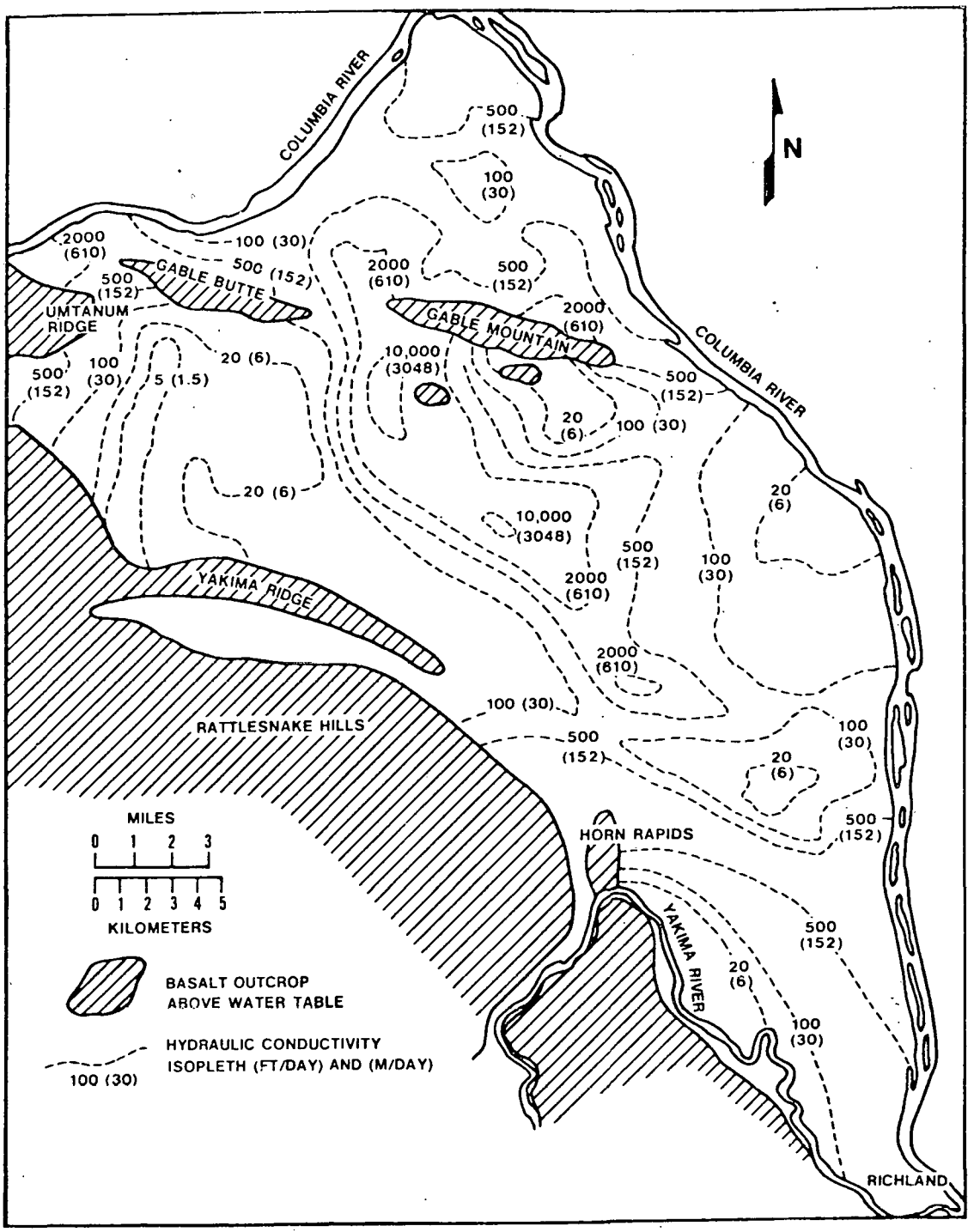

FIGURE 6.3

VERTICALLY AVERAGED HYDRAULIC CONDUCTIVITIY DISTRIBUTION IN THE UNCONFINED AQUIFER

TABLE 6.3

LABORATORY HYDRAULIC CONDUCTIVITY VALUES
OF SEDIMENTARY CORES FROM THE UNCONFINED AQUIFER

WELL NUMBER	DEPTH (feet)	MATERIAL	HYDRAULIC CONDUCTIVITY (feet per day)
699-54-17C	104	Silty conglomerate	5.1×10^{-2}
	133	Sand	100
	217	Silty clay	5.6×10^{-3}
	259	Silty clay	4.9×10^{-2}
	290	Sand	2.2
	314	Silty clay	8.7×10^{-1}
699-49-100	360	Sandy gravel	29
699-43-42	163	Sandy gravel	2.1
299-W11-26	265	Silty sand	10
299-W19-10	285	Sand	2.3

6.3.2 Upper Basalts and Interbeds

The upper basalts and interbeds form a series of confined aquifers which constitute the major intermediate flow system or systems beneath the Pasco Basin. Under this category, we include the lower Ringold Formation to the Vantage Member, which overlies the Grande Ronde Basalt.

Tests in the lower Ringold have been reported for several wells within the Pasco Basin.[16] The hydraulic conductivities obtained range from 0.10 to 7.0 feet per day. The lower Ringold confined aquifer may be connected to the unconfined aquifer in places where the subsurface strata were subjected to deformation or erosion.

Accurate results for water-bearing zones in the Saddle Mountains and Wanapum basalts are only available from testing Well DC-1 (Figure 6.4). The Saddle Mountains Basalt includes members made up of 1 to 3 flows. Some of these flows occur over limited geographic extent. Interbeds are common and are more extensive west of the Pasco Basin. As Table 6.4 shows, dense interiors make up only 55 percent of the formation and 43 percent of interbeds. The hydraulic conductivity of the dense interiors calculated from pumping tests in Well DC-1 is an order of magnitude larger than that of the Wanapum Basalt. The hydraulic conductivities of the interflows which make up only 2 percent of the formation are similar to those of the older formation. The hydraulic conductivities of the interbeds are approximately the same as those of the interbeds in the Wanapum Basalt.

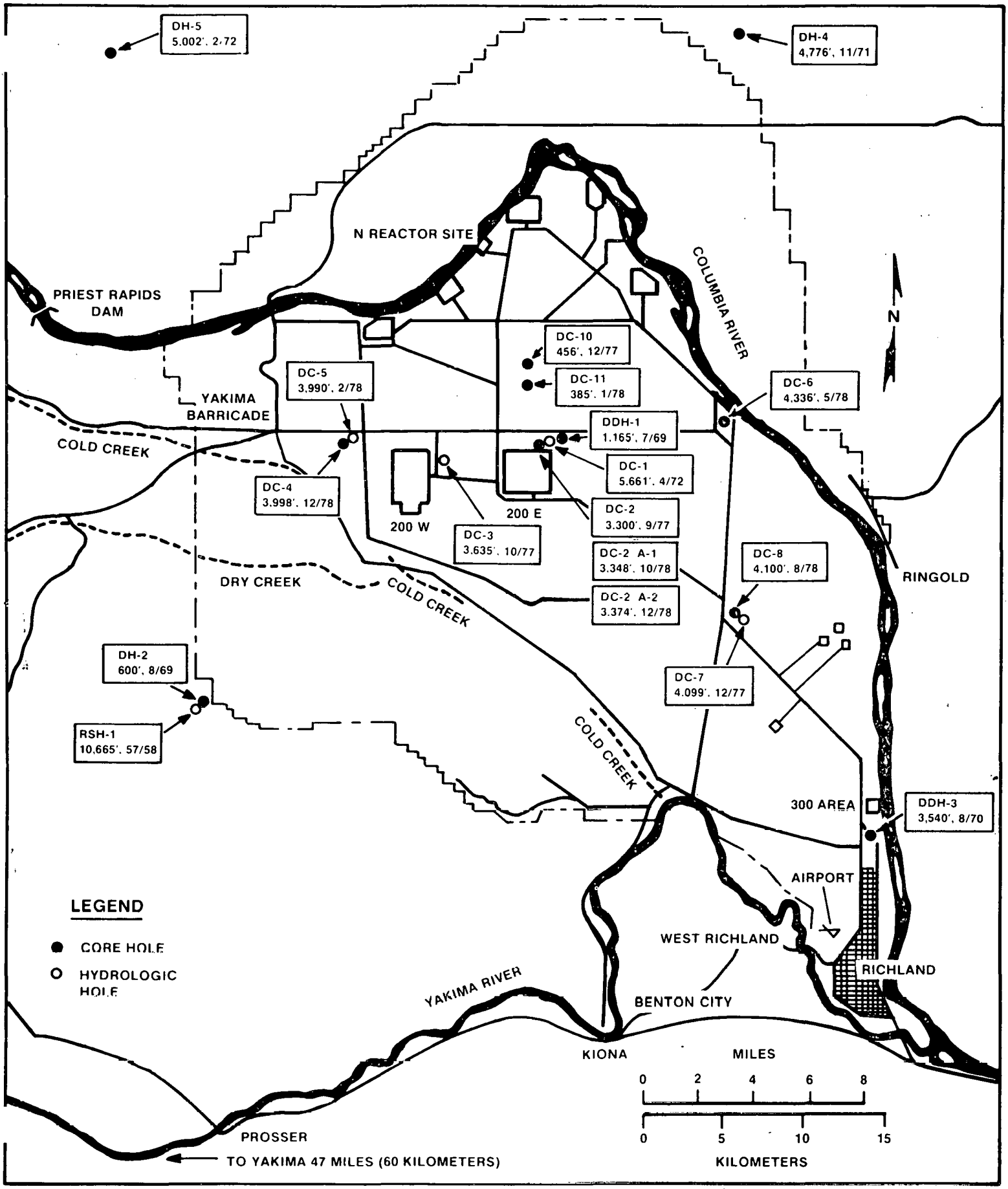

FIGURE 6.4

BASALT WASTE ISOLATION PROGRAM DRILL HOLES

TABLE 6.4

CALCULATED LITHOLOGIC AND MEAN HYDRAULIC CONDUCTIVITY OF SADDLE MOUNTAINS AND WANAPUM FORMATIONS, YAKIMA BASALT SUBGROUP IN WELL DC-1[17]

[Hydraulic Conductivity (k_h) is in feet per day]

FORMATION	DENSE BASALT			VESICULAR BASALT			BASALT FRACTURED, WEATHERED OR BRECCIATED			TUFF			SAND, GRAVEL CLAY		
	THICKNESS feet	%	k_h	THICKNESS feet	%	k_h	THICKNESS feet	%	k_h	THICKNESS feet	%	k_h	THICKNESS feet	%	k_h
Saddle Mountains	425	55	.030	0	-	-	15	2	.03	0	-	-	330	43	2
Wanapum	855	65	.002	25	2	.007	105	8	.09	220	18	.01	85	6	1

The Wanapum Basalt includes interbeds that geologists recognize over extensive areas plus several members made up of 2 or more flows. Table 6.4 shows that dense interiors with low hydraulic conductivity make up 67 percent of the formation. Hydraulic conductivity of the interflows, which make up only 8 percent of the formation, is similar to that of interflows in the Saddle Mountains Basalt. The hydraulic conductivity of the interbeds tends to be larger than that of the interflows.

The storage coefficient for the Saddle Mountains and Wanapum basalts can be estimated from the data of LaSala and Doty,[17] from Price's test of the Walla Walla City Well No. 3,[18] and from a calculation using the Young's modulus, Poisson's ratio, and bulk porosity values reported by Agapito, et al.[19] The storage coefficient of both the Wanapum and Saddle Mountains basalts is comparable ranging between 1.2×10^{-3} and 2.7×10^{-5}.

Porosity values were obtained from laboratory measurements in the Pomona Member of the Saddle Mountains Basalt using cores from Wells DC-10 and DC-11 (Figure 6.4). Porosity values for 7 determinations ranged from 1.0 percent to 3.95 percent.

6.3.3 Grande Ronde Basalt

The Grande Ronde Basalt is stratigraphically beneath the Wanapum Basalt. Within the Pasco Basin, the Grande Ronde Basalt contains few interbeds which are invariably very thin. Many Grande Ronde flows are so extensive that they cross the entire Pasco Basin. Table 6.5 summarizes the pumping data for Well DC-1[17] and shows that dense interiors with very low hydraulic conductivity make up about 71 percent of the formation. Another important fact noted in Table 6.5 is that the DC-1 data show that the hydraulic conductivity of the interflows and the interbeds is, with a few exceptions, as low as that of the dense interiors.[20] The hydraulic conductivities reflected by the data shown on Table 6.5 are comparable to results of laboratory analysis using rock cores from test Well DC-1 (Table 6.6). As Table 6.6 shows, the hydraulic conductivity of these samples is very low, even though all the samples, except Sample 13 (Umtanum), were from vesicular basalts. Sample 13 is from the Umtanum dense interior and shows a lower hydraulic conductivity and a much lower porosity.

Well RSH-1 (Figure 6.4) was tested by Raymond and Tillson.[21] They ran 4 drill stem tests in interflow zones and one across a moderately fractured zone. Their hydraulic conductivity values range from 4×10^{-2} to 7×10^{-5} feet per day.

In 1977, carefully run drill stem tests were conducted in the Grande Ronde Basalt at RSH-1. Tests centered on the Umtanum flow. Table 6.7 shows the results of the testing. Hydraulic conductivity values calculated for the low-density (flow tops) basalts at RSH-1 ranged between 4.8×10^{-4} and 1.1×10^{-5} feet per day.[22] In addition to the tests reported in Table 6.7, 3 other drill stem tests were conducted across portions of the Grande Ronde Basalt at RSH-1. Inasmuch as no measurable pressure change was observed, no hydraulic conductivity could be calculated for these three tests.

TABLE 6.5

LITHOLOGIC AND MEAN HYDRAULIC CONDUCTIVITY OF GRANDE RONDE BASALT IN WELL DC-1, 1971[17]

[Hydraulic conductivity (k_h) is in feet per day]

FORMATION	DENSE BASALT			VESICULAR BASALT			BASALT FRACTURED WEATHERED OR BRECCIATED			TUFF			SAND, GRAVEL CLAY		
	THICKNESS feet	%	- k_h	THICKNESS feet	%	- k_h	THICKNESS feet	%	- k_h	THICKNESS feet	%	- k_h	THICKNESS feet	%	- k_h
Grande Ronde	1,420	59	.003	270	12	.308	505	23	.08	105	5	.003	35	1	.003

TABLE 6.6

RESULTS OF LABORATORY TESTS ON CORE FROM WELL DC-1

CORE NO.	DEPTH (feet) FROM	TO	HYDRAULIC CONDUCTIVITY (feet per day)	POROSITY (%)
6	2,381.4	2,384.6	3.68×10^{-5}	9.8
7	2,779.0	2,779.8	5.96×10^{-5}	10.5
8	2,946.8	2,950.1	3.12×10^{-5}	25.4
13*	3,127.1	3,128.0	1.90×10^{-5}	2.1
28	4,285.0	4,285.5	3.97×10^{-5}	10.9

*Umtanum Basalt

TABLE 6.7

RESULTS OF HYDRAULIC TESTING IN WELL RSH-1

(Modified from R. E. Gephart, et al.[22])

TEST NUMBER	TEST INTERVAL (feet)	ROCK CHARACTER	HYDRAULIC CONDUCTIVITY (feet per day)	SKIN	RADIUS OF INFLUENCE*** (feet)
1	2,780 - 2,820	Low-density basalt*	4.8×10^{-4}***	-4	<1
2	2,825 - 2,860	Low-density basalt	8.5×10^{-5} - 9.9×10^{-5}	-4	<1
3	2,700 - 2,770	High-density basalt	1.3×10^{-5} - 1.7×10^{-5}	-3	<1
4	2,740 - 2,770	High-density basalt**	3.1×10^{-5} - 3.9×10^{-5}	-1	<1
5	2,780 - 2,820	Low-density basalt	2.2×10^{-5} - 2.5×10^{-5}	-2	<1
6	2,717 - 2,739	High-density basalt	4.3×10^{-5}***	-3	<1
7	2,622 - 2,676	Low-density basalt	1.1×10^{-5} - 1.6×10^{-5}	-2	<1

*Low-density basalt (2.4 - 2.6 grams per cubic centimeter).

**High-density basalt (2.7 - 2.9 grams per cubic centimeter).

***Identical values were calculated using recorder and electric line measurements of water pressures.

****Cone porosity assumed.

The negative skin values reported in Table 6.7 reveal that the basalts immediately adjacent to the borehole are slightly more permeable than the overall rock stratum. Because of the negative skin, less of a pressure drop (ΔP) is obtained across the test zone proportional to the rate of fluid production or injection (Q). In tests where the radius of influence is small, a large negative skin reveals that the permeability measured is probably greater than the undisturbed rock permeability. However, the skin values reported in Table 6.7 show:

- There was no interfering mud cake across the test horizons which would have produced a positive skin; and
- The reported hydraulic conductivity values are probably characteristic and conservative for the rocks tested.

The low values for the radius of influence are a measure of the tightness of the basalts permitting only limited rock volumes to be stressed. It can then be assumed that the test results are characteristic of the basalt rock within the immediate vicinity of the borehole. However, given the negative skin values, one can conclude that the hydraulic conductivity values obtained are conservative.

In 1978, five drill stem (injection) tests were run in Well DC-6 (Figure 6.4).[23] These tests were mostly run across vesicular flow tops in the upper part of the Grande Ronde Basalt section. Results are shown in Table 6.8 and are comparable to values from RSH-1 and DC-1.

TABLE 6.8

HYDRAULIC CONDUCTIVITY VALUES
DETERMINED IN WELL DC-6

DEPTH RANGE (feet) from	to	ROCK TYPE	HYDRAULIC CONDUCTIVITY (feet per day)
2,260	2,295	Vesicular flow top	10^{-10}
2,439	2,482	Vesicular flow top	1
2,544	2,576	Vesicular flow top	$<10^{-4}$
2,576	2,618	Basalt columns*	$<10^{-4}$
2,670	2,711	Vesicular flow top	10^{-4}

*Columns is a general term referring to either the entablature or colonnade portion of a basalt flow unit.

In 1978, carefully controlled drill stem tests using sensitive quartz transducers were run in Well DC-2 (Figure 6.4).[9] Calculations of hydraulic conductivity were made for 6 zones--4 in the colonnade/entablature sections and 2 in basalt flow top sections. Table 6.9 summarizes the results of the tests specifying the analytical method used for interpretation. Three of the 6 zones tested were in the Umtanum entablature/colonnade and showed values of hydraulic conductivity 3 orders of magnitude less than the other zones tested. For the Umtanum entablature/colonnade tests, no curve matching techniques (Papadopulous, et al.)[9] could be used due to the negligible volume of flow in the interval tested over the duration of the test period.

The storage coefficients obtained from the tests in DC-2 were less than 10^{-4}.

6.3.4 Basalts and Interbeds Outside the Pasco Basin

Some pumping tests are available from deep wells outside the Pasco Basin. These pumping tests generally have a large contributing interval and, thus, cannot be ascribed to a specific unit. Results are shown in Table 6.10.[20] Values of the hydraulic conductivity average around 10-20 feet per day.

6.3.5 Vertical Hydraulic Conductivity

The only expressed estimate of vertical hydraulic conductivity $\overline{k}_v$ derives from the simulation by Tanaka, et al., of the Columbia Basin Irrigation Project area where the estimated $\overline{k}_v$ for the dense interiors ranges from .000001 to .000037 feet per day,[24] and from MacNish and Barker[25] who say that in the Walla Walla River Basin the vertical hydraulic conductivity may be as low as .004 feet per day. We believe that in the interflows and interbeds the horizontal hydraulic conductivity $\overline{k}_h$ is slightly larger than $\overline{k}_v$; whereas the dense interiors $\overline{k}_h$ is much less than the $\overline{k}_v$.

6.4 SUMMARY

Table 6.11 lists the basic hydraulic properties for the hydrostratigraphic units beneath the Pasco Basin. The most significant variability takes place in the hydraulic conductivity of the glaciofluvial and Ringold sediments.

The unconfined aquifer comprised of these sediments is the largest carrier of ground water in the basin accounting for over 95 percent of the flow volumes beneath the basin (see Chapter 10.0). Fortunately, this unconfined aquifer is the best understood flow regime in the basin. Data shown in Table 6.11 and in preceding tables in this section also demonstrate the very low values found for hydraulic conductivity in the various Grande Ronde Basalt horizons.

Porosities in the basalt are usually less than 3 percent, except in brecciated horizons where very large values can be found in small samples.

All storage coefficients for the basalt horizons are near or below the limit of measurement.

TABLE 6.9

RESULTS OF HYDRAULIC TESTING IN WELL DC-2

INTERVAL	DEPTH (feet)	LENGTH (feet)	Rock Type	GEOLOGIC DESCRIPTION	HYDRAULIC CONDUCTIVITY (feet per day) PAPADOPULOUS	U. S. BUREAU OF RECLAMATION	HVORSLEV
1	2376.36 to 2409.08	32.72	Entablature	Moderately fractured, dense, dark, some glass, some flow banding, scattered amygdules	5.6×10^{-3}	1.3×10^{-4} to 3.6×10^{-4}	4.5×10^{-6}
2A and 2B	2343.57 to 2376.29	32.72	Flow top	Highly fractured, vesicular (15%), and breccia and flow rubble with clay matrix, zeolites; upper part of interval base of overlying colonnade of dense, dark, finely phaneritic nature; lower part of interval is top of entablature, moderately fractured, competent, with brown-yellow clay	1.5×10^{-2}	4.5×10^{-4} to 7.9×10^{-3} 3.1×10^{-4} to 6.5×10^{-3}	1.2×10^{-5}
4	3018.81 to 3071.45	52.65	Umtanum entablature	Dark, dense, aphyric with filled and unfilled fractures mostly hairline and irregular, rare amygdules	N/A	7.3×10^{-7}	1.5×10^{-8}
5	3068.94 to 3121.59	52.65	Umtanum entablature/ colonnade	Zones of moderate fracturing with high-angle orientation hairline fractures.	N/A	1.6×10^{-6}	4.2×10^{-8}
6	3116.14 to 3170.30	54.16	Umtanum colonnade	Moderately fractured rock, high-angle hairline fractures, black and glass zones; more fractured toward the base	N/A	8.2×10^{-7}	3.9×10^{-8}
7	2954.38 to 3006.54	54.16	Umtanum flow top	Flow top consisting of a competent rubble zone well indurated with little alteration underlain by a glassy scoria in a well-indurated matrix, some vugs; the underlying entablature is a dense, dark aphyric basalt with some low-angle fractures	7.1×10^{-4}	3.9×10^{-4} to 1.7×10^{-3}	4.8×10^{-7}

TABLE 6.10

SUMMARY OF PUMPING TESTS OF WELLS IN BASALT OUTSIDE OF PASCO BASIN

PUMPED WELL	ALTITUDE (feet)	DEPTH TO BOTTOM OF CASING (feet)	DEPTH TO WATER (feet)		TOTAL DEPTH (feet)	LENGTH OF CONTRIBUTION INTERVAL (b) (feet)		TRANSMISSIVITY (T) (feet^2/day)	APPROXIMATE MEAN HYDRAULIC CONDUCTIVITY (K_h = T/b)ft/d	
			Static	Maximum Pumping		Maximum	Minimum			
Walla Walla City Well #3	1,320	178	164	222	1,169	1,005	947	53,000	50	S = .0002 S_s = 2 x 10^{-7}/ft
Municipal Wells Walla Walla	-	-	-	-	-	-	-	40,000	-	
Test Well 6N35E.18	670	710	174	222	1,280	570		4,700	8	Wanapum Basalt
Geiger Field Near Spokane	-	-	-	-	-	-	-	670	-	
Bierly Farm Well	-	-	-	-	-	490		3,000	6	
Well Near Pilot Rock, OR	-	-	-	-	-	-	-	1,000	-	
Hermiston, OR 4N28E-11cac	453	55?	12		962	~900		9,000 to	9 to	
4N28E-11cca	446	44?	11		918	~875		17,000	20	
George Well (18/25-15E1)	1,157	343	165	191	975	632		40,000	60	Wanapum Basalt and Grande Ronde Basalt
Basalt Explorer #1	-	-	232? 230?	315? 264	1,600 2,300	1,370? 2,000?	1,300?	12,000 18,000	9 9	
Almira Well (24/31-16)	-	60	363	368	750	382		30,000	80	
Hangman Creek Area	-	-	-	-	-	-		9,000	-	S = 1.1 x 10^{-3} to 3.5 x 10^{-4}

TABLE 6.11

SUMMARY OF HYDRAULIC PROPERTIES

MATERIAL	HYDRAULIC CONDUCTIVITY (feet per day)	STORAGE COEFFICIENT	POROSITY (%)	REMARKS
Unconfined Aquifer	1,200 - 12,000	5×10^{-2} - 4×10^{-1}	Estimated	Mostly dry (above water table)
Glaciofluvial sediments	(6,000)	(3×10^{-2})	5 - 20	
Unconfined Aquifer	1 - 200	8×10^{-4} - 2×10^{-1}	Estimated	-
Upper and middle Ringold sediments	(60)	(1×10^{-3})	<12	
Confined Aquifer	.10 - 7	Estimated	Estimated	Extremely clayey material
Lower Ringold	(2)	$\sim 10^{-3}$	5 - 20	
Saddle Mountains Basalt	.030 - 10	2.7×10^{-5} - 1.2×10^{-3}	1.00 - 3.95	Most of the hydraulic conductivity is through the interbeds
Dense basalts	(.030)			
Brecciated basalts	(.030)	(1×10^{-4})	(2.00)	
Interbeds	(2)			
Wanapum Basalt	.020 - 10	2.7×10^{-5} - 1.2×10^{-3}	1.00 - 4.00	Most of the hydraulic conductivity is through the interbeds
Dense basalt	(.020)			
Brecciated basalts	(.080)	(1×10^{-4})	(2.00)	
Interbeds	(1)			
Grande Ronde Basalt	7.3×10^{-7} - 1×10^{-2}	1×10^{-5} - 1×10^{-3}	1.00 - 25.00*	Lowest hydraulic conductivities found
Umtanum	(1×10^{-6})			
Dense basalt	(.003)			
Brecciated basalts	(.01)	($<1 \times 10^{-4}$)	(3.00)	
Interbeds	(.003)			

*High value in one sample of brecciated basalt.

6.5 REFERENCES

1. D. K. Todd, Ground Water Hydrology, John Wiley and Sons, Inc., New York, New York (1959 et seq.).

2. J. H. Moran and E. E. Finklea, "Analysis of Pressure Build-up Data Obtained by the Wire Line Formation Tester," Paper SPE 177; 36th Annual Fall Meeting SPE, Dallas, October (1961).

3. P. J. Jones, "Draw Down Exploration, Reservoir Limit, Well and Formation Evaluation," Permian Basin Oil Recovery Conference of AIME, Midland, Texas (April 1957).

4. W. Hurst, O. K. Hanie, and R. N. Walker, "Some Problems in Pressure Build-up," Paper SPE 145, 36th Annual Fall Meeting, Dallas, Texas (October 1961), also "New Concept Extends Pressure Build-up Analysis," Petroleum Engineering (August 1962) 34 No. 9, p. 41.

5. L. F. Maier, "Recent Developments in the Interpretation and Application of DST Data," Journal of Petroleum Technology, XIV (11) (November 1962).

6. A. F. Everdingen, "The Skin Effect and its Influence on the Productive Capacity of a Well," Trans., AIME, 198 (1953) pp. 171-176.

7. M. F. Hawkins, Jr., "A Note on the Skin Factor, " Trans., AIME, 207 (1956).

8. R. A. Deju, The Hanford Field Testing Program, ARH-C-00004, Atlantic Richfield Hanford Company, Richland, Washington (September 1974).

9. Hydrologic Testing in Borehole DC-2, Science Applications, Inc., RHO-BWI-C-36, Rockwell Hanford Operations, Richland, Washington (September 1978).

10. D. R. Horner, "Pressure Build-up in Wells," in Proceedings of the Third World Petroleum Congress, E. J. Brill, Editor, Leiden Publishing II (1951) p. 503.

11. I. S. Papadopulous, J. D. Bredehoeft, and H. H. Cooper, "On the Analysis of Slug Test Data," Water Resources Research, Vol. 9, No. 4 (1973). pp. 1087-1089.

12. W. I. Duvall, R. J. Miller, and F. D. Wang, Preliminary Report on Physical and Thermal Properties of Basalt Drill Holes DC-10, Pomona Flow, Gable Mountain, RHO-BWI-C-11, Rockwell Hanford Operations, Richland, Washington (May 1978).

References (continued)

13. R. C. Newcomb, J. R. Strand, and F. J. Frank, "Geology and Ground Water Characteristics of the Hanford Reservation of the U. S. Atomic Energy Commission, Washington," U. S. Geological Survey Professional Paper 717 (1972).

14. J. L. Liverman, Final Environmental Statement - Waste Management Operations - Hanford Reservation, Richland, Washington, ERDA-1538 UC-60, United States Energy Research and Development Administration, Richland, Washington (December 1975).

15. R. A. Deju and W. K. Summers, Transmissivity and Hydraulic Conductivity of Saturated Sedimentary Rocks in the Hanford Reservation, ARH-C-00007, Atlantic Richfield Hanford Company, Richland, Washington (April 1975).

16. R. A. Deju and R. K. Ledgerwood, Hydrogeology of the Uppermost Confined Aquifers Underlying the Hanford Reservation, ARH-SA-253, Atlantic Richfield Hanford Company, Richland, Washington (March 1976).

17. A. M. LaSala, Jr. and G. C. Doty, Preliminary Evaluation of Hydrologic Factors Related to Radioactive Waste Storage in Basaltic Rocks at the Hanford Reservation, Washington Open-File Report, United States Geological Survey in Cooperation with the United States Atomic Energy Commission (1970) p. 68.

18. C. W. Price, Artificial Recharge of a Well Tapping Basalt Aquifers, Walla Walla Area, Washington, Water-Supply Bull. 7, Washington State Department of Ecology (1960) p. 50.

19. J.F.T. Agapito, M. P. Hardy, and D. R. St. Laurent, Geo-Engineering Review and Proposed Program Outline for the Structural Design of a Radioactive Waste Repository in Columbia Plateau Basalts, RHO-ST-6, Rockwell Hanford Operations, Richland, Washington (1977).

20. W. K. Summers and Associates, A Survey of the Ground-Water Geology and Hydrology of the Pasco Basin, Washington, RHO-BWI-C-41, Rockwell Hanford Operations, Richland, Washington (December 1978).

21. J. R. Raymond and D. D. Tillson, Evaluation of a Thick Basalt Sequence in South-Central Washington, AEC Research and Development Report, BNWL-776, Battelle Northwest (April 1968).

22. R. E. Gephart, R. A. Deju, and P. A. Eddy, Geophysical Logging and Hydrologic Testing of Deep Basalt Flows in the Rattlesnake Hills Well Number One, RHO-BWI-ST-1, Rockwell Hanford Operations and Pacific Northwest Laboratory (January 1979).

23. Staff, Basalt Waste Isolation Program Annual Report - Fiscal Year 1978, RHO-BWI-78-100, Rockwell Hanford Operations, Richland, Washington (October 1978).

24. H. H.Tanaka, Aquifer Test of Well 18/25-15E in Grant County, Washington, Washington State Department of Ecology, Olympia, Washington (1977) 3 p.

25. R. D. MacNish and R. A. Barker, Digital Simulation of a Basalt Aquifer System, Walla Walla River Basin, Washington and Oregon, Washington State Department of Ecology, Olympia, Washington (1973) 25 p.

7.0 HYDROCHEMISTRY

7.1 GENERAL

We can use hydrochemical data, coupled with ground water age determinations obtained by isotopic methods, to interpret ground water flow patterns because the ambient water chemistry in a particular part of the flow continuum depends on such factors as:

- The antecedent water chemistry;
- Residence time of the water;
- The chemical composition of the continuum; and
- The temperature-pressure relationships in the continuum that control water-rock reactions.

Because ground water flow systems are three-dimensional and flow may be across bedding or stratigraphic units, as well as parallel to them, the chemical character of water in a formation does not necessarily reflect chemical changes due exclusively to flow through that formation.

Conversely, local, intermediate, and regional flow systems (as described in earlier sections) can in some places be identified by their chemical characteristics, even though all flow is essentially horizontal.

Recharging ground waters are among the youngest waters in a ground water flow system. They have comparatively low concentrations of soluble salts and contain relatively few ionic species. They may not be at equilibrium with the surrounding rock.

As the waters move into and through the flow continuum, their residence times and travel paths become increasingly longer, and their concentrations of total dissolved solids increase, as does the diversity of ionic species. The water and rock tend to come to equilibrium. Thus, observed differences in water chemistry in a flow continuum may reflect distance traveled from the recharge area or length of residence time.

In discharge areas, waters of one or more flow systems, each with different chemistries, converge (so that water samples apparently from the same source have substantially different compositions). Discrimination of flow systems in a discharge area is difficult because water samples rarely represent one flow system exclusively.

7.2 ANALYTICAL RESULTS

Extensive chemical analyses are available from ground waters found within the Pasco Basin. The largest concentration of the data is found for the unconfined aquifer, with more meager results for the deep regional system. Most of the data are concentrated on the Hanford Site.[1,2] Table 7.1 depicts the average composition ascribed to waters in the unconfined aquifer (local flow system) and uppermost confined aquifer (intermediate flow system).

R. A. Deju[2] reported results of a study where a number of wells (DB-1, DB-2, DB-4, DB-7, DDH-3, 699-53-103, and 699-52-52) were sampled by Pacific Northwest Laboratory for the Atlantic Richfield Hanford Company during the month of August 1976. Complete chemical analyses were obtained for Wells DB-1, DB-2, DB-7, and DDH-3. Carbon-14 age dates were determined for all wells, and $^{18}O/^{16}O$ ratios were measured for all except Well DB-4. Tritium-3 analyses were obtained for DB-1, DB-2, DB-7, DDH-3, and 699-53-103. In addition, Well RSH-1 was sampled in May 1977 by Atlantic Richfield Hanford Company and a complete chemical analysis was obtained. No age-dating data are available for Well RSH-1. The locations of all wells sampled are shown in Figure 7.1.

All sampling was done by the Water and Land Resources Section of Pacific Northwest Laboratory, except for Well RSH-1 which was sampled by Atlantic Richfield Hanford Company. Well DB-1 has a water level within a few feet of the ground surface. A conventional centrifugal pump was used to both flush the well and subsequently sample it. Well 699-53-103 is artesian flowing and a water sample was directly obtained. For all other wells sampled, the water levels in the wells were below the capabilities for a centrifugal pump, and, therefore, an air lift method was employed. The method entails the use of a long sampling tube being lowered into the well and air pressure from an air compressor used as the driving force to bring the water to the surface. All wells were sampled until a reasonably clean sample was obtained. In the case of DDH-3, diesel oil and drilling mud contamination was detected and could not be removed even after extensive well clean out. Thus, DDH-3 results are not representative of aquifer water and are simply given for completeness. For all other water samples obtained, the air lift method provided reproducible results. Well RSH-1 was sampled using a swab unit while testing for hydraulic conductivity in selected zones of the Grande Ronde Formation.

Duplicate samples for chemical composition were taken in all wells sampled and are reported in Tables 7.2 and 7.3. Results of the ^{14}C and ^{18}O analyses are summarized in Table 7.4. Table 7.5 summarizes the results of the H^3 analyses.

TABLE 7.1

AVERAGE COMPOSITION OF WATERS FROM AQUIFERS UNDERLYING THE PASCO BASIN

(Numbers in parentheses denote the range of values found.)

CONSTITUENTS (milligrams per liter)	UNCONFINED AQUIFER (local flow system)	UPPERMOST CONFINED AQUIFERS (intermediate flow system)
Sodium	29 (16-64)	40 (4.1-122)
Calcium	48 (31-72)	15 (1-18)
Magnesium	12 (7.1-14)	7 (0-11)
Chloride	13 (3.1-24)	16 (3.8-81)
Sulfate	58 (20-150)	9 (0-29)
Bicarbonate	172 (115-315)	152 (93-180)
Carbonate	0 (0)	3 (0-15)
Hardness, total	170 (110-220)	66 (3-96)
Potassium	6.8 (4.6-13)	9.0 (4.5-17)
pH	8.0 (7.5-8.1)	8.0 (7.2-8.7)

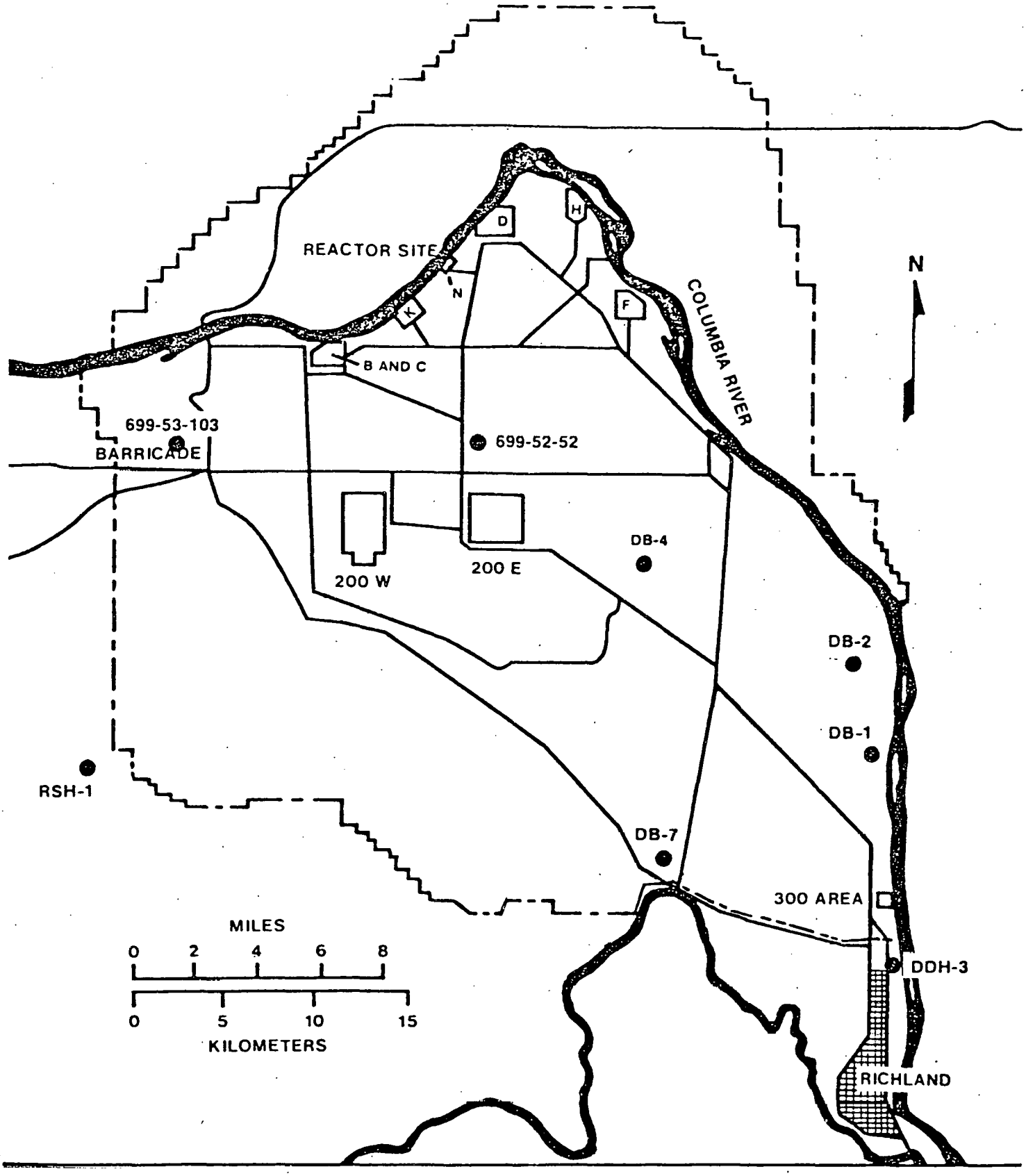

FIGURE 7.1

HANFORD AREA MAP SHOWING LOCATION OF WELLS SAMPLED

TABLE 7.2

MAJOR CONSTITUENTS: ANALYTICAL RESULTS

(Sampling dates are in parentheses.)

Constituent	DB-1 (8-9-76)		DB-2 (8-17-76)		DB-7 (8-11-76)		DDH-3* (8-11-76)		RSH-1 (5-11-77)		Units
SiO_2	27.8	28.8	31.6	31.8	36.4	36.4	29.0	29.0	22.5	22.5	ppm
Na	75.0	75.0	150.0	150.0	106.0	117.0	166.6	172.3	30.0	25.0	ppm
K	14.0	14.0	12.5	12.5	12.5	12.5	23.0	22.0	9.0	7.7	ppm
Ca	3.5	8.0	4.2	4.5	2.5	2.5	10.5	8.0	6.5	8.5	ppm
Mg	0.70	0.90	0.18	0.20	0.50	0.50	1.40	1.20	1.0	2.2	ppm
Fe	.155	.105	0.53	0.63	2.72	3.82	3.8	4.0	.08	<.02	ppm
HCO_3	208.8	219.6	196.4	192.8	135.7	121.4	192.8	191.0	42.8	67.3	mg/ℓ $CaCO_3$
CO_3	0	0	21.4	21.4	35.7	50.0	99.9	114.2	0	0	mg/ℓ $CaCO_3$
SO_4	<.5	<.5	.5	.5	1.0	.5	1.0	1.0	23.0	15.0	ppm
Cl	12.2	11.8	134.5	117.5	53.0	52.0	83.5	82.5	16.2	8.8	ppm
F	3.0	3.5	2	<1	7.0	8.7	15.0	18.0	0.7	0.7	ppm
NO_3	.5	.5	<.5	<.5	.5	.5	<.5	<.5	<.05	.20	ppm
B	.25	.25	.6	.6	.8	.7	.5	.4	<.05	<.05	ppm
T.D.S.	345	307	430	417	531	505	861	914	118	112	mg/liter
TOC	29	28	14	16	27	28	160	160	9	9	mg/liter
Cond.	400	430	430	440	450	475	460	560	250	250	micromhos/cm
pH	8.2	8.3	8.6	8.6	9.0	9.0	9.1	9.1	7.3	7.4	
	Water from Mabton Interbed sampled with centrifugal pump.		Water from Mabton Interbed sampled with air-lift device and air compressor.		Water from Mabton Interbed sampled with air-lift device and air compressor.		Water from Lower Frenchman Springs and Vantage members sampled with air-lift device and air compressor.		Water from Grande Ronde Formation sampled by swabbing.		

*Anomalously high metal ion content confirmed sampling of stagnant water containing diesel oil and drilling muc.

TABLE 7.3

TRACE CONSTITUENTS: ANALYTICAL RESULTS

(Sampling dates are in parentheses.)

Trace Constituent	DB-1 (8-9-76)		DB-2 (8-17-76)		DB-7 (8-11-76)		DDH-3 (8-11-76)		RSH-1 (5-11-77)	
Zn	24	16	14	15	600	655	700	750	2,560	39,000
Cu	15	15	10	12	15	19	30	25	20	50
Hg	<.05	<.05	<.05	<.05	<.05	<.05	<.05	<.05	<.05	<.05
Sb	10	<8	<8	<8	10	15	70	55	<3	<3
Ba	22	30	39	35	43	42	74	53	140	50
Be	.8	.9	1.3	1.2	.8	1.2	.8	1.1	NA	NA
Cd	<.5	<.5	<.5	<.5	1.0	1.5	1.5	1.5	.2	.6
Cr	2	<1	<1	<1	14	33	750	480	<25	<25
Co	6	7	7	5	6	5	8	5	2	2
Pb	19	17	15	13	31	41	38	15	7	12
Mo	67	20	<1	<1	40	15	107	120	2	2
Ni	7	10	8	11	15	13	19	11	NA	NA
Ag	1.5	1.0	1.0	1.5	0.8	0.8	1.5	0.5	<2.5	<2.5
Sr	7	5	2	3	4	3	8	5	NA	NA
Sn	14	17	14	14	5	5	6	10	NA	NA
Tl	11	11	12	15	11	13	7	8	NA	NA
V	<2	<2	8	9	13	14	22	19	NA	NA
Unit Sampled	Mabton Member		Mabton Member		Mabton Member		Lower Frenchman Springs/Vantage Member		Grande Ronde Formation	

NA = Not analyzed for.

* = All constituents are expressed in parts per billion.

TABLE 7.4

^{14}C AND ^{18}O ANALYSES

WELL	^{14}C AGES (years)	^{18}O VERSUS SMOW*
DB-1	20,500 ± 500	-17.6
DB-2	23,000 ± 500	-17.6
DB-7	15,400 ± 500	-17.4
DDH-3	4,200 ± 140**	-15.2**
699-53-103	16,800 ± 250	-18.0***
DB-4	15,400 ± 250	NA†
699-52-52	19,900 ± 500	-18.0††

*Standard Mean Ocean Water.

**Anomalously high metal ion content indicates sampling of stagnant water containing diesel oil and drilling mud.

***Mixed water from several confined aquifers.

NA - Not analyzed for.

† Water from between the Mabton and Vantage (see stratigraphic chart in Chapter 3.0 of this report).

†† Water from the uppermost confined aquifers.

TABLE 7.5

RESULTS OF ^{3}H ANALYSES

WELL	H^3 RANGES
DB-1	Below detection
DB-2	Below detection
DB-7	Below detection
DDH-3	46-53 pCi/ℓ*
699-53-103	Below detection
Upper confined aquifers range	1-30 pCi/ℓ
Unconfined aquifer	10^3 pCi/ℓ - 3 x 10^6 pCi/ℓ
Concentration guide USDOE Manual Chapter 0524	3 x 10^6 pCi/ℓ
Level of detection	1 pCi/ℓ

*Contaminated sample.

W. K. Summers and Associates[3] compiled chemical data from wells throughout the Pasco Basin. Their compilation includes 48 nearly complete water chemistry suites from basalt-confined aquifers and 91 suites from the unconfined aquifer. The analyses reported by W. K. Summers and Associates[3] are comparable to those reported by Deju[2] and those reported earlier by Newcomb.[4] Results of the ^{14}C age dating work agree with data from Robinson[5] (Table 7.6), Silar,[6] Crosby and Chatters,[7] and Newcomb.[4]

TABLE 7.6

AGE DATING RESULTS

(From Robinson[5])

WELL	WATER AGE (years)	ALTITUDE OF OPEN INTERVAL IN WELL (feet) From	To	Ca++ + Mg++ (percent) Σcations	REMARKS
1S/26E-1dad	Modern	-	-	-	Interval open to well is 30 -70 feet deep
4N/27E-8dda	6,700	359	162	29.1	
3N/26E-5cbd	27,290	341	-409	26.0	

7.3 INTERPRETATION

Results of the above analyses show that waters from the unconfined aquifer are characterized by a high bicarbonate and magnesium content. They can be described as calcium-magnesium-sulfate-bicarbonate waters. On the other hand, the waters in the uppermost confined aquifers are primarily of the sodium-bicarbonate type.

Generally, waters from basaltic aquifers are characterized by high ratios of calcium to sodium and of magnesium to calcium, a relatively high silica content, and a relatively high fluoride content.[8] The waters in the uppermost confined aquifers (Table 7.1) are atypical basalt waters and appear to be influenced by the sedimentary interbeds and not the basalt proper. The water from Well RSH-1, obtained from the Grande Ronde Formation, is slightly different and can be described as a sodium-calcium water; however, its composition is also atypical of basalt waters.

LaSala and Doty[9] have examined numerous water analyses of Columbia Plateau basaltic aquifers. They concluded that the waters were typical of those found in sedimentary aquifers. The silica content of these waters indicates near equilibrium with a silica phase having properties similar to those of chalcedony or cristobalite. The silica probably comes into solution

from feldspars and other minerals, but at a concentration higher than that at which it would be in equilibrium with quartz. The solubility of quartz is particularly low and would account for only 5 to 15 parts per million SiO_2 in the water. Other silicate minerals, however, have solubilities intermediate between quartz and amorphous silica (40 parts per million).

LaSala and Doty[9] analyzed the ^{14}C content of the bicarbonate dissolved in water from the uppermost confined aquifers in Well DC-1 within the Hanford Site. Their measured ^{14}C content was then adjusted for the dilution effects of carbonate mineral solution using the ^{13}C value of bicarbonate.[10] They found an adjusted age of about 13,000 years before present. The same procedure was followed for the wells in Figure 7.1 whose dates are reported in Table 7.5. Adjusted ages range from 15,400 to 23,000 years before present.

Silar[6] dated 44 samples of water from wells in east-central Washington. He concluded that the age of ground water in the top few hundreds of feet of basalt ranged from 0 to 16,275 ± 1,465 years before present. Thirty-seven of the ages were 6,000 years or less and 4 were greater than 10,000 years.

Crosby and Chatters[7] obtained age dates on 33 samples of ground water taken from wells in the basalt of Pullman and Moscow. The ages ranged from about 1,700 to more than 32,000 years. Newcomb[4] suggests that their data indicate that age may increase downward roughly correlating with depth with the exceptions being due to mixing of waters of different ages because of concentrated pumping for irrigation.

The $\delta^{18}O$ versus standard mean ocean water values reported in Table 7.5 are representative of waters recharged during a glacial stage when a colder climate prevailed.

Further, the ^{3}H results (Table 7.5) show very low ^{3}H in the confined aquifer system sampled, probably due to lack of interconnection between these and aquifers closer to the land surface.

Total iron concentration in Pasco Basin deep ground waters is very low. These low levels of iron indicate that the aqueous solution is poorly poised with respect to the Fe^{+3} - Fe^{+2} couple. The sulfur system is also poorly poised in Pasco Basin ground waters.

Ground water composition is also affected by secondary minerals found in a given rock formation. Benson[11] reports that 3 phases dominate secondary mineral assemblages to a depth of approximately 4,000 feet: (1) the zeolite clinoptilolite; (2) the smectite nontronite; and (3) a silica phase (usually cristobalite or quartz). Minor amounts of calcite, gypsum, potassium feldspar, chabazite, mordenite, pyrite, apatite, and opal have also been noted.

Using the preceding data on ground water chemistry, one can make a preliminary correlation with the ground water flow system of the Pasco Basin. We believe the following generalities describe the conceptual ground water flow systems underlying Hanford.

- Water in the recharge areas and in local flow systems (unconfined aquifer) contains Ca^{++}, Mg^{++}, and HCO_3^- with low (200-300 milligrams) per liter) total dissolved solids. This water is young water (less than 500 years before present).

- Water in intermediate flow systems is like water in local flow systems near the recharge area, but downstream the water contains more $SO_4^=$, larger total dissolved solids (300-500), and is older (more than 500 years before present).

- Water in regional flow systems contain Na^+, HCO_3^-, $CO_3^=$, Cl^-, and F^- and is usually much older than 2,000 years, in many cases as much as 30,000 years old.

- In discharge areas, water from local, intermediate, and regional flow systems converge, so the character of the water sampled depends upon how and where the sample was obtained.

7.4 REFERENCES

1. J. L. Liverman, Final Environmental Statement - Waste Management Operations - Hanford Reservation, Richland, Washington, ERDA-1538 United States Energy Research and Development Administration, Washington, D. C. (December 1975).

2. R. A. Deju, Preliminary Analysis of Some Waters from the Unconfined Aquifers Underlying the Hanford Site, RHO-BWI-LD-12, Rockwell Hanford Operations, Richland, Washington (September 1978).

3. W. K. Summers and Associates, A Survey of the Ground-Water Geology and Hydrology of the Pasco Basin, Washington, RHO-BWI-C-41, Rockwell Hanford Operations, Richland, Washington (December 1978).

4. R. C. Newcomb, Quality of the Ground-Water in Basalt of the Columbia River Group, Washington, Oregon, and Idaho, Geological Survey Water-Supply Paper 1999-N (1972), p. 71.

5. J. H. Robinson, Hydrology of Basalt Aquifers in the Hermiston-Ordinance Area, Umatilla and Morrow Counties, Oregon, Hydrologic Investigations Atlas HA-387, United States Geological Survey, Washington, D. C. (1971).

References (continued)

6. J. Silar, Ground Water Structures and Ages in the Eastern Columbia Basin, Washington, Bulletin 315, College of Engineering, Washington State University, Pullman, Washington (November 1969) p. 165.

7. J. W. Crosby, III and R. M. Chatters, Water-Dating Techniques as Applied to the Pullman-Moscow Ground-Water Basin, Washington State University Research Division Bulletin 296 (1965) p. 21.

8. S. N. Davis and R.J.M. DeWiest, Hydrogeology, Wiley and Sons, New York, New York (1966).

9. A. M. LaSala, Jr. and G. C. Doty, "Preliminary Evaluation of Hydrologic Factors Related to Radioactive Waste Storage in Basaltic Rocks at the Hanford Reservation, Washington," U. S. Geological Survey Open-File Report (1971).

10. F. J. Pearson, Jr. and B. B. Hanshaw, "Sources of Dissolved Carbonate Species in Groundwater and Their Effects on Carbon-14 Dating," in Symposium on Use of Isotopes in Hydrology, International Atomic Energy Agency, Vienna, Austria (1970) pp. 271-286.

11. L. V. Benson, Secondary Mineral, Oxidation Potential, Pressure and Temperature Gradients in the Pasco Basin of Washington State, Topical Report #1, RHO-BWI-C-34, Rockwell Hanford Operations, Richland, Washington (November 15, 1978).

8.0 CONTAMINANT TRANSPORT

8.1 GENERAL

The migration rates of radionuclides traveling from a repository location to the biosphere can be calculated by utilizing transport models based on the equation of mass conservation. To utilize these models, one needs to obtain a number of additional properties of the hydrologic regime. These are: (1) the dispersion coefficients; (2) sorption coefficients; (3) characteristics of the waste source; (4) chemical reaction constants; and (5) radioactive decay rates. These factors define differences in the movement of a ground water fluid and its associated contaminants.

Mathematically, the expression of transport is simply a continuity equation for each chemical species written as:[1]

$$\frac{\partial n C_i}{\partial t} = - (\nabla \cdot C_i \bar{V}) - (\nabla \cdot \bar{j}_i) + R_i \qquad (8\text{-}1)$$

$$i = 1, 2, 3 \ldots n \text{ (transport species)}$$

where

C_i = the mass or radioactivity concentration of species i, $[ML^{-3}]$

t = time, $[T]$

n = porosity [dimensionless]

∇ = the Del operator $= \frac{\partial}{\partial x} + \frac{\partial}{\partial y} + \frac{\partial}{\partial z}$, [dimensionless]

$\bar{V}$ = the mass average Darcian velocity of the fluid, $[LT^{-1}]$

$\bar{j}_i$ = the mass flux of species i relative to $\bar{V}$, $[M L^{-2} T^{-1}]$

R_i = the net rate of production or consumption of species i (source/sink term) $[ML^{-3}T^{-1}]$.

The term on the left of Equation 8-1 is the time rate of change of species i (transient term). The $- (\nabla \cdot C_i \bar{V})$ term is usually referred to as the advective term. This term represents change in concentration of the system resulting from the movement of fluid in which species i is dissolved. The velocity vector of the fluid mixture, $\bar{V}$, is in general a function of time, space, temperature, and the chemical composition of the mixture. If $\bar{V}$ is constant with respect to time, the flow field is said to be steady; if $\bar{V}$ is zero, the fluid is stationary.

The $-(\nabla \cdot \bar{j}_i)$ term is often referred to as dispersion and is the macroscopic mixing caused by a combination of the molecular type diffusion, microscopic velocity variations within the pore space flow paths, and small-scale variations in advection resulting from the separation of the contaminated fluid into slightly different flow paths. Dispersion causes a given mass of contaminant to spread into a continuously expanding volume of porous medium. Whereas the first two elements of dispersion may be directly related to physical or chemical processes at the microscopic level, the third element is largely a measure of apparent mixing produced by unidentified variations in the porous material which are responsible for changes in the direction and velocity of ground water flow. The magnitude of the latter component of dispersion is, therefore, often a function of the scale of porous medium property identification[2] and becomes more significant as the degree of nonhomogeneity of the medium increases. This type of dispersion has been called macroscopic dispersion.[2] The combination of velocity variations at the microscopic level and the macroscopic dispersion may be termed mechanical dispersion.[3] Considerable progress in the field of porous media flow has been made in describing dispersion resulting from molecular diffusion and microscopic velocity variations. This has been accomplished primarily through small-column laboratory studies. However, Schwartz[2] noted that the few results that are available from field trials suggest that dispersion effects are considerably different from laboratory results. The difference between laboratory and field results is caused by macroscopic dispersion.[1]

Unidentified variations in a porous material result from the technical and economic difficulties in obtaining sufficient data to completely define a porous medium. The system blocks in a regional model are, thus, often larger than the true representative elementary volumes (REV). In reality, the mechanical dispersion should be included in the advection term to be rigorously consistent. Since its effect is normally small relative to large-scale fluid movement, it is usually associated with molecular diffusion, and included as part of the $-(\nabla \cdot \bar{j}_i)$ term. The molecular diffusion is composed of ordinary (concentration) diffusion, pressure diffusion, forced (electro-osmotic) diffusion, and thermal diffusion. The pressure, forced, and thermal types of diffusion are not normally important in large-scale ground water problems because of the lack of steep pressure, gravity, electrical, or thermal gradients necessary to make these diffusion mechanisms significant in a given problem.

The last term of Equation 8-1 represents the net production or consumption of species i and is often called the source/sink term. It is the sum of the changes due to reactive or radioactive decay mechanisms and the input or withdrawal of species i associated with the fluid recharge/discharges. Mathematically, this can be expressed as:

$$R_i = r_i + m_i \qquad (8\text{-}2)$$

where

r_i = the net rate of production or consumption of species i by reactive means $[ML^{-3}T^{-1}]$

m_i = the net rate of input/withdrawal of species i such as from a discharge source or pumped well $[ML^{-3}T^{-1}]$.

Some of the reaction mechanisms represented by r_i include ion exchange, precipitation, complex formation, and radioactive decay. The reactivity of a system may be a function of temperature and any or all of the n mass concentrations in the mixture. This term should, in theory, consist of a series of rate expressions which represent all known mechanisms by which species i can react in a given system. Species for which r_i is zero are referred to as conservative species, since they do not change by reactive means within the ground water system. Because r_i can, in general, be a function of all n components of the mixture, it is through this term that the system of n transport equations is coupled.

Practical solutions of the transport equations can be obtained by assuming that advection-dispersion and reaction occur sequentially within a simulation time step. This simplification can be justified on the basis that ground water systems, in general, exist at near chemical equilibria. The reaction rates for most important reactions are extremely rapid with respect to the velocity with which the fluid is moving. Also, the amount of coupling among the equations for different species may be reduced by assuming that trace (contaminant) species do not affect the chemistry of either the significant naturally occurring species or other trace species.

The mass flux of the dispersion term may be expressed as:

$$\bar{J}_i = -E^i \nabla C_i \qquad (8\text{-}3)$$

where

Ei = the coefficient of dispersion of species i and in the general three-dimensional case is a second-rank tensor $[L^2T^{-1}]$.

Equation 8-1 thus reduces to:

$$\frac{\partial n C_i}{\partial t} = - \nabla \cdot C_i \overline{V} + \nabla \cdot (E^i \nabla C_i) + R_i$$

E^i has components defined by:

$$E^i_{xx} = D^i_l \cos^2\psi \cos^2\theta + D^i_t (\sin^2\theta + \sin^2\psi \cos^2\theta)$$

$$E^i_{xy} = (D^i_l - D^i_t) \sin\theta \cos\theta \cos^2\psi$$

$$E^i_{xz} = (D^i_l - D^i_t) \sin\psi \cos\psi \cos\theta$$

$$E^i_{yx} = E^i_{xy}$$

$$E^i_{yy} = D^i_l \cos^2\psi \sin^2\theta + D^i_t (\cos^2\theta + \sin^2\psi \sin^2\theta)$$

$$E^i_{yz} = (D_l - D_t) \sin\psi \cos\psi \sin\theta$$

$$E^i_{zx} = E^i_{xz}$$

$$E^i_{zy} = E^i_{yz}$$

$$E^i_{zz} = D^i_l \sin^2\psi + D^i_t \cos^2\psi$$

where

ψ,θ are the principal angles between movement caused by convection and the coordinate axes

$D^i_l = \frac{\alpha l}{n} |u|$ is the longitudinal dispersion scaler

$D^i_t = \frac{\alpha t}{n} |u|$ is the transverse dispersion scalar $[L^2T^{-1}]$

$|u|$= the magnitude of the fluid velocity, $[LT^{-1}]$

α_l = the longitudinal dispersivity [L]

α_t = the transverse dispersivity [L].

The dispersivities, α_l and α_t are characteristics of the porous medium alone. Specification of dispersivities is one of the data requirements for a transport model.

8.2 DISPERSION

As noted in the preceding section, dispersion is the result of a microscopic and a macroscopic mechanism. The former occurs as a result of a continuous division and redivision of a fluid mass as it flows through a given material. Variations in local velocity, both in regard to direction and magnitude, along tortuous flow paths and the velocity distribution within each pore lead to contaminant spreading. Macroscopic dispersion, on the other hand, is the apparent mixing produced by unresolved variations in the regional media being studied. The overall impact of dispersion processes, however, on an analysis of transport processes is of second order by comparison to the effect of sorption and radioactive decay. This secondary importance, coupled with the difficulty of measuring dispersivities, accounts for the lack of dispersion data. In general, the approach that is usually taken is to estimate dispersivities rather than measure them.

R. A. Deju[4] reported contour plots of the x and y directional components of dispersion of the unconfined aquifer underlying the Hanford Site. These plots were computed using the calculated 1970-1971 ground water velocity distribution in the saturated zone.

Longitudinal and transverse dispersivities (α_l and α_t) for the Hanford Site unconfined aquifer have been estimated as 100 feet and 60 feet, respectively,[5] based on the average values required to give a match of historical tritium movements in the unconfined aquifer resulting from Hanford waste management practices. These values are high compared to typical laboratory values. The transverse dispersivity of 60 feet is much greater relative to the longitudinal dispersivity that has been suggested by DeJong.[6]

Longitudinal dispersion values for crystalline rocks, such as basalts, have been reported by Hill and Grimwood.[7] Their work gives a value for D_l^i = 10 square meters per day = 107 square feet per day and a high figure for the ground water velocity of u = 0.3 meter per day = 0.98 foot per day. Thus, the longitudinal dispersivity for a dense flow of porosity .01 is:

$$\alpha_l = \frac{D_l^i n}{|u|} = 1.1 \text{ feet} \qquad (8\text{-}5)$$

For a more vesicular basalt flow with porosity 0.1, the value of α_l would be 11 feet. Thus, in the dense basalts we can assume 1.1 feet $\leq \alpha_l \leq$ 11 feet. α_t can then be estimated as approximately[7] .6 α_l .7 feet $\leq \alpha_t \leq$ 7 feet.

8.3 SORPTION

Sorption is a measure of the decrease in the concentration of a component of a solution as it flows through a porous medium. One measure of sorption for species which are present in chemically trace amounts is the distribution coefficient, K_d

$$K_d = \frac{[A]eq}{[B]eq} \qquad (8\text{-}6)$$

where

K_d = distribution or sorption coefficient (milliliter per gram)

[A]eq = equilibrium trace concentration associated with the solid phase (milliequivalent per gram)

[B]eq = equilibrium trace concentration in the solution phase (milliequivalent per gram).

There are two types of reactions that result in changes in K_d with time.[8] The first is a sorption-desorption reaction with the rock. This type of reaction is relatively rapid and is probably diffusion controlled. The second is extremely slow and involves the reaction of geologic media with macro-components of the ground water. Possible reactions include mineral transformation, mineral dissolution, and precipitation of dissolved minerals and other ground water components.

R. A. Deju[4] has reported contours of the sorption coefficient for ground water containing ^{90}Sr flowing through the unconfined aquifer underlying the Hanford Site within the Pasco Basin. These results are shown in Figure 8.1 and were obtained from five field tests.

Results from various sources are shown in Table 8.1. These data include K_d values for various radionuclides in sediments from the unconfined aquifer beneath the Pasco Basin. These results are from laboratory columns and batch tests.

R. C. Routson[9] has studied K_d values for the unconfined aquifer using laboratory columns and batch tests. His results show that enormous volumes of water would be required to leach ^{90}Sr, ^{137}Cs, Pu, U, and ^{241}Am; whereas ^{3}H and ^{99}Tc are likely to move essentially with the liquid except for dispersion.

D. W. Rhodes[10] conducted laboratory equilibrium studies on sediments from the unconfined aquifer as a function of pH. His results are shown in Table 8.2. T. Tamura [11] later noted that, since plutonium can exist in different oxidation states and is subject to hydrolysis in the pH range normally encountered in natural-water systems, its adsorption from a water system is not by ion exchange, but more likely by scavenging of the hydroxide or oxide precipitates.

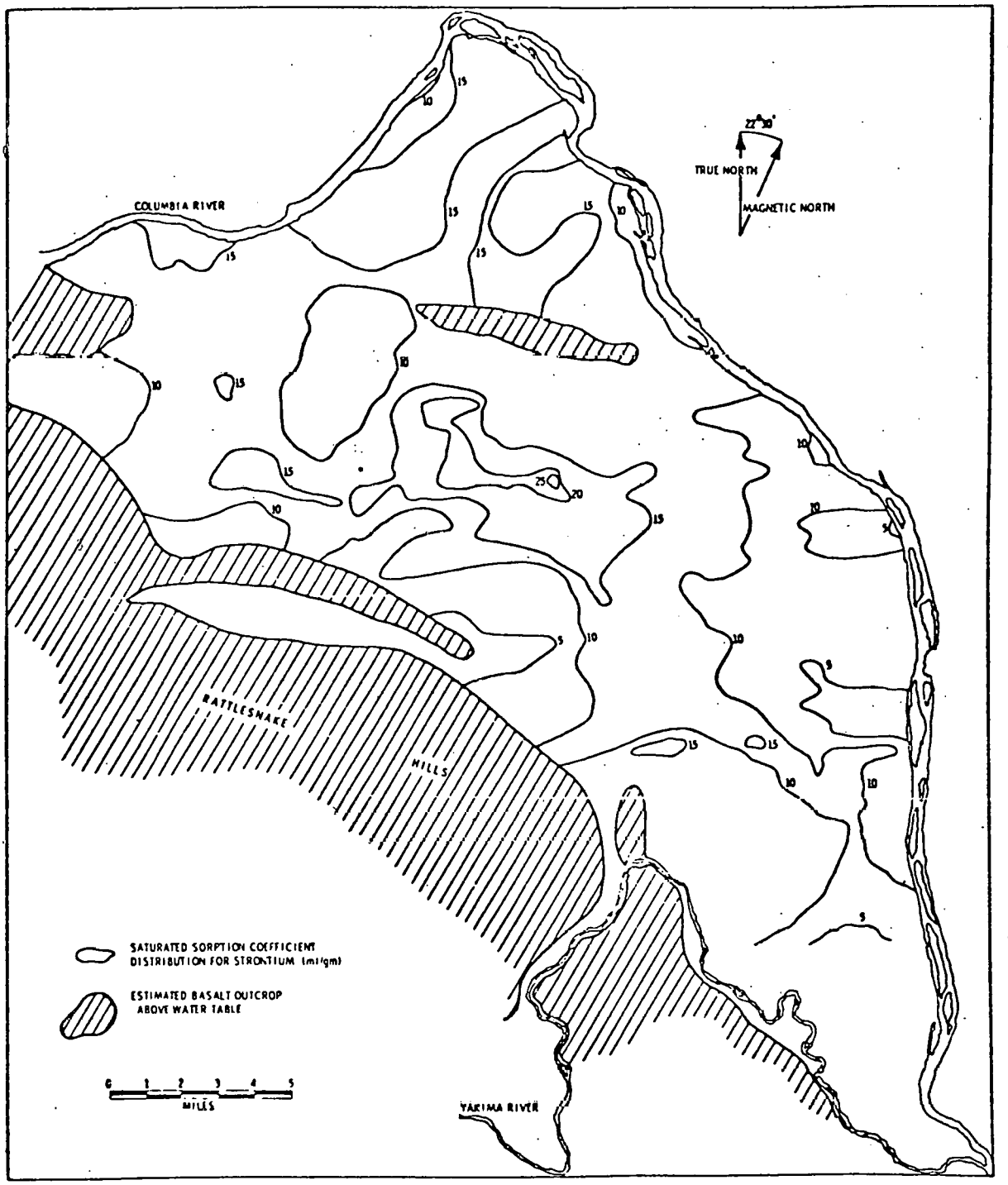

FIGURE 8.1

SATURATED SORPTION COEFFICIENT
DISTRIBUTION FOR STRONTIUM

TABLE 8.1

SORPTION (DISTRIBUTION) COEFFICIENTS FOR
SELECTED RADIONUCLIDES ON UNCONFINED AQUIFER SEDIMENTS

RADIONUCLIDE	K_d (ml/g)
^{90}Sr	5-38
^{137}Cs	12-200
Pu	200
U	<1
^{241}Am	~1,200
^{99}Tc	Very low (<<1)
^{89}Ru	26-750

TABLE 8.2

EQUILIBRIUM DISTRIBUTION COEFFICIENT VALUES
FOR ^{239}Pu AS A FUNCTION OF pH[9]

pH	K_d (ml/g)	pH	K_d (ml/g)
0	18	6.5	1,314
1.0	28	7.1	>1,980
2.2	>1,980	8.4	>1,980
2.7	>1,980	9.3	200
3.5	>1,980	11.1	178
4.4	>1,980	12.0	96
5.3	>1,980	13.0	1,980
6.0	888	14.0	1,980

K. J. Schneider and A. M. Platt[12] and Routson, et al.,[13] have determined K_d values for neptunium using typical Pasco Basin unconfined aquifer sediments. The former reported values of 15 milliliters per gram. Routson, et al., reported values of between 0.36 and 3.90 milliliters per gram using batch tests.

K. J. Schneider and A. M. Platt[12] have estimated a K_d value of 2,000 milliliters per gram for americium in the case of water and a typical western desert sediment. They have also estimated a K_d value of 600 milliliters per gram for curium between water and a typical western desert sediment.

G. S. Barney and M. W. Grutzeck[8] measured K_d values using batch experiments with Umtanum flow basalt samples (from an outcrop at Sentinel Gap, Washington) and typical deep basalt waters from the Pasco Basin (Table 8.3). Since the extent of sorption is directly proportional to the surface area, Barney has also reported the modified distribution coefficient K_d':

$$Kd' = \frac{K_d}{\text{Surface area } (m^2)/g} \qquad [ml/m^2] \qquad (8\text{-}7)$$

Barney measured the surface area using the Brinnell-Emmett-Teller apparatus and averaged the results of 2 determinations. His average surface area for basalt was 5.1 square meters per gram.

TABLE 8.3

SUMMARY OF K_d AND K_d' VALUES WITH BASALT

	K_d ml/g*	K_d' (ml/m^2)
^{137}Cs	296 ± 31	58.0 ± 6.1
^{90}Sr	151 ± 18	29.6 ± 3.5
^{106}Ru	38.0 ± 8.1	7.45 ± 1.59
Pu	19.8 ± 4.0	3.88 ± 0.78
^{241}Am	231 ± 18	45.3 ± 3.5

*The error given is the standard deviation for five replicate experiments.

S. Fried, et al.,[14,15] conducted experiments on the surface adsorption coefficient, K, of plutonium and americium on limestones and basalts. This coefficient, K, was defined as:

$$K = \frac{\text{(activity of actinide/ml of solution)}}{\text{(activity of actinide/cm}^2\text{ of rock)}} \qquad (8\text{-}8)$$

The results of Fried's experiments showed that, on a surface area basis, basalts sorbed more plutonium than limestone. Results from Fried's experiments are depicted in Figure 8.2.

Ames[16] has conducted K_d batch tests using basalt, heulandite $[(Ca, Na_2)\ Al_2\ Si_7\ O_{18} \cdot 6H_2O]$, and nontronite $[(Fe, Al)_2\ (Al, Si)_4\ O_{10} \cdot XH_2O]$. The latter two are common secondary minerals found within the Pasco Basin basalts. The basalt used was a sample of Umtanum basalt collected from just below Priest Rapids Dam on Umtanum Ridge.

The work of Ames included determination of K_d variations with time for natural uranium, ^{266}Ra, ^{75}Se, ^{125}I, ^{60}Co, ^{85}Sr, ^{137}Cs, ^{95m}Tc, and ^{237}Pu. The K_d data for strontium and cesium are shown in Table 8.4. Typical K_d values for other elements are shown in Table 8.5.

Examination of the cesium and strontium data indicate that, in 60 days, equilibrium or near-equilibrium conditions were not achieved. Since the chemical forms of cesium and strontium are not sensitive to changes in redox potential, they provide a good source of information regarding the required equilibration time.

In all cases except uranium, sorption experiments showed that, on a unit surface area basis, basalt adsorbs larger quantities of radionclides than heulandite and nontronite. This is true of selenium, radium, iodine, and cobalt, as well; although unexplained fluctuations in K_d values occurred for selenium and cobalt. These are probably a result of the lack of control of redox potential and temperature in the experiments.

8.4 CHARACTERISTICS OF THE WASTE SOURCE

8.4.1 General

The waste form presently being considered for storage in a basalt repository is spent unreprocessed fuel (SURF) from a light-water reactor. Assemblies from both pressurized water reactors (PWR) and boiling water reactors (BWR) are being considered. The physical characteristics of these SURF assemblies are listed in Table 8.6.[17]

If the decision were made to reprocess spent fuel with its resultant high-level waste stream, a vitrification process yielding a glass product would probably be the leading contender. In addition, supercalcine formulations have recently been studied as a potential waste form. The basic properties of these waste forms are noted in Table 8.7.[18]

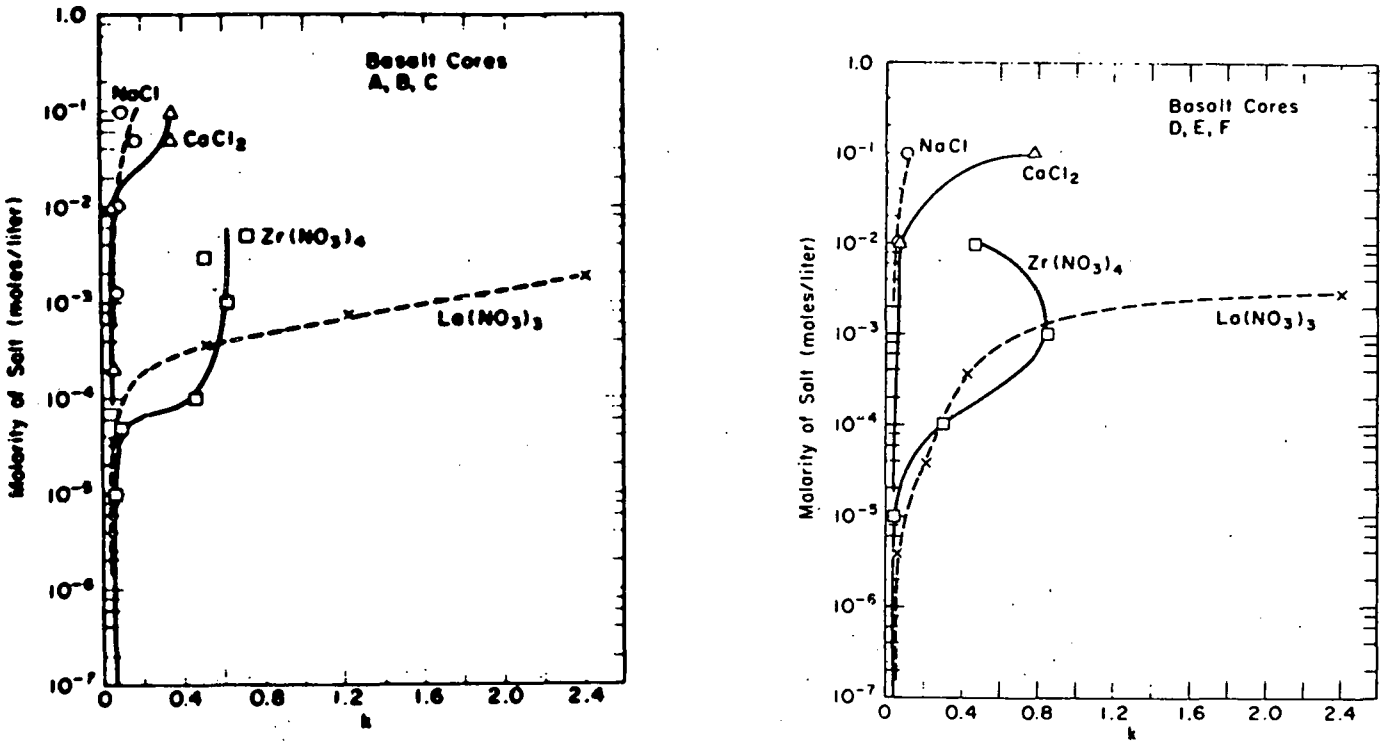

FIGURE 8.2

SURFACE ADSORPTION COEFFICIENT OF PLUTONIUM AS A FUNCTION OF THE CONCENTRATION OF OTHER SALTS FOR (A) DENSE AND (B) POROUS BASALT CORES

(From Fried, et al.[15])

TABLE 8.4

CESIUM AND STRONTIUM K_d VARIATIONS WITH TIME AT 23 DEGREES CENTIGRADE

		Kd (milliliters per gram)						
		3 DAYS	7 DAYS	14 DAYS	28 DAYS	55 DAYS	90 DAYS	120 DAYS
Basalt	^{137}Cs	623 ± 42	605 ± 36	566 ± 59	710 ± 5	828 ± 36	771 ± 50	882.1 ± 60.7
	^{85}Sr	79 ± 6	86 ± 5	89 ± 4	113 ± 3	121 ± 6	70 ± 12	120.4 ± 11.6
Heulandite	^{137}Cs	328 ± 27	409 ± 147	333 ± 95	461 ± 100	598 ± 277	331 ± 42	324.6 ± 75.4
	^{85}Sr	180 ± 6	231 ± 34	221 ± 9	333 ± 53	422 ± 55	495 ± 84	444.8 ± 74.6
Nontronite	^{137}Cs	1000 ± 37	899 ± 96	1056 ± 10	992 ± 46	1238 ± 212	1466 ± 14	1626 ± 74
	^{85}Sr	970 ± 86	992 ± 90	744 ± 40	950 ± 44	1020 ± 73	1328 ± 100	1046 ± 121
		K_d(s) (milliliters per square meter)						
Basalt	^{137}Cs	35.2 ± 2.4	34.2 ± 2.0	32.0 ± 3.3	40.1 ± 0.3	46.8 ± 2.0	43.6 ± 2.8	49.8 ± 3.4
	^{85}Sr	4.5 ± 0.3	4.9 ± 0.3	5.0 ± 0.2	6.4 ± 0.8	6.8 ± 0.3	3.9 ± 0.7	6.80 ± 0.65
Heulandite	^{137}Cs	6.0 ± 1.3	7.4 ± 2.7	6.1 ± 1.7	8.4 ± 1.8	10.9 ± 5.0	6.0 ± 0.8	5.90 ± 1.37
	^{85}Sr	3.3 ± 0.1	4.2 ± 0.6	4.0 ± 0.2	6.1 ± 1.0	7.7 ± 1.0	9.0 ± 1.5	8.09 ± 1.36
Nontronite	^{137}Cs	1.16±0.04	1.05 ± 0.1	1.22± 0.01	1.15±0.005	1.44±0.25	1.70± 0.02	1.89 ± 0.09
	^{85}Sr	1.13±0.10	1.15 ± 0.1	0.86± 0.05	1.10±0.05	1.18± 0.08	1.54± 0.02	1.21 ± 0.14

TABLE 8.5

TYPICAL K_d VALUES AND THEIR STANDARD DEVIATIONS AT 23 DEGREES CENTIGRADE FOR SEVERAL RADIONUCLIDES

(Equilibration time in days is indicated in each case.)

	^{237}Pu, 38 DAYS	^{226}Ra, 66 DAYS	^{60}Co, 30 DAYS	U, 42 DAYS	^{125}I, 30 DAYS	^{75}Se, 30 DAYS
	K_d (milliliters per gram)					
Basalt	65 ± 2	731 ± 327	315 ± 45.8	3.09 ± 15.8	6.2 ± 2.3	11.1 ± 0.8
Heulandite	66 ± 16	975 ± 660	234 ± 32	-1.28 ± 3.93	2.0 ± 2.7	0
Nontronite	1456 ± 609	1441 ± 331	8393 ± 428	314 ± 102	-3.0 ± 2.8	21.7 ± 1.3
	K_d (milliliters per square meter)					
Basalt	3.67 ± 0.11	41.3 ± 13.4	17.8 ± 2.6	0.175 ± 0.892	0.35 ± 0.13	0.63 ± 0.045
Heulandite	1.20 ± 0.29	17.7 ± 12.0	4.3 ± 0.6	-0.023 ± 0.071	0.036 ± 0.049	0
Nontronite	1.69 ± 0.71	1.67 ± 0.38	9.75 ± 0.50	0.365 ± 0.118	-0.003 ± 0.003	0.025 ± 0.002

TABLE 8.6

PHYSICAL CHARACTERISTICS OF UNIRRADIATED
REFERENCE LIGHT WATER REACTOR ASSEMBLIES[21]

	PRESSURIZED WATER REACTOR	BOILING WATER REACTOR
Overall assembly length, meters	4.640	4.350
Cross section, centimeters	20.8 x 20.8	13.9 x 13.9
Fuel element length, meters	3.851	4.065
Active fuel height, meters	3.658	3.660
Fuel element OD, centimeters	1.12	1.252
Fuel element array	14 x 14	8 x 8
Assembly total weight, kilogram	657.9	275.7
Uranium assembly, kilogram	461.4	183.3
UO_2 assembly, kilogram	523.4	208.0
Zircaloy assembly, kilogram	108.4**	57.9*
Hardware assembly,*** kilogram	26.1††	9.77†
Total metal assembly, kilogram	134.5	67.7

* Includes zircaloy fuel element spacers.

** Includes zircaloy control rod guide thimbles.

*** There are also light-water reactor fuels that have stainless steel control rod guide thimbles and cladding.

† Includes stainless steel tie-plates and inconel springs.

†† Includes 10 kilogram stainless steel nozzles and inconel 718 grids.

TABLE 8.7

WASTE FORM PROPERTIES[18]

PROPERTY	UNITS	SUPERCALCINE		GLASS		SURF
		POWDER	CERAMIC	PHOSPHATE	BORO-SILICATE	PELLETS
SOLUTION RATE	$\frac{mg}{m^2 sec}$	10^{-6} to 10^{-4}	10^{-7} to 10^{-5}	10^{-5} to 0.7	10^{-5} to 0.01	10^{-2} to 10^{-5}
CORROSION TO CLAD MATERIAL	nm/sec	0 to 10	0 to 10	0 to 10	0 to 10	*
RESIDUAL NITRATE AND/OR WATER	%	0.005 to 0.05	0.005 to 0.01	0.005 to 0.05	0.005 to 0.05	<.005
MAXIMUM PROCESSING TEMPERATURE	°K	1,370 to 1,570	1,370 to 1,570	1,170	1,270 to 1,670	NA
RUTHENIUM VOLATILIZED AT PROCESSING	%	≤7.0	≤5.0	3 to 15	≤2.0	NA
VOLATILITY	NA	1,570°K some Ru & Cs	1,670°K much Ru & Cs	<1,500°K all Ru & Cs	<1,500°K all Ru & Cs	NA
SPECIFIC VOLUME	$\frac{m^3}{MgU}$	0.070	0.070	0.036 to 0.078	0.04 to 0.1	—
WEIGHT PERCENT WASTE PRODUCT OXIDES	MAXIMUM	≤75%	≤75%	≤25%	≤ 50%	5%
	TYPICAL	45%	45%	20%	20-35%	4%
SPECIFIC AREA	$\frac{m^2}{Kg}$	10,000 to 20,000	0.005 to 0.05	0.005 to 0.05	0.005 to 0.05	—
FORM	NA	Powder	Monolithic	Fractured Monolith	Fractured Monolith	Fractured Pellets
STRUCTURAL QUALITY	NA	Soft & Crumbly	Very Hard & Brittle	Very Hard & Brittle	Very Hard & Brittle	Very Hard & Brittle
POROSITY	%	40 to 80	2 to 20	≤5.0	≤1.0	2 to 10
DENSITY	$\frac{Kg}{m^3}$	4,000	3,500 to 4,000	2,700 to 3,000	3,000 to 3,600	10,000 to 10,500**
COEFFICIENT OF LINEAR EXPANSION	x 10^{-6}/°K	~8.3	8 to 10	8 to 10	8 to 10	~10**
THERMAL CONDUCTIVITY	$\frac{W}{m°K}$	0.6	0.8 to 2	0.8 to 1.3	0.9 to 1.3	2** to 6
HEAT CAPACITY	$\frac{J}{Kg°K}$	670	1,100 to 1,200	1,100 to 1,200	750	238** to 330
LIQUIDUS TEMPERATURE	°K	1,670 to 1,870	1,670 to 1,870	820 to 1,020	800 to 1,500	~3,138**
TRANSITION TEMPERATURE	°K	NA	NA	770	870 to 970	NA

KEY TO SYMBOLS

— = Not Available.

NA = Not Applicable.

* = Mostly stress corrosion cracking which is localized, variable, and dependent upon the chemical species.

** = Based on UO_2 with approximately 2-10 percent porosity.

*** = Alloy has a transition temperature.

8.4.2 Spent Unreprocessed Fuel

8.4.2.1 General

The chemical state of SURF is altered from the state of fresh fuel by the presence of fission, activation and decay products, and by the radial temperature gradient which exists in the fuel during irradiation. The central portion of the fuel pin, which is typically at temperatures in the range of 1,800 to 2,500° C during irradiation, restructures forming large, dense columnar grains with radial orientation. An annular central void also can occur during restructuring (Figure 8.3).[19] The fuel restructuring is essentially a sintering process which occurs early in irradiation life. Typically, only refractory oxide and noble metal components, which have very low vapor pressures, remain in the central portion of the fuel. Other fission products migrate radially to cooler regions. The most mobile components are found at the fuel surface in the fuel cladding gap and at the fuel column ends or plenum regions.

The chemical components of SURF (excluding cladding) can be divided into chemical groups for the purpose of assessment of the chemical state. The groups consist of the following: actinides; yttrium and the rare earths; noble metals; other metals; alkaline earths (Ba, Sr); alkali (Cs, Rb); other elements (H, Se, Te, I); and inert gases (He, Kr, Xe). The groups as listed are roughly ordered from lowest to highest mobility in an intact fuel pin. However, two factors which strongly influence the state of SURF components are temperature and oxygen chemical potential.

8.4.2.2 Fuel Solid Solution

The primary phase in SURF is an oxide fuel solid solution. The fuel solid solution phase contains the actinides, Y + rare earths, and much of the Zr in a fluorite structure oxide phase of nominal MO_2 stoichiometry. Calculated bulk composition of the cation elements in the oxide fuel solid solution are given in Table 8.8.

TABLE 8.8

FUEL SOLID SOLUTION COMPOSITION
(Percent)

	1 YEAR	10,000 YEARS
U	97.632	97.874
Pu	0.931	0.524
Np	0.045	0.171
Am	0.018	0.004
Cm	0.002	---
Y + rare earths	1.013	1.013
Zr	0.359	0.413
Th	---	0.001
Others	<0.001	<0.001

*Assumes all ZrO_2 and no MoO_2 are dissolved in the fuel solid solution phase.

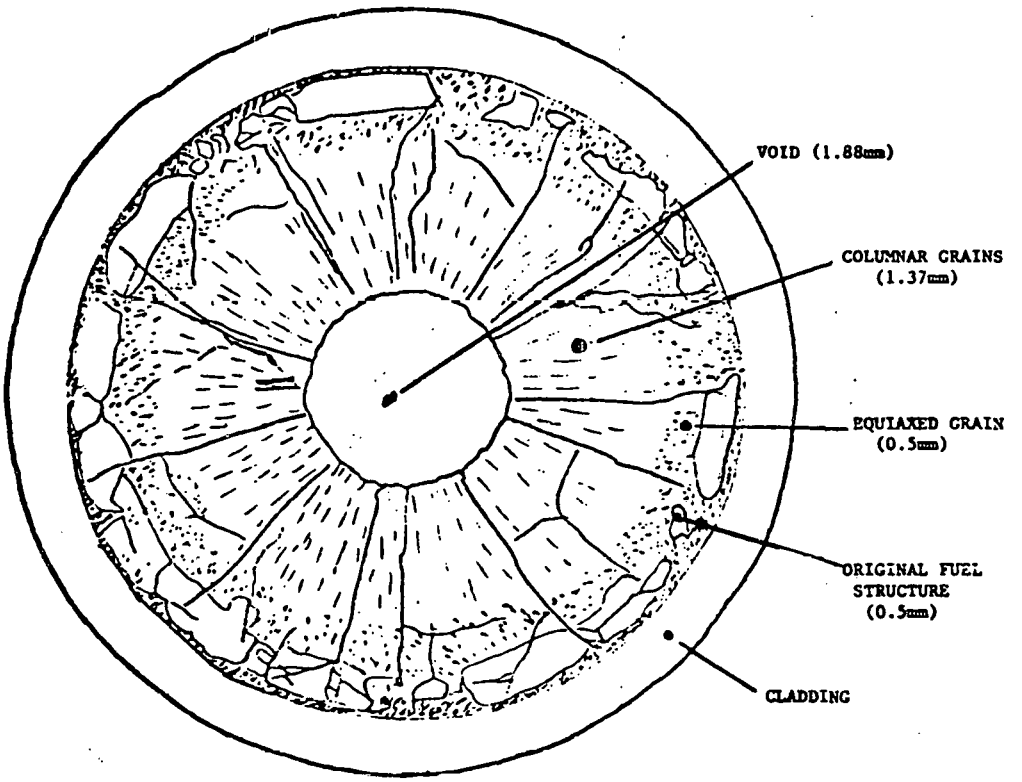

FIGURE 8.3

SCHEMATIC CROSS SECTION OF A TYPICAL SPENT FUEL PIN

Some radial concentration gradients in the fuel solid solution composition occur as a result of the radial temperature gradients during irradiation.

In a flooded repository (no air) under hydrothermal conditions, oxidative degradation of the fuel structure would depend on oxygen potential and pH characteristics of the ground water. However, solubility of the actinides, Y+ rare earths, and Zr oxides or salts in the neutral aqueous solutions is quite low and their polyvalent cations tend to be highly complexed in solutions. Solubility and mobility of these species is expected to increase with decreasing ground water pH.

8.4.2.3 Noble Metals

The noble metals, primarily Te, Ru, Rh and Pd, are present as metallic ingots in the fuel. Depending on oxygen potential, the ingots may also contain Mo. The equilibrium oxygen potential for formation of MoO_2 is close to the oxygen potential of stoichiometric MO_2 fuel. Rhodium, Ru, and Tc form oxides when heated in air. After a few hundred years, only Tc and Pd have any significant radioactive isotopes in SURF.

8.4.2.4 Other Metals

Zirconium and molybdenum are the major elements in this group. The majority of Zr is most likely dissolved in the primary fuel oxide phase. However, Zr may also be found as $BaZrO_3$ and $SrZrO_3$ zirconates in a second phase oxide. The molybdenum will be partitioned between the primary fuel oxide phase, the noble metal ingots, and $CsMoO_4$ phase in the fuel cladding gap. At full burnup, the majority of the Mo is most likely in the ingots or in the gap as $CsMoO_4$. Oxidation of Mo to MoO_2 occurs at oxygen potential values near that of the primary fuel oxide at stoichiometry (O/M = 2.0). The chemical state of minor metal elements in this category will also depend on oxygen potential.

8.4.2.5 Alkaline Earths

The alkaline earth elements barium and strontium are present as second-phase oxides in the fuel. The second-phase oxide may include zirconium as in $BaZrO_3$ and $SrZrO_3$.[20] Strontium would be leached out of the fuel if contacted by neutral or slightly acidic ground water. However, the deep Pasco Basin ground waters are fairly basic. Availability of strontium to interact with the repository system will be greatly increased by conditions leading to disruptive oxidation of the oxide fuel.

8.4.2.6 Alkali Metals

Cesium is the only alkali with significant radioactivity. At 100 years, cesium accounts for more than half of the calculated SURF radioactivity. Cesium-135 contributes small amounts of activity for great lengths of time due to a 2×10^6 year half-life. Cesium forms compounds with YO_2 and MoO_2 in the fuel cladding gap and may also be present as CsI and Cs_2Te.

8.4.2.7 Other Elements

All elements in this category have relatively high potential for migration from stored SURF. However, except for ^{129}I and initial contributions from tritium, activity from these elements is quite low. Iodine and Se would most likely be present in the fuel cladding gap along with Cs-containing phases. Carbon-14 and ^{36}Cl may also occur as activation products.

8.4.2.8 Inert Gases

A portion of the fission gas is released from the fuel during irradiation and may occasionally also be released to the reactor coolant through cladding breaches.

Retained fission gas is probably on the order of half the fission gas generated. Gas generated in the hotter central portions of the fuel diffuses out of the fuel structure as it is generated. Release of retained fission gas would be expected under conditions resulting in oxidation of UO_2 to U_3O_8.

8.4.2.9 Bulk Composition

Calculated typical spent fuel compositions at post-irradiation times from 1 to 10^4 years are given in Table 8.9. This table is derived from ORIGEN-2 computations for a PWR fuel assembly at 33,000 MWD/MT burnup,(21) and includes heavy metals, fission products, and decay products. Elements derived from light element neutron activation products, the cladding, or subassembly are not included in Table 8.9. The fission and decay product total is 3.38 percent of the original heavy metal weight indicating 3.38 atom percent burnup.

8.4.2.10 Spent Unreprocessed Fuel Activities

The elements whose chemical state is of most concern are those containing the highest long-lived radionuclide activities. Calculated activities at post-irradiation times from 1 to 10^4 years are given in Table 8.10. Activities less than 10^{-8} curies per subassembly are tabulated as zero. Several activation products not listed in Table 8.8 are included in Table 8.10 (i.e., ^{14}C, ^{36}Cl . ^{54}Mn, ^{55}Fe, ^{58}Co, ^{60}Co, ^{59}Ni, ^{63}Ni, ^{65}Zn.) Where decay chains occur, activities of short-lived isotopes are included in the longer-lived isotope activity. For example, in the decay chain:

$$^{144}Ce \xrightarrow{295d} {}^{144}Pr \xrightarrow{17m} {}^{144}Nd \quad \text{(stable)},$$

Prometium-144 activity is part of the tabulated Ce activity. Similarly, ^{137}Ba is included in the Cs activity, ^{103}Rn and ^{106}Rh are included in the Ru activity, and so on. The Zr, Nb activity includes:

$$^{95}Zr \xrightarrow{65d} Nb \xrightarrow{35d} {}^{85}Mo \quad \text{(stable)}$$

$$^{93}Ar \xrightarrow{10^6y} {}^{93m}Nb \xrightarrow{3.7y} {}^{93}Nb \quad \text{(stable)}.$$

Total spent fuel activities as a fraction of the total activity at 1 year are 14.1 percent, 1.44 percent, 0.074 percent, and 0.024 percent at 10, 100, 1,000, and 10,000 years, respectively. It appears that a majority of the fission products are of concern for less than 100 years. Beyond 1,000 years, most of the SURF activity results from actinide decay.

TABLE 8.9

PWR SPENT FUEL COMPOSITION IN GRAMS PER ASSEMBLY
(excluding cladding)
(From C. W. Alexander, et al.[21])

	1 YEAR	10 YEARS	100 YEARS	1,000 YEARS	10,000 YEARS
Actinides	446,000	446,000	446,000	446,000	446,000
Ac → Es					
Alkali Metals					
Li	8.9×10^{-5} →				
Rb	157	162	168	168	168
Cs	1,250	1,108	723	680	667
Total	1,307	1,270	891	848	835
Alkali Earths					
Sr	403	355	183	162	162
Ba	657	796	1,181	1,236	1,236
Total	1,060	1,151	1,364	1,398	1,398
Rare Earths (&γ)					
Y	210	210	210	210	210
La	561	561	561	561	561
Ce	1,168	1,096	1,096	1,096	1,096
Pr	515	515	515	515	515
Nd	1,784	1,856	1,856	1,856	1,856
Pm	52	5	10^{-10}	0	0
Sm	353	400	401	398	398
Eu	73	60	54	57	57
Gd	40	53	63	63	63
Tb	1	1	1	1	1
Dy	1	1	1	1	1
Ho	6×10^{-2} →				
Er	2×10^{-2} →				
Tm	2×10^{-5} →				
Yb	7×10^{-6} →				
Total	4,758	4,758	4,758	4,758	4,758

Table 8.9 (continued)

	1 YEAR	10 YEARS	100 YEARS	1000 YEARS	10,000 YEARS
Noble Metals					
Tc	359	359	359	358	348
Ru	1,044	1,005	1,005	1,006	1,016
Rh	217	217	217	217	217
Pd	592	631	631	631	631
Ag	35	35	35	35	35
Total	2,247	2,247	2,247	2,247	2,247
Other Metals*					
Zr	1,624	1,672	1,844	1,865	1,863
Nb	0.7	10^{-3}	10^{-2}	0.2	2.4
Mo	1,533	1,535	1,535	1,535	1,535
Cd	49	49	49	49	49
In	1	1	1	1	1
Sn	41	41	41	41	40
Sb	13	9	8	8	8
	3,261.7				
Other Elements					
I	10^{-2}	10^{-2}	10^{-4}	0	0
Se	26	26	26	26	26
Te	218	223	223	223	224
I	108	108	108	108	108
	352				

*Mn, Fe, Co, Ni, and Zn were listed only in curies as activation products, Zr does not include cladding.

TABLE 8.10

PWR SPENT FUEL ACTIVITIES IN CURIES PER ASSEMBLY

(446 Kg Heavy Metal; 33,000 MWD/MT)

(From C. W. Alexander, et al.[21])

	1 YEAR	10 YEARS	100 YEARS	1000 YEARS	10,000 YEARS
Actinides					
Ac→Cm	60,700	38,300	3,140	785	204
Alkali					
Cs	142,000	76,400	9,310	0.2	0.2
Alkali Earths					
Sr	36,900	27,300	2,960	10^{-6}	0
Rare Earths					
Y	6,400	0	0	0	0
Ce	458,000	15	0	0	0
Pm	48,400	4,480	0	0	0
Sm	175	163	84	0.1	0
Eu	7,290	2,944	2	0	0
Total	520,265	7,602	86	0.1	0
Noble Metals					
Tc	6.1	6.1	6.1	6.1	5.9
Ru	264,000	544	0	0	0
Pd	0.1	0.1	0.1	0.1	0.1
Total	264,000	550.2	6.2	6.2	6.0
Other Metals					
Mn	20	10^{-2}	0	0	0
Fe	1,970	179	10^{-8}	0	0
Co	3,272	972	10^{-2}	0	0
Ni	305	286	146	2	2
Zn	23	10^{-3}	0	0	0
Zr,Nb	45,400	3	3	3	3
Mo	10^{-2}	10^{-2}	10^{-2}	10^{-2}	10^{-2}
Sn	1,200	1	0.6	0.6	0.5
Sb	7,370	750	10^{-7}	0	0
Total	59,560	2,190	150	5.6	5.5

Table 8.10 (continued)

	1 YEAR	10 YEARS	100 YEARS	1000 YEARS	10,000 YEARS
Others					
^{3}H	356	214	1.3	0	0
C	0.7	0.7	0.7	0.6	0.2
Se	0.2	0.2	0.2	0.2	0.2
Cl	10^{-3}	10^{-3}	10^{-3}	10^{-3}	10^{-3}
I	10^{-2}	10^{-2}	10^{-2}	10^{-2}	10^{-2}

8.4.3 Other Waste Forms

The reference properties of both glasses and supercalcine have been summarized by Deju, et al.,[18] Ross,[22] Mendel, et al.,[23,24] Gray,[25] Turcotte and Wald,[26] and Ross, et al.,[27] have extensively detailed the properties of borosilicate glass wastes. McCarthy, et al.,[28-32] have extensively covered the properties of supercalcine formulations.

8.5 CHEMICAL REACTION CONSTANTS

A simulation of reactions between basalt and ground water has been made using techniques which permit the calculation of the progressive mass transfer between solids and an aqueous phase as a function of reaction progress.[33] Reactions involving SURF, basalt, and ground water have also been extensively studied and reported.[34-36]

In order to understand the chemistry of the natural environment in which contaminant transport takes place, chemical thermodynamic data are needed to summarize this environment. A summarization[8] was made of thermodynamic data of aqueous complexes and solid phases of plutonium, neptunium, americium, and curium likely to form in the natural environment. Data summarized includes:

- Free-energy data for the aqueous and solid species;
- Reaction constant data;
- Reactions studies;
- Techniques used;
- Nature of the aqueous media;
- Reaction-free energy;
- eH-pH diagrams.

Thermodynamic data on aqueous complexes and solid phases of other ions are presently being summarized as part of the Waste Isolation Safety Assessment Program.

8.6 RADIOACTIVE DECAY RATES

Radioactive decay rates are a measure of the amounts of a given radionuclide present in a given system at any one time. The half-life of a radionuclide is a measure of the time for the activity of a radionuclide to decay to half its value. Half-lives for the most important radionuclides from a contaminant transport analysis standpoint are given in Table 8.11.

TABLE 8.11

RADIOACTIVE DECAY RATES

ISOTOPE	HALF-LIFE (years)
^{241}Am	432
^{14}C	5,730
^{135}Cs	2.3×10^{6}
^{137}Co	30.17
^{60}Cm	5.27
^{244}Cm	18.11
^{3}H	12.33
^{129}I	1.59×10^{7}
^{237}Np	2.14×10^{6}
^{239}Pu	2.4×10^{4}
^{241}Pu	14.7
^{226}Ra	1,600
^{79}Se	10,000
^{90}Sr	29
^{99}Tc	2.13×10^{5}
^{234}U	2.44×10^{5}
^{238}U	4.47×10^{9}

8.7 REFERENCES

1. R. C. Arnett, R. A. Deju, R. W. Nelson, C. R. Cole, and R. E. Gephart, Conceptual and Mathematical Modeling of the Hanford Groundwater Flow Regime, ARH-ST-140, Atlantic Richfield Hanford Company, Richland, Washington (October 1976) 103 p.

2. F. W. Schwartz, "Macroscopic Dispersion in Porous Media: The Controlling Factors," Water Resources Research (1977).

3. J. Bear, Dynamics of Fluids in Porous Media, American Elsevier (1972).

4. R. A. Deju, A Comprehensive Review of Mathematical Models Construction to Describe the Hydrology of the Hanford Reservation, ARH-C-00003, Atlantic Richfield Hanford Company, Richland, Washington (April 1974).

5. Multicomponent Mass Transport Model: Theory and Numerical Implementation (Discrete-Parcel-Random-Walk Version), BNWL-2127, Battelle, Pacific Northwest Laboratory, Richland, Washington (May 1977).

6. J. DeJong, "Longitudinal and Transverse Diffusion in Granular Deposits," Transactions American Geophysical Union, 39 (1958).

7. M. D. Hill and P. D. Grimwood, Preliminary Assessment of the Radiological Protection Aspects of Disposal of High Level Waste in Geologic Formations, R69, National Radiological Protection Board Report, United Kingdom (1978).

8. R. J. Serne, Editor, Proceedings of the Task 4 Contractor Information Meeting; Waste Isolation Safety Assessment Program, PNL-SA-6957, Pacific Northwest Laboratory, Richland, Washington (September 1978).

9. R. C. Routson, A Review of Soil-Waste Relationships on the Hanford Reservation from 1944 to 1967, BNWL-1464, Battelle, Pacific Northwest Laboratory, Richland, Washington (March 1973).

10. D. W. Rhodes, "The Effects of pH on the Uptake of Radioactive Isotopes from Solution by a Soil," Soil Science Society of American Proceedings, 21, (1957) pp. 389-392.

11. T. Tamura, "Sorption Pehnomena Significant in Radioactive-Waste Disposal," Underground Waste Management and Environmental Implications, Proceedings of the Symposium December 6-9, 1971, Houston, Texas, published by American Association of Petroleum Geologists, 18, pp. 318-330.

12. K. J. Schneider and A. M. Platt, (Editors), High-Level Radioactive Waste Management Alternatives, BNWL-1900, Volume 1, Battelle, Pacific Northwest Laboratory, Richland, Washington (1974).

References (continued)

13. R. C, Routson, G. Jansen, and A. V. Robinson, Sorption of ^{99}Tc, ^{237}Np, and ^{241}Am on Two Subsoils from Differing Weathering Intensity Areas, BNWL-1889, Battelle, Pacific Northwest Laboratories, Richland, Washington (1975).

14. S. Fried, A. M. Friedman, J. J. Hines, R. W. Atcher, L. A. Quarterman, and A. Volesky, The Migration of Plutonium and Americium in the Lithosphere, (1976) p. 33.

15. S. Fried, A. M. Friedman, and R. Weeber, "The Distribution of Plutonium in a Rock Containment Environment," in M. H. Campbell, Editor, High Level Radioactive Waste Management, Advances in Chemistry Series No. 153, American Chemical Society, Washington, D.C., pp. 136-133.

16. L. L. Ames, "Radionuclide Batch K_d Values on Basalt, Heulandite, and Nontronite," in Basalt Waste Isolation Program Annual Report - Fiscal Year 1978, RHO-BWI-78-100, Rockwell Hanford Operations, Richland, Washington (October 1978).

17. Staff, Spent Unreprocessed Fuel Facility - Engineering Studies, RHO-LD-2, Rockwell Hanford Operations, Richland, Washington (October 1977).

18. R. A. Deju, R. K. Ledgerwood, P. E. Long, Reference Waste Form, Basalts, and Ground Water Systems for Waste Interaction Studies, RHO-BWI-LD-11, Rockwell Hanford Operations, Richland, Washington (September 1978).

19. G. J. McCarthy, S. Komarneni, and B. E. Scheetz, "The Chemical Interactions of Simulated Spent Unreprocessed Fuel and Basalts of the Columbia Plateau," in Basalt Waste Isolation Program Annual Report - Fiscal Year 1978, RHO-BWI-78-100, Rockwell Hanford Operations, Richland, Washington (October 1978).

20. D. R. Olander, Fundamental Aspects of Nuclear Fuel Elements, RID-26711-P1 (1976).

21. C. W. Alexander, C. W. Kee, A. G. Croff, and J. O. Blomeke, Projections of Spent Nuclear Fuel to be Discharged by the U. S. Nuclear Power Industry, ORNL/TM-6008, Oak Ridge National Laboratory, Oak Ridge, Tennessee (ctober 1977) p. 80.

22. W. A. Roos, Development of Glass Formulations Containing High-Level Nuclear Wastes, PNL-2481, Pacific Northwest Laboratory, Richland, Washington (February 1978).

23. J. E. Mendel, et al., A Program Plan for Comprehensive Characterization of Solidifed High-Level Wastes, BNWL-1940, Battelle, Pacific Northwest Laboratories, Richland, Washington (December 1975).

24. J. E. Mendel, et al., Annual Report on the Characterization of High-Level Waste Glasses, BNWL-2252, Battelle, Pacific Northwest Laboratories, Richland, Washington (June 1977).

References (continued)

25. W. J. Gray, Volatility of a Zinc Borosilicate Glass Containing Simulated High-Level Radioactive Waste, BNWL-2111, Battelle, Pacific Northwest Laboratories, Richland, Washington (October 1976).

26. R. P. Turcotte and J. W. Wald, Devitrification Behavior of a Zinc Borosilicate Nuclear Waste Glass, PNL-2247, Pacific Northwest Laboratory, Richland, Washington (May 1978).

27. W. A. Ross, et al., Annual Report on the Characterization of High-Level Waste Glasses, PNL-2625, Pacific Northwest Laboratory, Richland, Washington (June 1978).

28. G. J. McCarthy and M. T. Davidson, "Ceramic Nuclear Waste Forms: I. Crystal Chemistry and Phase Formation in Calcine," American Ceramic Society Bulletin, 54, p. 782-786 (1975).

29. G. J. McCarthy, M. T. Davidson, D. E. Pfoertsch, C. A. Smith, S. A. Gallagher, and R. G. Johnston, "Oxide Ceramic Nuclear Waste Forms," American Ceramic Society Bulletin, 54, p. 459 (1975).

30. G. J. McCarthy, "High-Level Waste Ceramics" Materials Considerations, Process Simulation and Product Characterization," Nuclear Technology, 32, p. 92-105 (1977).

31. G. J. McCarthy, "Ceramics and Glass Ceramics as High-Level Waste Forms," Ceramic and Glass Radioactive Waste Forms, D. W. Readey and C. R. Cooley, Editors, CONF-770102, U. S. Energy Research and Development Administration, Washington, D.C. (April 1977).

32. G. J. McCarthy, Advanced Waste Forms Research and Development. Comprehensive Progress Report, COO-2510-12, The Pennsylvania State University, University Park, Pennsylvania (1977).

33. J. A. Apps, The Simulation of Reactions Between Basalt and Groundwater, UCID-8066, University of California, Lawrence Berkeley Laboratory, Berkeley, California (October 1978).

34. G. J. McCarthy and B. E. Scheetz, High-Level Waste-Basalt Interactions, Annual Progress Report for the Period February 1, 1977 to September 30, 1977, RHO-BWI-C-2, Rockwell Hanford Operations, Richland, Washington, (May 1978).

35. G. J. McCarthy, B. E. Scheetz, S. Komarneni, M. Barnes, C. A. Smith, J. F. Lewis, and D. K. Smith, Simulated High-Level Waste-Basalt Interaction Experiments, First Interim Progress Report, RHO-BWI-C-12, Rockwell Hanford Operations, Richland, Washington (March 24, 1978).

36. G. J. McCarthy, B. E. Scheetz, S. Komarneni, M. Barnes, C. A. Smith, D. K. Smith, and J. F. Lewis, Simulated High-Level Waste-Basalt Interaction Experiments, Second Interim Progress Report, RHO-BWI-C-16, Rockwell Hanford Operations, Richland, Washington (June 30, 1978).

9.0 MODELING

9.1 GENERAL

The ultimate objective of our research and development effort in the basalt waste repository program is to assess the risk of siting a repository in a given subsurface stratum. The data given in the preceding chapters of this report are aimed at supplying the basic input parameters to flow and ground water transport models that serve as the basis for the assessment of risk from a basalt repository. The data requirements of these models are shown in Table 9.1. In this table, we have included a list of the sections of this report where individual input items are discussed. In this table, we depicted the flow models as separated from the transport process. This separation of flow from transport is based upon the assumption that the movement of waste contaminants from a repository would not cause any significant changes in the hydraulic properties of individual rock strata. The flow models are required input to the transport models, inasmuch as one must first describe the flow field that will be responsible for moving the radioactive contaminants.

To date, models have been developed and used in a preliminary way to model specific portions of the flow system; i.e., the unconfined aquifer,[1] and the deep repository environment,[2] but have not yet been applied to the total system. This latter objective is part of the effort in our risk assessment studies. Data from this report will be used in these regional modeling applications.

9.2 SIMPLIFIED CONCEPTUAL MODEL

A model can be defined as a simplified representation of a given system. Models must behave in a manner analogous to the actual system under a set of specified conditions. The objective of constructing a model is generally to assess the impact of certain actions and/or conditions on the actual system.

Generally, in modeling a system, one begins by conceptualizing the overall description of the actual system. This report has presented our conceptual model of the surface hydrology of the Pasco Basin (Chapter 4.0) and our conceptual model of the subsurface hydrology of the Pasco Basin (Chapter 5.0). The hydrologic properties of the various subsurface strata are part of the data requirements for our conceptual understanding of the subsurface regime and have been discussed in Chapter 6.0.

The picture that emerges from these analyses is that the Pasco Basin, in essence, consists of a sequence of water-bearing zones, generally confined from one another, and separated into three distinct flow systems. Flow paths in these flow systems appear to lengthen as we move to deeper zones.

TABLE 9.1

DATA REQUIREMENTS FOR MODELING

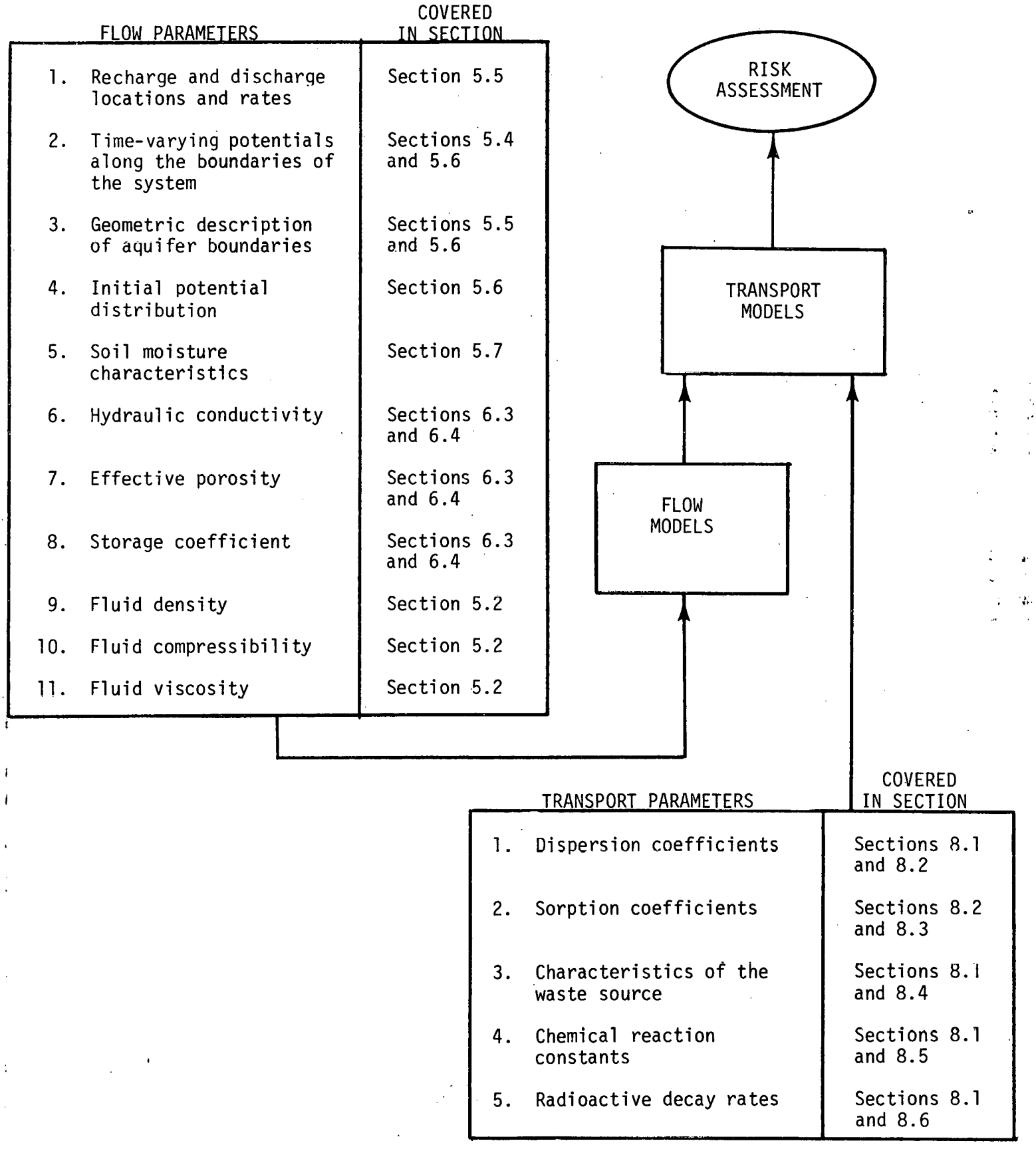

FLOW PARAMETERS	COVERED IN SECTION
1. Recharge and discharge locations and rates	Section 5.5
2. Time-varying potentials along the boundaries of the system	Sections 5.4 and 5.6
3. Geometric description of aquifer boundaries	Sections 5.5 and 5.6
4. Initial potential distribution	Section 5.6
5. Soil moisture characteristics	Section 5.7
6. Hydraulic conductivity	Sections 6.3 and 6.4
7. Effective porosity	Sections 6.3 and 6.4
8. Storage coefficient	Sections 6.3 and 6.4
9. Fluid density	Section 5.2
10. Fluid compressibility	Section 5.2
11. Fluid viscosity	Section 5.2

TRANSPORT PARAMETERS	COVERED IN SECTION
1. Dispersion coefficients	Sections 8.1 and 8.2
2. Sorption coefficients	Sections 8.2 and 8.3
3. Characteristics of the waste source	Sections 8.1 and 8.4
4. Chemical reaction constants	Sections 8.1 and 8.5
5. Radioactive decay rates	Sections 8.1 and 8.6

The total amount of flow from individual aquifers can be calculated using Darcy's law. Such a calculation was done for Well DC-1 using the data contained in Chapter 6.0. The results of these calculations are shown in Table 9.2, which indicates that the bulk of the ground water underflowing a unit column at the location of Well DC-1 is coming through the upper unconfined aquifer with minimal amounts by comparison being contributed by the deeper zones, especially within the Grande Ronde Formation.

In Chapter 6.0, it was also shown that our present model of the regional flow system, based upon piezometric head testing to date, indicates downward flow in this system trending from east to west within the Pasco Basin.

By describing the surface hydrology and the subsurface hydrology and, in addition, defining the hydrologic properties of individual subsurface strata, one can physically describe the flow characteristics of the ground water regime. In addition, in siting a repository, one is interested in understanding the transport potential of such a regime. To conceptualize this transport, a series of additional properties is necessary. These have been described in Chapter 8.0.

To conceptualize the transport process, we will consider a source of radioactive contaminant defined mathematically as a body of finite dimensions containing a given amount of radioactive material. This radioactive material is leached at a given rate and will undergo sorption and dispersion based on the basic physical/chemical properties of the repository basalt system. These basic properties are heavily dependent on the waste form and rock material through which the waste would have to be transported.

This general conceptual model will form the basis for our mathematical studies to analyze the behavior of the basic hydrologic system under various repository conditions. A number of mathematical models is available to define and describe the behavior of this system under various circumstances.[3] These models will be used to analyze the behavior of a saturated flow system adjacent to the canisters of nuclear waste, to analyze the effect of ground water on the stability of underground caverns, and to understand the flow and transport processes that take place in the subsurface of the Pasco Basin.

9.3 MODELING TO DATE

Mathematical models are representations of a system by means of a set of equations satisfying a number of conditions which occur in the actual system. Mathematical models can be further classed into two groups: (1) stochastic; and (2) deterministic. Stochastic models are such that one or more variables in the system are regarded as random or as Kisiel[4] defines them: "In the stochastic approach uncertainty by way of probability laws is woven onto the fabric of hydrodynamic and phenomenological relations which define mean-value behavior of a system with zero mean-square error." Deterministic models, on the other hand, involve only variables that are free from random variation. The modeling approach discussed herein is of a deterministic nature. To date, modeling work has included model development, sensitivity testing, and preliminary verification.

TABLE 9.2

GROUND WATER CALCULATIONS AT
THE SITE OF WELL DC-1

ZONE	T TOTAL TRANSMISSIVITY (square feet per day)	ϕ EFFECTIVE POROSITY (percent)	dh/dx HYDRAULIC GRADIENT (dimensionless)	$q = -\frac{T}{\phi}\frac{dh}{dx}$ Unit Flow (square feet per day)	PERCENT OF FLOW
Unconfined aquifer Ringold and glaciofluvial	40,000	5	1.8×10^{-4}	1,440	95.31
Saddle Mountains Formation	1,443	2	9.0×10^{-4}	65	4.30
Wanapum Formation	99	2	9.0×10^{-4}	4.5	0.30
Grande Ronde Formation	47	3	9.0×10^{-4}	1.4	0.09

To date, models for describing ground water and contaminant movement in the unsaturated zone and the unconfined aquifer have been developed and tested against analytical solutions and field data. The testing provided confidence in the mathematical methods and the approach used. Verification with field data showed areas where data coverage was inadequate and pointed up the need for development of a technique to compute uncertainties in the output based on known uncertainties in the input data.

In general, the Pasco Basin modeling is divided into three categories: (1) unsaturated zone analysis capability; (2) saturated ground water analysis capability; and, (3) transport capability. The unsaturated and saturated portions of the ground water system were considered separately in order to develop feasible models. The transport phenomena were assumed to be affected by, but not to affect, the convective flow patterns.

The model development effort is separated into three major categories: (1) data models; (2) hydraulic models; and (3) contaminant transport models. Data models are used to calculate input characteristics required for operation of the hydraulic and transport models. The hydraulic models utilize the ground water movement calculated by the hydraulic models with rock-waste reactions for predicting the contaminant movement rate. The ground water convective transport is often simulated independent of waste movement.

Reliable estimation of model parameter distributions both in time and space is a challenging enterprise in view of uncertainties in sampling, data analysis and interpretation, and the model structure. Hence, data models which assist in the process of producing such parameter distributions can be as important as the simulative models they serve. In a recent review of parameter estimation techniques applicable to Hanford ground water modeling, McLaughlin[5] examined a number of the better known methods. Statistical parameter estimation methods were recommended because they can account for significant measurement uncertainties and have a more general applicability to a variety of problems. Such statistical methods are being integrated into the Rockwell modeling effort. Earlier, a major data model, the Transmissivity Iterative Routine (TIR) was developed for calculating the hydraulic conductivity distribution in highly heterogeneous aquifers where characterization by field measurement alone would be prohibitive.[6] The TIR has been useful in developing a spatial distribution of hydraulic conductivity for the Hanford unconfined aquifer, but is limited by a lack of an objective measure of performance, the necessity of engineering intervention at various stages of the estimation process, and by the fact that it is rather highly specialized and application dependent.[5]

The basic hydraulic models are the Variable Thickness Transient Ground Water Flow Model (VTT),[7] the Simultaneous Heat and Moisture Transport Model (SEMTRA),[8] the PATHS Model,[9] and versions of the DAVIS FE Model.[9] The VTT Model was developed to predict the changing height of the water table (phreatic surface) throughout the unconfined aquifer. It provides for the simulations of two-dimensional flow in an unconfined aquifer. The model utilizes the non-linear transient Boussinesq equation with the appropriate initial and boundary conditions. The heterogeneous permeability distribution input has been calculated by the TIR Model. A successive line over-relaxation technique with unequal time steps is used for numerical solution. The VTT Model has recently been enhanced to have a multi-aquifer capability with variable thickness features for the unconfined stratum. The VTT Model can solve both transient and steady-state problems. More detailed solution at a finer difference grid spacing is possible by a sequential solution process, wherein the results of a large-region simulation are used as boundary conditions for a smaller region.[7]

The SEMTRA Model[8] is a finite element model for use in the analysis of transport processes in arid site vadose (unsaturated) zones. The numerical model is designed to provide detailed simulations of the interactions between climatic conditions and natural moisture movement in a dry soil system. The theoretical framework of the models considers processes of coupled heat and moisture transport, soil-atmosphere interactions, and spatially varying soil properties.

The mathematical formulation of the non-isothermal model consists of the coupled form of the pressure-based flow equation and the conduction equation. The flow equation models moisture flow as a function of the capillary, gravity, and thermal driving forces. The heat equation considers conduction and surface fluxes arising from atmospheric heating and cooling.

A Galerkin finite element approach is used to solve the set of governing equations. The non-linear, coupled equations are solved simultaneously using a Newton-Raphson iteration scheme. Quadratic basis functions are used to form the subdomain approximations for the principal variables and the spatially varying parameters. The soil hydraulic relationships are represented by cubic spline functions. A log transform approach is introduced to alter the form of the pressure-based flow equation.

Results of numerical experiments including comparisons with: (1) an analytical solution for linearized-coupled heat and moisture flow; (2) a numerical solution for isothermal imbibition; and, (3) actual field data demonstrate that the combined use of the cubic splines and the log transform approach significantly improve the solution convergences at low saturations.

The PATHS Model[9] is a two-dimensional analysis tool for determining saturated ground water arrival times at a river-type outflow boundary. The code was purposely designed to provide a realistic balance between model complexity and the limited input data usually available. Accordingly, the basis of the code is an idealized, two-dimensional analytical solution for the ground water potential distribution. From the potential distribution, the path line differential equations are numerically solved by the code to give the paths of the fluid particles and their advance with time along the paths toward the outflow boundary. The program uses an interactive BASIC front end which leads the user through the program input, requesting the data needed, and helping the user to select the necessary control parameters. After the input is completed, the BASIC part of the program automatically submits a "batch" job, thereby capitalizing on the economy available during heavy computing while solving the simultaneous equations. The results are available as: (1) summary tables obtained interactively; (2) detailed computer printouts when desired; or (3) as Calcomp plots, if that option is selected.

Three-dimensional ground water models based upon the DAVIS FE Model, developed by S. K. Gupta, et al., while with the Water Science and Engineering Section, University of California at Davis, are being applied.[10] The model considers saturated confined flow in three dimensions with both the fluid and porous material considered compressible. The time dependence arising from compressibilities is considered through a backward difference and the spatial discretization is through finite element.

Three-dimensional isoparametric elements are used that can be deformed in any of the three coordinate directions. The spatial basis functions for the isoparametric shapes along any element edge may be either linear, quadratic, or cubic in functional form. Such functional forms are incorporated by inserting additional node points along the element edge; i.e., the two end points are used for the linear form, adding a node at the center provides the quadratic variation, and the cubic is obtained through adding internal nodes at the one-third points along the element side. This procedure allows flexibility, particularly in satisfying irregular boundary conditions, yet maintains the advantages of using the simpler Chapeau basis functions for the potential or head representation.

Among the transport codes available are MMT and GETOUT. The GETOUT Code assumes that, at some arbitrary time after the waste is emplaced, the contents of the site are dissolved at a specified constant rate into an underground water body. The ground water flows at constant velocity through a homogeneous, one-dimensional column of the geologic medium and discharges to a surface water body. The dissolved radionuclides are assumed to be in sorption equilibrium at all points in the geologic medium. Radioactive decay (including chain decay of the actinides) is modeled both at the disposal site and during migration through the geologic medium.[9]

The MMT Code is based on the two-dimensional form of the diffusion-convection equation. The model considers variable dispersion coefficients, variable media thickness, and sink and/or source terms. The model has two major components: (1) the macroion segment handles dissolved minerals that are typically present in ground water systems; and (2) the microion segment predicts movement of the contaminants that are normally present in trace quantities (in comparison with the naturally occurring materials). The model combines the compound problem of multicomponent transport with simultaneous chemical reactions and includes the general transport mechanisms of advection, dispersion, and sorption, as well as radioactive decay. Each segment can be run as a separate model.

9.4 REFERENCES

1. J. L. Liverman, Final Environmental Statement - Waste Management Operations - Hanford Reservation, Richland, Washington, ERDA-1538, United States Energy Research and Development Administration, Washington, D. C. (December 1975).

2. M. P. Hardy, "Numerical Modeling for Repository Design," in Basalt Waste Isolation Program Annual Report - Fiscal Year 1978, RHO-BWI-78-100, Rockwell Hanford Operations, Richland, Washington (October 1978).

3. R. C. Arnett, R. A. Deju, R. W. Nelson, and C. R. Cole, Conceptual and Mathematical Modeling of the Hanford Groundwater Flow Regime, ARH-ST-140, Atlantic Richfield Hanford Company, Richland, Washington (October 1976) 103 p.

4. C. C. Kisiel, "Time Series Analysis of Hydrologic Data," Advances in Hydroscience, Academic Press, New York and London (1969) p. 119.

References (continued)

5. D. B. McLaughlin, Hanford Groundwater Modeling - Review of Parameter Estimation Techniques, RHO-C-19, Rockwell Hanford Operations, Richland, Washington (April 1979).

6. D. B. Cearlock, K. L. Kipp, and D. R. Friedricks, The Transmissivity Iterative Calculations Routine - Theory and Numerical Implementation, BNWL-1706, Battelle, Pacific Northwest Laboratory, Richland, Washington (1974).

7. K. L. Kipp, A. E. Reisenauer, C. R. Cole, and C. A. Bryan, Variable Thickness Transient Groundwater Flow Model Theory and Numerical Implementation, BNWL-1703, Battelle, Pacific Northwest Laboratory Richland, Washington (1976).

8. J. R. Raymond, Workshop on Transport Modeling for Nuclear Waste Repositories, PNL-SA-7468, Pacific Northwest Laboratory, Richland, Washington (July 25-26, 1977).

9. R. G. Baca, I. P. King, and W. R. Horton, Finite Element Models for Simultaneous Heat and Moisture Transport in Unsaturated Soils, RHO-SA-31, Rockwell Hanford Operations, Richland, Washington (March 1978).

10. S. K. Gupta, K. K. Tanji, and J. N. Luthin, "A Three-Dimensional Finite Element Ground Water Model," in Bulletin of the Water Resources Center, University of California at Davis, Davis, California (November 1975).

DISTRIBUTION

Number of Copies	
1	AMOCO
	G. Servos
1	ATOMICS INTERNATIONAL
	H. C. Weiseneck
6	BATTELLE-OFFICE OF NUCLEAR WASTE ISOLATION
	N. E. Carter Library
2	BECHTEL INCORPORATED
	R. A. Langley, Jr.
1	R. E. BROWN
2	CENTRAL WASHINGTON UNIVERSITY
	Department of Geology Library
2	EASTERN WASHINGTON UNIVERSITY
	Department of Geology Library
1	GEOSCIENCE RESEARCH CONSULTANTS
	J. G. Bond
2	IDAHO BUREAU OF MINES AND GEOLOGY
	M. M. Miller Library
1	LAWRENCE LIVERMORE LABORATORY
	L. D. Ramspott
1	LOS ALAMOS SCIENTIFIC LABORATORY
	K. Wofsberg
1	OREGON STATE DEPARTMENT OF GEOLOGY AND MINERAL INDUSTRIES
	J. D. Beaulieu

Distribution (continued)

Number of Copies	
2	OREGON STATE UNIVERSITY Department of Geology Library
2	PACIFIC NORTHWEST LABORATORY J. R. Raymond Library
5	SANDIA LABORATORIES E. H. Beckner R. C. Lincoln A. E. Stephenson L. D. Tyler W. D. Weart
1	STANFORD UNIVERSITY I. Remson
5	W. K. SUMMERS AND ASSOCIATES
4	U. S. ARMY CORPS OF ENGINEERS Seattle District Geologist Seattle District Librarian Walla Walla District Geologist Walla Walla District Librarian
1	U. S. BUREAU OF MINES J. W. Corwine
1	U. S. BUREAU OF RECLAMATION D. Newmann
2	U. S. DEPARTMENT OF ENERGY-ALBUQUERQUE OPERATIONS OFFICE D. T. Schueler
1	U. S. DEPARTMENT OF ENERGY-COLUMBUS PROGRAM OFFICE J. O. Neff

Distribution (continued)

Number of Copies	
5	U. S. DEPARTMENT OF ENERGY-HEADQUARTERS
	C. R. Cooley
	M. W. Frei
	C. H. George
	C. A. Heath
	D. L. Vieth
1	U. S. DEPARTMENT OF ENERGY-NEVADA OPERATIONS OFFICE
	R. M. Nelson
9	U. S. DEPARTMENT OF ENERGY-RICHLAND OPERATIONS OFFICE
	T. A. Bauman (4)
	R. B. Goranson
	A. G. Lassila
	B. L. Nicoll
	D. J. Squires
	F. R. Standerfer
6	U. S. GEOLOGICAL SURVEY
	C. Collier (3)
	W. W. Dudley, Jr.
	R. Schneider
	D. A. Swanson
5	U. S. NUCLEAR REGULATORY COMMISSION
	R. Boyle
	J. O. Bunting, Jr.
	J. C. Malaro
	J. B. Martin
	E. P. Regnier
2	UNIVERSITY OF ARIZONA
	E. S. Simpson
	Library
3	UNIVERSITY OF IDAHO
	R. Williams
	Department of Geology
	Library
2	UNIVERSITY OF OREGON
	Department of Geology
	Library

Distribution (continued)

Number of Copies	
2	UNIVERSITY OF WASHINGTON S. D. Malone S. W. Smith Department of Geology Library
1	VANDERBILT UNIVERSITY F. L. Parker
1	WASHINGTON PUBLIC POWER SUPPLY SYSTEM, INC. D. D. Tillson
3	WASHINGTON STATE DEPARTMENT OF ECOLOGY P. M. Grimstad (2) Library
2	WASHINGTON STATE DEPARTMENT OF NATURAL RESOURCES V. E. Livingston Library
4	WASHINGTON STATE UNIVERSITY J. C. Brown J. W. Crosby Department of Geology Library
1	A. C. WATERS
2	WESTINGHOUSE WIPP PROJECT R. C. Mairson
43	ROCKWELL HANFORD OPERATIONS H. Babad R. L. Biggerstaff D. J. Brown D. J. Cockeram T. A. Curran (5) R. A. Deju R. E. Gephart R. J. Gimera A. G. Law R. K. Ledgerwood C. W. Myers S. M. Price W. H. Price (5) M. J. Smith Basalt Waste Isolation Program Library (15) Document Control (4) Records Retention Center (2)